Peptidyl-Prolyl Isomerases as Promising Targets for Natural Product-Inspired Therapeutics

by

Bryan M. Dunyak

**A dissertation submitted in partial fulfillment
of the requirements for the degree of
Doctor of Philosophy
(Biological Chemistry)
in the University of Michigan
2016**

Doctoral Committee:

**Adjunct Associate Professor Jason E. Gestwicki, Co-Chair, University of
      California at San Francisco
Professor Janet L. Smith, Co-Chair
Professor Robert S. Fuller
Associate Professor Mark A. Saper
Assistant Professor Matthew B. Soellner**

Dedication

This work is dedicated to my parents, Donna S. Dunyak and Stephen A. Dunyak.

They taught me an appreciation for science from an early age, and my successes

would not be possible without them.

Acknowledgements

I would like to thank my advisor, Dr. Jason E. Gestwicki, for his unwavering support during this thesis work. Jason is an inspirational scientist and his passion for discovery is infectious. He has played a fundamental role in my development as a scientist, and I am eternally grateful. I have been privileged to be a member of his laboratory where he has taught me what it means to be an interdisciplinary researcher, a leader, and a mentor. To other members of the Gestwicki laboratory, past and present, I would like to express my sincerest gratitude. This work would not have been possible without your dedication to the "Gestwicki Gang" and scientific insight.

I am indebted to the contribution of my committee members: Dr. Janet L. Smith, Dr. Mark A. Saper, Dr. Robert S. Fuller, Dr. Paul F. Hollenberg, and Dr. Matthew B. Soellner. I appreciate all of the time they have taken to provide me feedback and direction during my graduate career.

I am grateful to my friends and family who have supported me throughout this journey, it is difficult to succinctly summarize everything that every one of you has done for me along the way. To Douglas Aho, Robert Kubiak, Collin Magin, and Matthew Schau, your friendship and confidence in me has been a core element of

Preface

This thesis is a compilation of published and unpublished work investing the underlying properties of the bifunctional natural product FK506 and how it may be leveraged in the design of effective therapeutics. In Chapter 1, I introduce the super family of Peptidyl-prolyl isomerases, their role in disease, and the mechanism of the bifunctional natural products FK506, rapamycin and cyclosporine. A portion of this Chapter was published as: "Dunyak, B.M. & Gestwicki, J.E. Peptidyl-Proline Isomerases (PPIases): Targets for Natural Products and Natural Product-Inspired Compounds. *J. Med. Chem.* In press. (2016)." In Chapter 2, I synthesized bifunctional molecules related to FK506 that simultaneously bind FKBP12 and HIV protease and characterized them using biochemical assays. In Chapter 3, I explored the cyto-selective properties of our bifunctional molecules using a cell-based GFP reporter and live virus HIV infectivity assays. These results suggested key design principles underlying cyto-selective bifunctional molecules and are published as "Dunyak, B.M., Nakamura, R.L., Frankel, A.D. & Gestwicki, J.E. Selective Targeting of Cells via Bispecific Molecules That Exploit Coexpression of Two Intracellular Proteins. *ACS Chem Biol* **10**, 2441-7 (2015)." In Chapter 4, FK506 was semisynthetically modified to furnish an amine substituted derivative, FK-NH2. This molecule was modified to develop potential Pin1 inhibitors, one of which had modest affinity for Pin1. This work is

currently ongoing. In Chapter 5, I summarize the work herein and highlight future

directions.

Table of Contents

List of Figures

List of Tables

List of Abbreviations

ACN   Acetonitrile

AD   Alzheimer's disease

ADME   Absorption, distribution, metabolism, and excretion

amu   Atomic mass unit

ANOVA   Analysis of variance

ANT   Adenine nucleotide translocase

APL   Acute promyelocytic leukemia

AR   Androgen receptor

ATP   Adenosine triphosphate

ATRA   All-trans retinoic acid

$A\beta$ Amyloid beta

Bcl-2   B-cell lymphoma 2

Bcl-xL   B-cell lymphoma-extra large

Boc   tert-Butyloxycarbonyl protecting group

C10   Carbon position 10

CD147   Cluster of differentiation 147

CD4   Cluster of differentiation 4

Cdc25   Cell division cycle 25

cDNA   Complimentary deoxyribonucleic acid

CID	Chemical inducer of dimerization
Cs_2CO_3	Cesium carbonate
CypA	Cyclophilin A
CypB	Cyclophilin B
CypD	Cyclophilin D
Da	Dalton
DABCYL	4-((4-(dimethylamino)phenyl)azo)benzoic acid
DCM	Dichloromethane
ddH_2O	Double-distilled H_2O
DIEA	N,N-Diisopropylethylamine
DMAP	4-Dimethylaminopyridine
DMEM	Dulbecco's modified eagle medium
DMF	Dimethylformamide
DMPU	1,3-Dimethyl-3,4,5,6-tetrahydro-2(1H)-pyrimidinone
DMSO	Dimethyl sulfoxide
DNA	Deoxyribonucleic acid
DTT	Dithiothreitol
EC_{50}	Half maximal effective concentration
EDANS	5-((2-Aminoethyl)amino)naphthalene-1-sulfonic acid ....
EDTA	Ethylenediaminetetraacetic acid
eq	Equivalence
ERK	Extracellular signal-regulated kinase
EtOH	Ethanol

FBS	Fetal bovine serum
FDA	Food and Drug Administration
FKBPs	FK506-binding proteins
Fmoc	Fluorenylmethyloxycarbonyl chloride
FP	Fluorescence polarization
FRB	FKBP-rapamycin binding
FRET	Förster resonance energy transfer
FRT	Flippase recombination target
GFP	Green fluorescent protein
GR	Glucocorticoid receptor
HAART	Highly active anti-retroviral therapy
HATU	1-[Bis(dimethylamino)methylene]-1H-1,2,3-triazolo[4,5-b]pyridinium 3-oxide hexafluorophosphate
HEK293	Human embryonic kidney 293 cells
HEPES	4-(2-hydroxyethyl)-1-piperazineethanesulfonic acid
HIV	Human immunodeficiency virus
HIVp	HIV protease
HPLC	High-performance liquid chromatography
Hr	Hour
Hsp72	Heat shock protein 72
Hsp90	Heat shock protein 90
IC_{50}	Half maximal inhibitory concentration
IPA	Isopropyl alcohol

IPTG	Isopropyl β-D-1-thiogalactopyranoside
ITK	IL-2 inducible T-cell kinase
M	Molar
MeOH	Methanol
MES	2-(N-Morpholino)ethanesulfonic acid
Methan(ol-d)	Deuterated methanol
MMP	Metalloproteinase
mP	Millipolarization units
MPT	Mitochondrial permeability transition
MS	Mass spectrometry
mTOR	Mammalian target of rapamycin
MW	Molecular weight
N_2	Nitrogen gas
Na_2SO_4	Sodium sulfate
NaCl	Sodium chloride
n-BuOH	n-Butanol
NF-AT	Nuclear factor of activated T-cells
NMR	Nuclear Magnetic Resonance
NTA	Nitrilotriacetic acid
PAGE	Polyacrylamide gel electrophoresis
PAMPA	Parallel artificial membrane permeability assay
Par14	Parvulin-14
Par17	Parvulin-17

PBS	Phosphate buffered saline
PEG	Polyethylene glycol
PHF	Paired helical filaments
Pin1	Peptidyl-prolyl cis/trans isomerase NIMA interacting protein 1
PML-RAR-α	Promyelocytic leukemia-retinoic acid receptor α
PPIases	Peptidyl-prolyl isomerases
ppm	Parts per million
pS/T-P	Phosphoserine/threonine-proline
PSI	Pounds per square inch
Rapa	rapamycin
RIPA	Radioimmunoprecipitation assay buffer
rRNA	Ribosomal ribonucleic acid
RU	Resonance units
SAR	Structure-activity relationship
SD	Standard deviation
SDS	Sodium dodecyl sulfate
SEM	Standard error of the mean
SH2	Src homology 2
SLF	Synthetic ligand for FKBP
SPR	Surface-plasmon resonance
TC	Tissue culture
Tet	Tetracycline
TEV	Tobacco etch virus

TFA	Trifluoroacetic acid
TFE	Trifluoroethanol
TGF-β	Transforming growth factor beta
T_h	T-helper cells
THF	Tetrahydrofuran
TIPS	Triisopropylsilane
TLC	Thin-layer chromatography
Tosylate	p-toluenesulfonate
TPR	Tetratricopeptide repeat
UV	Ultraviolet

Abstract

Peptidyl-prolyl isomerases (PPIases) are a ubiquitously expressed super family of proteins that catalyze the *cis/trans* isomerization of prolyl bonds. Proline conformation acts as a regulatory switch during folding, activation and/or degradation of "clients" that include proteins with roles in cancer and neurodegeneration. PPIase inhibitors, therefore, could be important therapeutics. However, the active site of PPIases is shallow and well conserved between members, challenging selective inhibitor design. Despite this, macrocyclic natural products, including FK506, rapamycin and cyclosporin, bind PPIases with nanomolar or better affinity. These natural products possess an unusual "bifunctional" binding mode and bind two separate proteins simultaneously, which is critical for their activity. They exhibit remarkable pharmacological properties, including oral bioavailability, and rapidly accumulate in cells with widespread tissue distribution.

Inspired by this mechanism, I synthesized a library of bifunctional molecules that bind both FKBP12 and HIV protease. Like FK506, we envisioned a model where coincident, high-level expression of both targets - as in HIV-infected lymphocytes with high levels of FKBP12 and HIV protease - would drive cyto-selective sequestration. The library possessed varying affinities for each target, retained

passive membrane permeability, and had cellular activity. Molecules highly potent for FKBP12 and HIV protease were selectively taken up into relevant cell populations. Treatment with FKBP12 inhibitors limited partitioning of the molecules, while FKBP12 overexpression enhanced it. This suggests that avidity effects drive selective accumulation of bifunctional molecules in cells expressing high levels of both protein partners.

We next focused on Pin1, a unique PPIase that binds prolines directly following phosphoserine/threonine residues. The requirement for an electronegative group in the Pin1 active site renders many inhibitors inactive from poor permeability. We hypothesized that the excellent pharmacological properties of FK506 might make it a suitable scaffold for engineering Pin1 inhibitors. However, FK506 has little affinity for Pin1, because it lacks the key electronegative region essential for Pin1 binding. To overcome this, we designed a novel semisynthetic strategy to modify FK506 at a position to improve affinity for Pin1. Installing a sulfamic acid significantly improved the affinity for Pin1 (>100-fold) *in vitro*. This strategy is designed to yield high-affinity membrane-permeable inhibitors of Pin1.

Chapter 1

The Superfamily of Peptidyl-Prolyl Isomerases: Targets of Macrocyclic Natural Products

1.1   Abstract

Peptidyl-prolyl isomerases (PPIases) are a chaperone superfamily comprising the FK506-binding proteins (FKBPs), cyclophilins and parvulins. PPIases catalyze the *cis*/*trans* isomerization of peptidyl-prolyl bonds, acting as a regulatory switch during folding, activation and/or degradation of many proteins. These "clients" include proteins with key roles in cancer, neurodegeneration and psychiatric disorders, suggesting that PPIase inhibitors could be important therapeutics. However, the active site of PPIases is well conserved between members, making selective inhibitor design challenging. Further, the active site is shallow and solvent-exposed. Despite these hurdles, macrocyclic natural products, including FK506, rapamycin and cyclosporin, bind PPIases with nanomolar or better affinity. Attempts to derive synthetic inhibitors de novo have been somewhat less successful, often showcasing the "undruggable" features of PPIases. Interestingly, the most potent synthetic molecules tend to integrate features of the natural products, including macrocyclization or proline mimicry strategies. Lastly, the

aforementioned macrocyclic natural products possess an unusual binding mode; they are naturally bifunctional and able to bind two separate protein targets simultaneously. For example, FK506 binds the FKBPs with one chemical face and calcineurin with another, non-overlapping motif to facilitate the formation of a stable ternary complex. In each case, binding two proteins at the same time is critical to the natural product's activity.

1.2 PPIases are a Superfamily of Molecular Chaperones

Peptidyl-prolyl isomerases (PPIases) are a superfamily of molecular chaperones that play widespread roles in protein folding and regulation through isomerization of proline residues.[1, 2] Unlike other chaperones,[3] PPIases do not utilize co-factors, such as ATP, to drive their activity; rather, they bind their "clients" using a shallow and promiscuous interface that is thought to favor proline isomerization through conformational selection. As discussed below, this deceptively simple mechanism is critical to the folding and function of numerous "clients". Indeed, genetic studies have shown that PPIases are essential to the function/folding of proteins important in cancer, neurodegenerative disorders, viral infection and psychiatric disorders.[4-7]

Despite the lack of deep, "druggable"[8] sites in the PPIases, nature has repeatedly found ways of creating potent PPIase inhibitors, as exemplified by the macrocycles FK506, rapamycin and cyclosporin. These natural products have been key probes for understanding PPIase function and were even used to identify members of the

PPIase family.[9] Here, we briefly discuss the structure and function of PPIases, their roles in disease, and our understanding of how natural products have informed recent developments in the search for selective, potent PPIase inhibitors.

1.3   Proline Isomerization in Protein Folding and Function

Peptide bonds in proteins are dominated by the *trans* conformation due to the steric clashes that occur at the alpha carbon in the *cis* orientation. However, proline is different (Figure 1.1A). The cyclized side chain of proline samples both the *cis* and *trans* conformations, typically in a ratio of ~20% *cis* to ~80% *trans*. Spontaneous isomerization of the Xaa-Pro bond is slow (on the timescale of
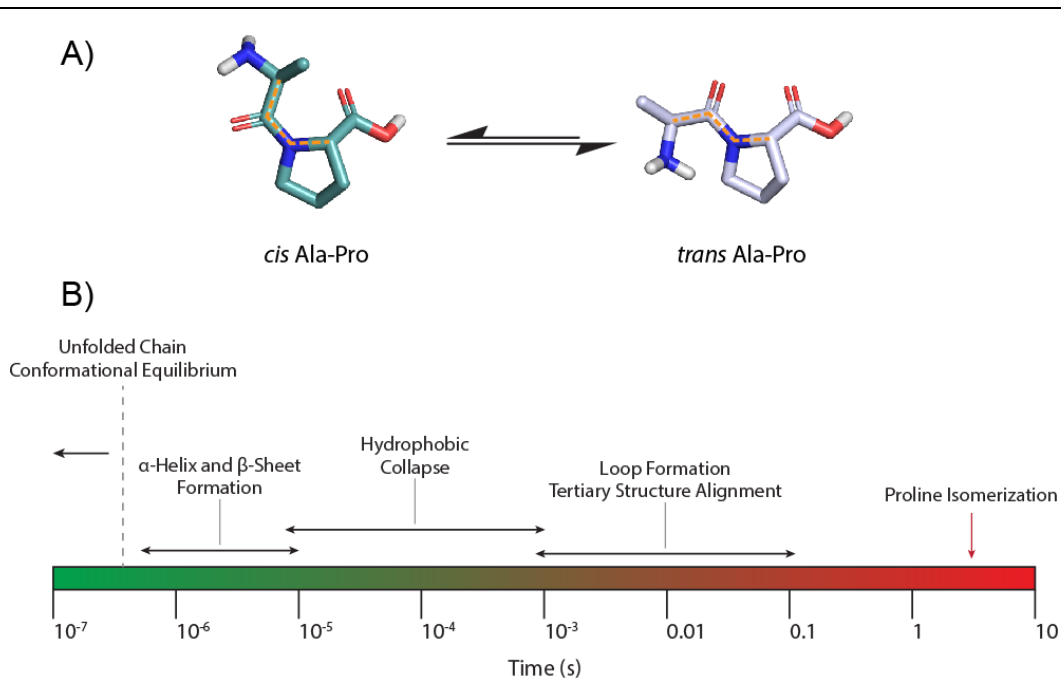
Figure 1.1) Proline can sample discrete *cis* and *trans* conformations, which isomerize on the timescale of milliseconds-to-seconds. A) Depiction of the proline conformations, with the backbone *cis* and *trans* orientations highlighted as an orange dotted line. B) Average timescales of processes important in protein folding, illustrating that uncatalyzed proline isomerization can often be a rate-limiting step.

milliseconds to seconds), creating a particular challenge to protein folding because the majority of folding events occur on the microsecond-to-millisecond timescale.[10] Thus, proline isomerization can be rate limiting, requiring PPIases to alleviate the bottleneck (Figure 1.1B).[11, 12] Beyond folding, this special feature of proline has been exploited as a regulatory switch in signal transduction. For example, oncogenic p53 is activated after binding of the PPIase Pin1, enhancing malignancy in transformed cells.[13, 14]

1.4   FKBPs, Cyclophilins and Parvulins

1.4.1 Architecture of the PPIase domain

PPIases are a superfamily consisting of the immunophilins and parvulins. In turn, the immunophilin family is further subdivided into the FKBPs and cyclophilins. In humans, there are 18 FKBPs, 24 cyclophilins and 3 parvulins.[15, 16] Each of the PPIases contains at least one PPIase domain. This domain is composed of antiparallel β-strangds that position a short α-helix. A shallow groove between the α-helix and β-sheet forms a small, solvent-exposed active site that binds to the
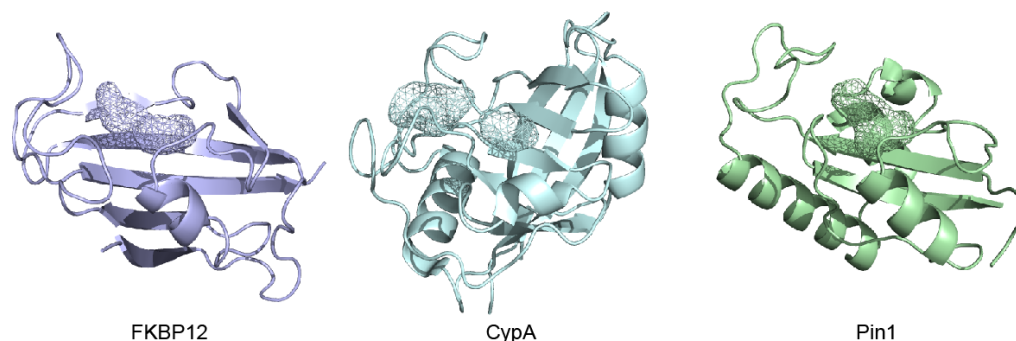
| FKBP12 | CypA | Pin1 |

Figure 1.2) Ribbon diagrams of the global folds of the representative PPIase domains of FKBP12, CypA and Pin1.The client binding pockets are depicted as a mesh cavity (produced in PyMol). (PDB: 1FKB, 1BCK, 1PIN, respectively)

target proline (Figure 1.2). Generally, a planar aromatic residue on the floor of the pocket mediates a critical hydrophobic interaction with proline. In the prototypical PPIases FKBP12, cyclophilin A (CypA) and Pin1, this interaction is facilitated by Trp-59, Phe-113 and Phe-134, respectively. The stabilizing role of Trp-59 has been extensively studied by NMR.[17] The catalytic mechanism of isomerization is not entirely clear, with previous studies suggesting that the PPIases may force a twisted-amide transition state.[18, 19] Stabilization is conferred by hydrophobic residues within the pocket alongside crucial hydrogen bonds formed with the proline backbone and adjacent residues (Figure 1.3A). In CypA, this interaction is carried out by Arg-55, which forms hydrogen bonds with the proline carbonyl oxygen in the *trans* state and proline amide nitrogen in the *cis* state.[20] These interactions have been studied by multi-temperature crystallography,[21] revealing the dynamical nature of the active site. The roles of the active site residues in FKBP12 are less clear, although mutagenesis experiments have implicated Asp-
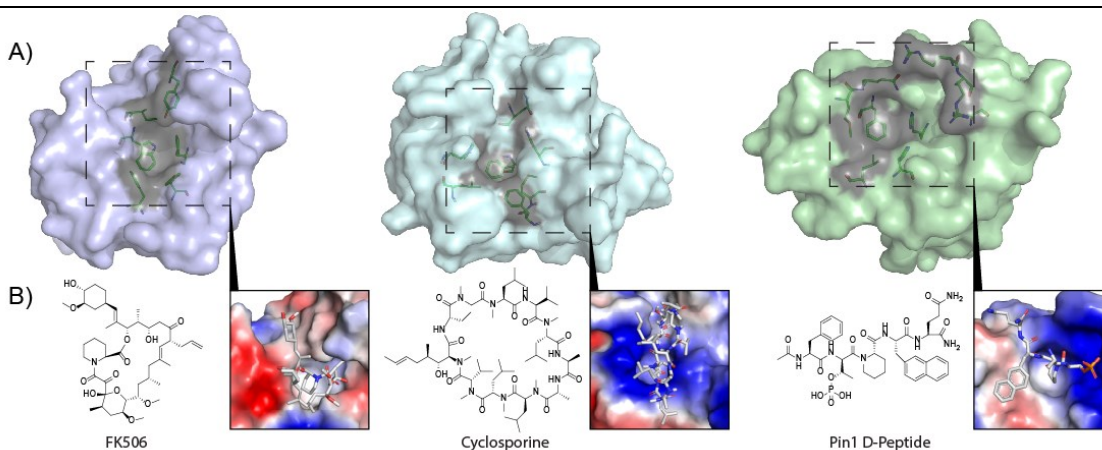
Figure 1.3) PPIases have a shallow, broad active site. A) Surface representation of the representative PPIase domains from FKBP12, CypA and Pin1. The active site region is shaded in gray, with critical residues for catalysis shown. B) High-affinity ligands for each PPIase are bound to the active site and engage the proline-binding pocket. Surface charges depicted (blue is positive, red is negative).

37 and His-87 in forming a hydrogen bond network between the pocket and bound client.[22] In Pin1, there is an active site Cys-113 that was initially thought to operate via covalent nucleophilic attack on the client. However, follow-up studies demonstrated that the cysteine could be mutated to serine (C113S) or aspartate (C113D) without loss of function, suggesting that hydrogen bonding is more important.[23] This model is further supported by the observation that Cys-113 is replaced by Asp-74 in the related family member, Parvulin-14.[24] Beyond this residue, a substantial hydrogen-bonding network involving His-59 and His-157, helps stabilize interactions with clients in Pin1.[24] Thus, all of the PPIases feature a key, floor residue that is supported by hydrophobic interactions and a hydrogen-bonding network surrounding the active site, although the exact identity of the residues often varies substantially. The best inhibitors of the PPIase access all of these regions (Figure 1.3B), which is a challenge given the extended dimensions of the pocket.

1.4.2 FKBPs

The FKBPs are a sub-family of 18 proteins and they are named for their apparent molecular mass. The 12 kDa family member, FKBP12 (gene *FKBP1A*), is composed of just a PPIase domain. It is widely expressed, but especially abundant in skeletal and cardiac muscle, the central nervous system, peripheral nerves and blood cells.[25, 26] The cellular roles of FKBP12 are not entirely clear despite its abundance; knockout mice exhibit a cardiac muscle phenotype and behavioral changes associated with several neurological disorders.[27, 28] FKBP12 likely

acts as a chaperone in protein folding and the knockout phenotypes suggest that its activity may be redundant with other PPIases in many instances. The other members of the FKBP family have, in addition to at least one PPIase domain, other modules. These other domains provide additional functions and often serve as scaffolds between the PPIase clients and other cellular pathways. For example, FKBP51 (gene *FKBP5*) and FKBP52 (gene *FKBP4*) share 70% sequence identify and possess three domains, two PPIase domains (FK1 and FK2) and a C-terminal tetratricopeptide repeat (TPR) domain.[6] The FK1 domain has PPIase activity and it binds both rapamycin and FK506 (FKBP51: $K_D^{Rapa} \approx 3.7$ nM, $K_D^{FK506} \approx 104$ nM; FKBP52: $K_D^{Rapa} \approx 4.2$ nM, $K_D^{FK506} \approx 23$ nM)[29] with similar affinity as FKBP12. The function of the FK2 domain is still largely unknown. FK2 does not bind FK506 or rapamycin and it does not have measurable isomerase activity *in vitro*. Through their TPR domains, FKBP51 and FKBP52 interact with the unstructured C-terminal tail of the chaperone, heat shock protein 90 (Hsp90), which links them to steroid hormone receptor maturation.[30-32] Interestingly, despite their high homology to each other, FKBP52 positively regulates the stability of androgen, glucocorticoid and progesterone receptors while FKBP51 acts as a negative regulator. Through this activity, FKBP52 has been implicated as a target in hormone-driven tumors, such as prostate cancer, colorectal adenocarcinomas, breast cancer and myelomas.[6] The functional differences between FKBP51 and FKBP52 have been isolated to dynamical changes in FK1.[33] In addition to steroid hormone signaling, the complex between Hsp90 and these FKBPs has also been shown to interact with intrinsically disordered proteins, such as tau.[34] In Alzheimer's

disease models, FKBP51-Hsp90 is associated with tau retention, while FKBP52-Hsp90 is linked to tau degradation through the proteasome.[35, 36] However, FKBP52 is also associated with promoting tau aggregation[37, 38] and inhibitors have shown promise in tauopathy models.[39] FKBP38 (gene *FKBP8*) has a single PPIase domain, which is normally inactive. However, this family member also has a TPR domain and a putative calmodulin-binding motif. Increases in Ca^{2+} trigger a conformational change that recruits calmodulin and activates the PPIase domain. In response to intracellular Ca^{2+}, activated FKBP38 then becomes competent for binding to the anti-apoptotic protein, Bcl-2. The exact role of FKBP38 in regulation of Bcl-2 activity remains enigmatic, with conflicting results suggesting that FKBP38 may either promote or inhibit apoptosis.[40]

1.4.3 Cyclophilins

Similar to the FKBPs, cyclophilins contain at least one PPIase domain and are widely distributed across tissue types.[41] The most abundant cyclophilin, cyclophilin A (CypA, gene *PPIA*), was named after the discovery of its ability to potently bind cyclosporin A ($K_D \approx 6$ nM).[42, 43] CypD, a mitochondrial cyclophilin, has been implicated in mitochondrial permeability transition (MPT) pore opening, allowing for the release of pro-apoptotic factors into the cytosol.[44] It is thought that CypD binds the adenine nucleotide translocase (ANT) machinery directly. Under stress conditions, this facilitates a Ca^{2+}-mediated conformational change in ANT, altering the role of ANT from a nucleotide transporter to an open pore.[45] Analogous to FKBP51/52, Cyp40 contains a TPR domain and interfaces with

Hsp90, facilitating complex formation with the estrogen receptor to modulate steroid hormone receptor maturation and trafficking.[46]

1.4.4 Parvulins

Lastly, the parvulins make up the smallest family of PPIases, consisting of: peptidyl-prolyl *cis*/trans isomerase NIMA interacting protein 1 (Pin1), Parvulin-14 (Par14) and Parvulin-17 (Par17). The parvulins were originally discovered as a novel PPIase family in *Escherichia coli*.[47] Human parvulins can be subdivided into two groups by substrate specificity. Par14 and Par17, products of alternative transcription initiation of the parvulin gene,[48] are similar to the prokaryotic parvulins and exhibit the conserved isomerase and chaperoning activity characteristic to most PPIases. The exact cellular functions of Par14 and Par17 are still cryptic. Par14 has been found both in the cytosol and nucleus, reportedly binding DNA[49] and assisting in rRNA processing for ribosome biogenesis.[50] Less is known about Par17, although it has been shown to promote microtubule assembly[51] and it contains a mitochondrial targeting sequence, where it is implicated in DNA binding.[52] Pin1, the third member of the parvulin family, is unique among all PPIases because it only recognizes prolines that are adjacent to phosphorylated serine/threonine residues (*i.e.* the pS/T-P motif). Pin1 also has an N-terminal WW domain, which similarly binds to the pS/T-P motif and shares an overlapping client profile with the PPIase domain. The WW domain consists of two antiparallel β-strands that connect via a short linker to the PPIase domain, forming a hydrophobic patch that binds to substrate and coordinates the phosphorylated

serine/threonine via Arg-17. The WW domain does not possess intrinsic isomerase activity and it is not clear why it has an overlapping substrate preference. It is thought that the WW domain may help recruit Pin1 to relevant clients, but the hand-off mechanism is unknown. What is clear is that Pin1 plays essential roles in cell division. For example, Pin1 regulates the activity of the phosphatase Cdc25, coordinating it with the cell cycle.[53] Pin1 also stabilizes the regulatory protein, cyclin D1, preventing its degradation and mediating its nuclear localization through the conformational switch of pThr286-Pro287.[54]

1.5   Mechanisms of Bifunctional PPIase Ligands

Two of the PPIases, FKBP12 and CypA, were discovered as the molecular targets of the natural products FK506, cyclosporin, and rapamycin, in a pre-genomic
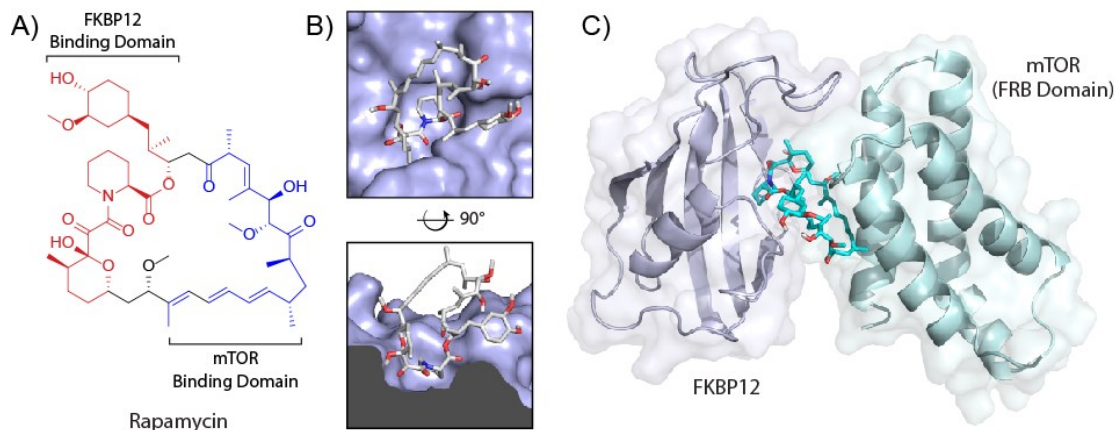
Figure 1.4) Bifunctional binding mode of the natural product rapamycin. A) Rapamycin forms a ternary complex with FKBP12 and the FRB) domain of mTOR). B) The pipecolyl α-ketoamide of rapamycin anchors it into the proline-binding pocket, while leaving the triene exposed for interactions with mTor. C) Crystal structure of the FKBP12-rapamycin-mTOR ternary complex, showing the rapamycin-mediated organization of both protein partners. (PDB: 1FAP)

example of pharmacology leading to the discovery of a protein function.[42, 55-57] Subsequent work showed that FK506 forms a ternary complex between FKBP12 (and other FKBPs)[58] and the phosphatase, calcineurin. Interestingly, cyclosporin and rapamycin have a conceptually similar way of binding their targets. Cyclosporin brings together CypA and calcineurin, while rapamycin facilitates the ternary complex between FKBPs and mTOR.[59] These molecules are able to bind both targets and are thus naturally "bifunctional"; rapamycin binds FKBPs with one chemical face and mTOR with another, non-overlapping motif (Figure 1.4A and 1.4B) to facilitate the formation of a stable ternary complex (Figure 1.4C). In each case, binding two proteins at the same time is critical to the natural product's immunsuppressive activity. For example, FK506 blocks the dephosphorylation and activation of the transcription factor NF-AT by using the steric bulk of FKBP12 to limit accessibility to the calcineurin active site.[60] It would be difficult for a small molecule to do this effectively on its own because of the shallow, open nature of the phosphatase pocket. Similarly, rapamycin blocks the G1 to S phase transition and prevents proliferation of activated T-cells by using FKBP12 to limit accessibility of substrates to mTOR.[61-63] Thus, the PPIase (*i.e.* FKBP12) isn't necessarily the target that drives the biological affect, it is simply "along for the ride".

1.6   *Chemically Induced Dimerization*

Over the last two decades, this mechanism has been exploited in dozens of chemical biology strategies. Synthetic, bifunctional molecules, which are based on the natural products, are used to control protein dimerization, stability, localization
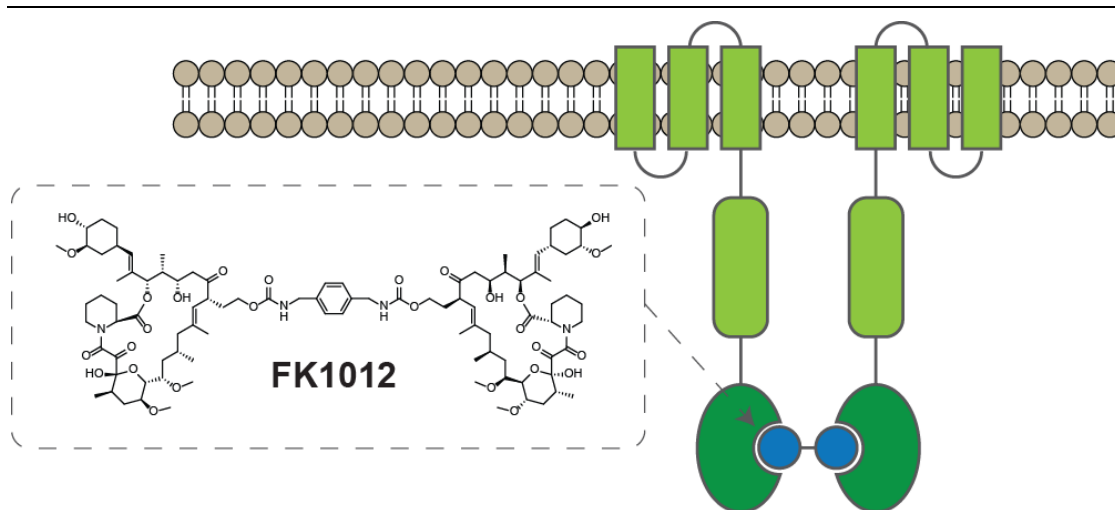
Figure 1.5) General schematic for Chemically Induced Dimerization (CID) to activate receptors. Receptor constructs fused to FKBPs (dark green) could be artificially dimerized by the addition of bifunctional FK506 ligands (inset and blue circles). This strategy can be used to study temporally controlled signaling events triggered by receptor oligomerization.

and function.[64-69] Synthetic molecules based on FK506 have a long history of important uses in chemical biology and drug discovery.[64, 68, 70-74] The first example of a synthetic FK506 bifunctional derivative was used as a Chemical Inducer of Dimerization (CID), a generalizable tool for understanding the mechanism of receptor dimerization and signaling. Cellular expression of constructs consisting of a receptor of interest fused to FKBPs could be activated by the addition of a synthetic bifunctional FK506 ligand. Receptor activation via intracellular dimerization and oligomerization events were triggered by the addition of a cell-permeable "FK1012" ligand (Figure 1.5). In this way, signaling cascades could be initiated by addition of the exogenous ligand, allowing for temporal control of dimerization and subsequent signaling events.

While FK506-based bifunctional ligands were effective as CIDs, their large molecular weight and overwhelming chemical complexity initially limited their usefulness. Further, these limitations presented challenges in the discovery of new ligands targeting the FKBPs as traditional chemical probes. Development of the early synthetic (*e.g.* non-natural product) FKBP12 inhibitors were designed to mimic the binding pose of FK506 (Figure 1.6A). The pipecolate core of FK506 is retained but the pyranose ring is replaced by a tert-pentyl substitution off the α-ketoamide.[75, 76] Derivatization and optimization of the pipecolic ester to represent the cyclohexylethenyl group and stereospecific substitution at the carbinol center ultimately resulted in SLF[74], or Synthetic Ligand for FKBP. SLF was designed to retain most of the affinity of FK506 ($K_i \approx 20$ nM), while also
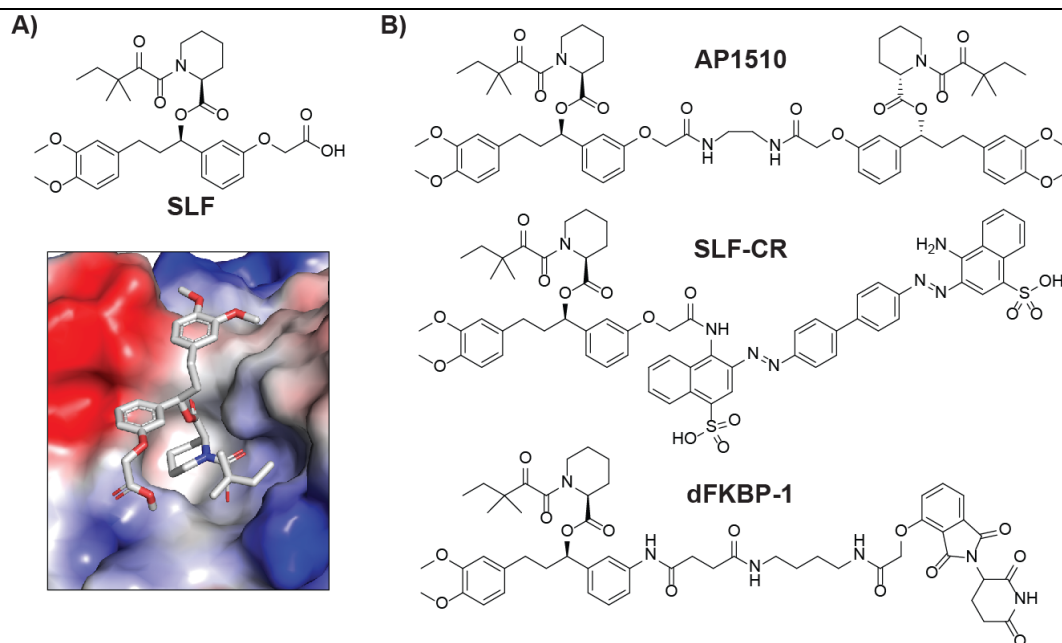
Figure 1.6) Synthetic Ligand for FKBP (SLF) binding to FKBP12 and representative SLF CIDs. A) SLF was designed to mimic the natural binding pose of FK506. B) Modification at the carboxylic acid allows for simple formation of bifunctional molecules for dimerization, recruitment of FKBPs to amyloids or delivery of FKBPs to E3 ubiquitin ligases for targeted degradation. (PDB: 4LAY, represented as an electrostatic surface)

including a pendant carboxylate that could be used to add additional functionalities that point away from the FKBP surface. Crystal structures confirmed that the compounds adopt a binding pose similar to FK506, largely driven by the pipecolyl ring interaction with Trp-59. The cyclohexylethenyl chain, replaced by the phenethyl fragments in the synthetic molecules, sits in the same hydrophobic groove, engaging in hydrophobic interactions with Ile-56 and Tyr-82. The most significant deviation from the FK506 pose occurs in the pyranose replacement, where a hydrogen bond with Asp-37 is lost. Nonetheless, native salt bridges are maintained and the tert-pentyl group makes productive Van der Waals contacts. Consistent with their design, these compounds lack immunosuppressant activity because they can no longer bind calcineurin.

1.7 Heterodimeric Bi-specific Ligands

In this way, SLF became a "go-to" molecule for creating CIDs (Figure 1.6B).[64, 77] Typical CIDs were assembled by coupling SLF either to itself (**AP1510**)[74] or to other molecules to form heterodimeric ligands. Synthetic FK506 mimetics were likewise used for various CID applications. With similar potency as FK1012, **AP1510** was able to dimerize FKBP12-Fas fusion proteins, activating Fas-mediated apoptosis in HT1080 cells.[74] SLF tethered to the amyloid-binding ligand Congo Red (**SLF-CR**) was able to recruit FKBP12 chaperone proteins to sites of protein misfolding and aggregation, blocking Aβ fibril formation *in vitro* and in cell models of disease.[78] In an alternate approach, thalidomides could selectively target proteins for degradation via specific ligand conjugates that recruit

the cereblon E3 ubiquitin ligase; here, SLF conjugated thalidomide (**dFKBP-1**) selectively bound FKBP12 which was subsequently degraded.[79] Inspired by the natural mechanism of FK506, synthetic bifunctional molecules are promising candidates for future clinical development.

In Chapters 2 and 3, I will explore a new aspect of bifunctional molecule design. Specifically, I synthesized bifunctional molecules that bind to FKBP12 on one end and HIV protease on the other. Using these molecules, I could selectively target cells that express both of the target proteins.

1.8   Roles of PPIases in Disease

More recently, the PPIases themselves have emerged as targets in their own right, and for a wide range of diseases.[80] The breadth of diseases linked to PPIases is staggering, likely because they have so many potential clients. For example, FKBP12 has been shown to modulate the activity of ryanodine receptor, inositol 1,4,5-triphosphate receptor, TGF-β receptor 1 and activin type 1 receptor.[81, 82] Similarly, as mentioned above, FKBP51 and FKBP52, are critical for maturation and activity of the steroid hormone receptors, such as androgen receptor (AR) and glucocorticoid receptor (GR) ,[83] FKBP38 is linked to the anti-apoptotic proteins Bcl-2/Bcl-xL matrix metalloproteinase 9 (MMP9),[40] FKBP25 regulates casein kinase II and nucleolin[84] and FKBP13 and FKBP65 control elements of the secretory pathway for protein trafficking and collagen biosynthesis.[85, 86] Similarly, the cyclophilins are involved in collagen remodeling,[87] function of the

steroid hormone receptors,[46, 88] and activation of numerous transcription factors.[41] The cyclophilins also play key roles in calcium signaling and homeostasis through activities on multiple clients.[45, 89] CypA binds the SH2 domain of ITK and regulates production of CD4$^+$ T$_h$2 cytokines.[90] Highly expressed in vascular smooth muscle cells, CypA may be excreted as an extracellular growth factor as a response to oxidative stress to mediate ERK1/2 [91] and CD147[92] activation. In addition to these roles, cyclophilins have been shown to be critical host-factors that are co-opted by viruses.[93] For example, CypA regulates multiple steps in the human immunodeficiency virus type-1 (HIV-1) life cycle and is repackaged into new virion particles during HIV replication and release. During Hepatitis C virus (HCV) infection, CypA and CypB bind the regulator protein NS5A and RNA polymerase NS5B, which are critical for HCV replication. Other cyclophilins, such as CypD, have been implicated in Alzheimer's disease through a direct interaction with Aβ.[94] The breadth of clients showcases how the PPIase active site must be shallow and malleable to accommodate a range of sequences and topologies around the central proline.

After its discovery as a crucial regulator of cell cycle progression, Pin1 has since been shown to be involved in numerous phosphorylation-dependent regulatory mechanisms. Pin1 works in tandem with 'proline-directed' kinases and phosphatases, binding and isomerizing the peptide backbone of the pS/T-P motifs to alter the prolyl *cis/trans* conformation. This is especially important in the context of pS/T-P motifs, as they have been shown to isomerize 8-fold slower than their
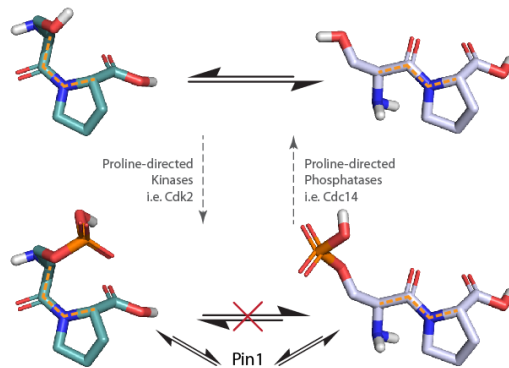
Figure 1.7) Pin1 is required for conformational switching of phosphoserine-proline. Increased steric bulk and transient backbone interactions of the phosphate group dramatically slow the rate of intrinsic isomerization, when compared to the unphosphorylated dipeptide. Pin1 selectively recognizes the negative charge adjacent to the proline and removes the isomerization bottleneck. The *cis* and *trans* conformations are illustrated as an orange dotted line.

non-phosphorylated counterparts.[95] Since proline isomerization already represents a significant bottleneck in protein folding and the conformational dynamics of proteins, phosphoprotein substrates of Pin1 require the specific isomerase activity of this chaperone to function (Figure 1.7). Pin1-mediated conformational changes act as a switch mechanism for activating transcription factors, facilitating dephosphorylation or degradation of clients, stabilizing protein-protein interactions and targeting proteins for specific subcellular localization.[96] Accordingly, Pin1 has been linked to a particularly wide-spread set of client proteins, including transcription factors, oncogenes and neurodegenerative amyloids.[97] Despite this, what determines a Pin1 "client" has been called into question.[98] Putative Pin1 binding sites have been challenging to substantiate, such as the unconventional bivalent interaction as seen with protein kinase C where both the WW and PPIase domains bind to disparate sites on the protein,[99]

or the role in controlling phosphorylated tau function for microtubule assembly and stabilization.[100]

Through the ability to control the folding or function of so many clients, PPIases have been suggested as potential drug targets for cancer, viral infection, neurodegeneration and other diseases. Indeed, Pin1 is one of the most widely over-expressed proteins in all cancers[101], including prostate, brain, breast, ovary, cervical and melanomas.[102] However, it has proven to be particularly challenging to target Pin1 with small molecules. The natural products, FK506 and rapamycin, do not effectively bind to Pin1 or inhibit its PPIase activity. As will be discussed in Chapter 4, attempts at developing synthetic inhibitors have not yet achieved good potency or selectivity.

1.9   Analysis and Prospectus

In this Chapter, I provide an introduction to the structure and function of the PPIases and their role(s) in disease. I also discussed how natural bifunctional molecules, such as FK506, have been key to discovering PPIases and understanding their roles. Moreover, I introduced how synthetic bifunctional molecules, inspired by FK506 and rapamycin, have subsequently been used in chemical biology strategies to bind two proteins simultaneously. Finally, the promise and particular challenge of Pin1 as a drug target in the PPIase superfamily was introduced. In the subsequent Chapters, I will describe my efforts to expand our knowledge of PPIases and their respective natural product inhibitors. I was

specifically interested in two emerging areas of PPIase research. In Chapter 2 and 3, I develop a new way of using synthetic, bifunctional molecules to selectively target cells that express high levels of FKBP12. Those studies both extend the use of chemical biology approaches based on FK506, while also teaching us about the possible mechanisms of the natural product. In Chapter 4, I develop a novel way to exploit the natural products to design promising new inhibitors of Pin1. Then, in Chapter 5, I conclude with an analysis of the future of PPIase research.

1.10   Notes

This chapter represents a portion of the work published in "Dunyak, B.M. & Gestwicki, J.E. Peptidyl-Proline Isomerases (PPIases): Targets for Natural Products and Natural Product-Inspired Compounds. *J. Med. Chem.* In press. (2016)."

1.11   References

1.   Fischer, G., Bang, H. & Mech, C. [Determination of enzymatic catalysis for the cis-trans-isomerization of peptide binding in proline-containing peptides]. *Biomed Biochim Acta* **43**, 1101-11 (1984).
2.   Galat, A. Peptidylprolyl cis/trans isomerases (immunophilins): biological diversity--targets--functions. *Curr Top Med Chem* **3**, 1315-47 (2003).
3.   Saibil, H. Chaperone machines for protein folding, unfolding and disaggregation. *Nat Rev Mol Cell Biol* **14**, 630-42 (2013).
4.   Theuerkorn, M., Fischer, G. & Schiene-Fischer, C. Prolyl cis/trans isomerase signalling pathways in cancer. *Curr Opin Pharmacol* **11**, 281-7 (2011).
5.   Frausto, S.D., Lee, E. & Tang, H. Cyclophilins as modulators of viral replication. *Viruses* **5**, 1684-701 (2013).
6.   Storer, C.L., Dickey, C.A., Galigniana, M.D., Rein, T. & Cox, M.B. FKBP51 and FKBP52 in signaling and disease. *Trends Endocrinol Metab* **22**, 481-90 (2011).

7. Koren, J., 3rd et al. Bending tau into shape: the emerging role of peptidyl-prolyl isomerases in tauopathies. *Mol Neurobiol* **44**, 65-70 (2011).

8. Makley, L.N. & Gestwicki, J.E. Expanding the number of 'druggable' targets: non-enzymes and protein-protein interactions. *Chem Biol Drug Des* **81**, 22-32 (2013).

9. Siekierka, J.J., Hung, S.H., Poe, M., Lin, C.S. & Sigal, N.H. A cytosolic binding protein for the immunosuppressant FK506 has peptidyl-prolyl isomerase activity but is distinct from cyclophilin. *Nature* **341**, 755-7 (1989).

10. Kim, P.S. & Baldwin, R.L. Specific intermediates in the folding reactions of small proteins and the mechanism of protein folding. *Annu Rev Biochem* **51**, 459-89 (1982).

11. Schonbrunner, E.R. et al. Catalysis of protein folding by cyclophilins from different species. *J Biol Chem* **266**, 3630-5 (1991).

12. Andreotti, A.H. Native state proline isomerization: an intrinsic molecular switch. *Biochemistry* **42**, 9515-24 (2003).

13. Zheng, H. et al. The prolyl isomerase Pin1 is a regulator of p53 in genotoxic response. *Nature* **419**, 849-53 (2002).

14. Girardini, J.E. et al. A Pin1/mutant p53 axis promotes aggressiveness in breast cancer. *Cancer Cell* **20**, 79-91 (2011).

15. He, Z., Li, L. & Luan, S. Immunophilins and parvulins. Superfamily of peptidyl prolyl isomerases in Arabidopsis. *Plant Physiol* **134**, 1248-67 (2004).

16. Somarelli, J.A., Lee, S.Y., Skolnick, J. & Herrera, R.J. Structure-based classification of 45 FK506-binding proteins. *Proteins* **72**, 197-208 (2008).

17. Fulton, K.F., Jackson, S.E. & Buckle, A.M. Energetic and structural analysis of the role of tryptophan 59 in FKBP12. *Biochemistry* **42**, 2364-72 (2003).

18. Rosen, M.K., Standaert, R.F., Galat, A., Nakatsuka, M. & Schreiber, S.L. Inhibition of FKBP rotamase activity by immunosuppressant FK506: twisted amide surrogate. *Science* **248**, 863-6 (1990).

19. Xu, G.G., Zhang, Y., Mercedes-Camacho, A.Y. & Etzkorn, F.A. A reduced-amide inhibitor of Pin1 binds in a conformation resembling a twisted-amide transition state. *Biochemistry* **50**, 9545-50 (2011).

20. Howard, B.R., Vajdos, F.F., Li, S., Sundquist, W.I. & Hill, C.P. Structural insights into the catalytic mechanism of cyclophilin A. *Nat Struct Biol* **10**, 475-81 (2003).

21. Keedy, D.A. et al. Mapping the conformational landscape of a dynamic enzyme by multitemperature and XFEL crystallography. *Elife* **4** (2015).

22. DeCenzo, M.T. et al. FK506-binding protein mutational analysis: defining the active-site residue contributions to catalysis and the stability of ligand complexes. *Protein Eng* **9**, 173-80 (1996).

23. Behrsin, C.D. et al. Functionally important residues in the peptidyl-prolyl isomerase Pin1 revealed by unigenic evolution. *J Mol Biol* **365**, 1143-62 (2007).

24. Barman, A. & Hamelberg, D. Cysteine-mediated dynamic hydrogen-bonding network in the active site of Pin1. *Biochemistry* **53**, 3839-50 (2014).

25. Carmody, M., Mackrill, J.J., Sorrentino, V. & O'Neill, C. FKBP12 associates tightly with the skeletal muscle type 1 ryanodine receptor, but not with other intracellular calcium release channels. *FEBS Lett* **505**, 97-102 (2001).

26. Lyons, W.E., Steiner, J.P., Snyder, S.H. & Dawson, T.M. Neuronal regeneration enhances the expression of the immunophilin FKBP-12. *J Neurosci* **15**, 2985-94 (1995).

27. Hoeffer, C.A. et al. Removal of FKBP12 enhances mTOR-Raptor interactions, LTP, memory, and perseverative/repetitive behavior. *Neuron* **60**, 832-45 (2008).

28. Shou, W. et al. Cardiac defects and altered ryanodine receptor function in mice lacking FKBP12. *Nature* **391**, 489-92 (1998).

29. Kozany, C., Marz, A., Kress, C. & Hausch, F. Fluorescent probes to characterise FK506-binding proteins. *Chembiochem* **10**, 1402-10 (2009).

30. Davies, T.H., Ning, Y.M. & Sanchez, E.R. A new first step in activation of steroid receptors: hormone-induced switching of FKBP51 and FKBP52 immunophilins. *J Biol Chem* **277**, 4597-600 (2002).

31. Assimon, V.A., Southworth, D.R. & Gestwicki, J.E. Specific Binding of Tetratricopeptide Repeat Proteins to Heat Shock Protein 70 (Hsp70) and Heat Shock Protein 90 (Hsp90) Is Regulated by Affinity and Phosphorylation. *Biochemistry* **54**, 7120-31 (2015).

32. Cheung-Flynn, J. et al. Physiological role for the cochaperone FKBP52 in androgen receptor signaling. *Mol Endocrinol* **19**, 1654-66 (2005).

33. LeMaster, D.M. et al. Coupling of Conformational Transitions in the N-terminal Domain of the 51-kDa FK506-binding Protein (FKBP51) Near Its Site of Interaction with the Steroid Receptor Proteins. *J Biol Chem* **290**, 15746-57 (2015).

34. Blair, L.J., Baker, J.D., Sabbagh, J.J. & Dickey, C.A. The emerging role of peptidyl-prolyl isomerase chaperones in tau oligomerization, amyloid processing, and Alzheimer's disease. *J Neurochem* **133**, 1-13 (2015).

35. Jinwal, U.K. et al. The Hsp90 cochaperone, FKBP51, increases Tau stability and polymerizes microtubules. *J Neurosci* **30**, 591-9 (2010).

36. Chambraud, B. et al. A role for FKBP52 in Tau protein function. *Proc Natl Acad Sci U S A* **107**, 2658-63 (2010).

37. Giustiniani, J. et al. The FK506-binding protein FKBP52 in vitro induces aggregation of truncated Tau forms with prion-like behavior. *FASEB J* **29**, 3171-81 (2015).

38. Giustiniani, J. et al. Immunophilin FKBP52 induces Tau-P301L filamentous assembly in vitro and modulates its activity in a model of tauopathy. *Proc Natl Acad Sci U S A* **111**, 4584-9 (2014).

39. Stocki, P. et al. Inhibition of the FKBP family of peptidyl prolyl isomerases induces abortive translocation and degradation of the cellular prion protein. *Mol Biol Cell* **27**, 757-67 (2016).

40. Edlich, F. & Lucke, C. From cell death to viral replication: the diverse functions of the membrane-associated FKBP38. *Curr Opin Pharmacol* **11**, 348-53 (2011).

41. Wang, P. & Heitman, J. The cyclophilins. *Genome Biol* **6**, 226 (2005).

42. Handschumacher, R.E., Harding, M.W., Rice, J., Drugge, R.J. & Speicher, D.W. Cyclophilin: a specific cytosolic binding protein for cyclosporin A. *Science* **226**, 544-7 (1984).

43. Fruman, D.A., Burakoff, S.J. & Bierer, B.E. Immunophilins in protein folding and immunosuppression. *FASEB J* **8**, 391-400 (1994).

44. Crompton, M. The mitochondrial permeability transition pore and its role in cell death. *Biochem J* **341 (Pt 2)**, 233-49 (1999).

45. Halestrap, A.P. & Brenner, C. The adenine nucleotide translocase: a central component of the mitochondrial permeability transition pore and key player in cell death. *Curr Med Chem* **10**, 1507-25 (2003).

46. Ward, B.K., Mark, P.J., Ingram, D.M., Minchin, R.F. & Ratajczak, T. Expression of the estrogen receptor-associated immunophilins, cyclophilin 40 and FKBP52, in breast cancer. *Breast Cancer Res Treat* **58**, 267-80 (1999).

47. Rahfeld, J.U. et al. Confirmation of the existence of a third family among peptidyl-prolyl cis/trans isomerases. Amino acid sequence and recombinant production of parvulin. *FEBS Lett* **352**, 180-4 (1994).

48. Mueller, J.W. et al. Characterization of novel elongated Parvulin isoforms that are ubiquitously expressed in human tissues and originate from alternative transcription initiation. *BMC Mol Biol* **7**, 9 (2006).

49. Surmacz, T.A., Bayer, E., Rahfeld, J.U., Fischer, G. & Bayer, P. The N-terminal basic domain of human parvulin hPar14 is responsible for the entry to the nucleus and high-affinity DNA-binding. *J Mol Biol* **321**, 235-47 (2002).

50. Fujiyama-Nakamura, S. et al. Parvulin (Par14), a peptidyl-prolyl cis-trans isomerase, is a novel rRNA processing factor that evolved in the metazoan lineage. *Mol Cell Proteomics* **8**, 1552-65 (2009).

51. Thiele, A. et al. Parvulin 17 promotes microtubule assembly by its peptidyl-prolyl cis/trans isomerase activity. *J Mol Biol* **411**, 896-909 (2011).

52. Kessler, D. et al. The DNA binding parvulin Par17 is targeted to the mitochondrial matrix by a recently evolved prepeptide uniquely present in Hominidae. *BMC biology* **5**, 1 (2007).

53. Stukenberg, P.T. & Kirschner, M.W. Pin1 acts catalytically to promote a conformational change in Cdc25. *Mol Cell* **7**, 1071-83 (2001).

54. Liou, Y.C. et al. Loss of Pin1 function in the mouse causes phenotypes resembling cyclin D1-null phenotypes. *Proc Natl Acad Sci U S A* **99**, 1335-40 (2002).

55. Liu, J. et al. Calcineurin is a common target of cyclophilin-cyclosporin A and FKBP-FK506 complexes. *Cell* **66**, 807-15 (1991).

56. Brown, E.J. et al. A mammalian protein targeted by G1-arresting rapamycin-receptor complex. *Nature* **369**, 756-8 (1994).

57.	Harding, M.W., Galat, A., Uehling, D.E. & Schreiber, S.L. A receptor for the immunosuppressant FK506 is a cis-trans peptidyl-prolyl isomerase. *Nature* **341**, 758-60 (1989).

58.	Weiwad, M. et al. Comparative analysis of calcineurin inhibition by complexes of immunosuppressive drugs with human FK506 binding proteins. *Biochemistry* **45**, 15776-84 (2006).

59.	Marz, A.M., Fabian, A.K., Kozany, C., Bracher, A. & Hausch, F. Large FK506-binding proteins shape the pharmacology of rapamycin. *Mol Cell Biol* **33**, 1357-67 (2013).

60.	Ho, S. et al. The mechanism of action of cyclosporin A and FK506. *Clin Immunol Immunopathol* **80**, S40-5 (1996).

61.	Sehgal, S.N. Rapamune (RAPA, rapamycin, sirolimus): mechanism of action immunosuppressive effect results from blockade of signal transduction and inhibition of cell cycle progression. *Clin Biochem* **31**, 335-40 (1998).

62.	Faivre, S., Kroemer, G. & Raymond, E. Current development of mTOR inhibitors as anticancer agents. *Nat Rev Drug Discov* **5**, 671-88 (2006).

63.	Yang, H. et al. mTOR kinase structure, mechanism and regulation. *Nature* **497**, 217-23 (2013).

64.	Spencer, D.M., Wandless, T.J., Schreiber, S.L. & Crabtree, G.R. Controlling signal transduction with synthetic ligands. *Science* **262**, 1019-24 (1993).

65.	Clackson, T. et al. Redesigning an FKBP-ligand interface to generate chemical dimerizers with novel specificity. *Proc Natl Acad Sci U S A* **95**, 10437-42 (1998).

66.	Sakamoto, K.M. et al. Protacs: chimeric molecules that target proteins to the Skp1-Cullin-F box complex for ubiquitination and degradation. *Proc Natl Acad Sci U S A* **98**, 8554-9 (2001).

67.	Braun, P.D. et al. A bifunctional molecule that displays context-dependent cellular activity. *J Am Chem Soc* **125**, 7575-80 (2003).

68.	Inoue, T., Heo, W.D., Grimley, J.S., Wandless, T.J. & Meyer, T. An inducible translocation strategy to rapidly activate and inhibit small GTPase signaling pathways. *Nat Methods* **2**, 415-8 (2005).

69.	Corson, T.W., Aberle, N. & Crews, C.M. Design and Applications of Bifunctional Small Molecules: Why Two Heads Are Better Than One. *ACS Chem Biol* **3**, 677-692 (2008).

70.	Thomis, D.C. et al. A Fas-based suicide switch in human T cells for the treatment of graft-versus-host disease. *Blood* **97**, 1249-57 (2001).

71.	Gray, D.C., Mahrus, S. & Wells, J.A. Activation of specific apoptotic caspases with an engineered small-molecule-activated protease. *Cell* **142**, 637-46 (2010).

72.	Banaszynski, L.A., Chen, L.C., Maynard-Smith, L.A., Ooi, A.G. & Wandless, T.J. A rapid, reversible, and tunable method to regulate protein function in living cells using synthetic small molecules. *Cell* **126**, 995-1004 (2006).

73. Grimley, J.S., Chen, D.A., Banaszynski, L.A. & Wandless, T.J. Synthesis and analysis of stabilizing ligands for FKBP-derived destabilizing domains. *Bioorg Med Chem Lett* **18**, 759-61 (2008).

74. Keenan, T. et al. Synthesis and activity of bivalent FKBP12 ligands for the regulated dimerization of proteins. *Bioorg Med Chem* **6**, 1309-35 (1998).

75. Armistead, D.M. et al. Design, synthesis and structure of non-macrocyclic inhibitors of FKBP12, the major binding protein for the immunosuppressant FK506. *Acta Crystallogr D Biol Crystallogr* **51**, 522-8 (1995).

76. Holt, D.A. et al. Design, synthesis, and kinetic evaluation of high-affinity FKBP ligands and the X-ray crystal structures of their complexes with FKBP12. *Journal of the American Chemical Society* **115**, 9925-9938 (1993).

77. DeRose, R., Miyamoto, T. & Inoue, T. Manipulating signaling at will: chemically-inducible dimerization (CID) techniques resolve problems in cell biology. *Pflugers Arch* **465**, 409-17 (2013).

78. Gestwicki, J.E., Crabtree, G.R. & Graef, I.A. Harnessing chaperones to generate small-molecule inhibitors of amyloid beta aggregation. *Science* **306**, 865-9 (2004).

79. Winter, G.E. et al. DRUG DEVELOPMENT. Phthalimide conjugation as a strategy for in vivo target protein degradation. *Science* **348**, 1376-81 (2015).

80. Romano, S. et al. FK506 binding proteins as targets in anticancer therapy. *Anticancer Agents Med Chem* **10**, 651-6 (2010).

81. Harikishore, A. & Yoon, H.S. Immunophilins: Structures, Mechanisms and Ligands. *Curr Mol Pharmacol* **9**, 37-47 (2015).

82. Yamaguchi, T., Kurisaki, A., Yamakawa, N., Minakuchi, K. & Sugino, H. FKBP12 functions as an adaptor of the Smad7-Smurf1 complex on activin type I receptor. *J Mol Endocrinol* **36**, 569-79 (2006).

83. Pratt, W.B. & Toft, D.O. Steroid receptor interactions with heat shock protein and immunophilin chaperones. *Endocr Rev* **18**, 306-60 (1997).

84. Jin, Y.J. & Burakoff, S.J. The 25-kDa FK506-binding protein is localized in the nucleus and associates with casein kinase II and nucleolin. *Proc Natl Acad Sci U S A* **90**, 7769-73 (1993).

85. Davis, E.C., Broekelmann, T.J., Ozawa, Y. & Mecham, R.P. Identification of tropoelastin as a ligand for the 65-kD FK506-binding protein, FKBP65, in the secretory pathway. *J Cell Biol* **140**, 295-303 (1998).

86. Bush, K.T., Hendrickson, B.A. & Nigam, S.K. Induction of the FK506-binding protein, FKBP13, under conditions which misfold proteins in the endoplasmic reticulum. *Biochem J* **303 (Pt 3)**, 705-8 (1994).

87. Cabral, W.A. et al. Abnormal type I collagen post-translational modification and crosslinking in a cyclophilin B KO mouse model of recessive osteogenesis imperfecta. *PLoS Genet* **10**, e1004465 (2014).

88. Harrell, J.M. et al. All of the protein interactions that link steroid receptor.hsp90.immunophilin heterocomplexes to cytoplasmic dynein are common to plant and animal cells. *Biochemistry* **41**, 5581-7 (2002).

89.   Kim, J. et al. Overexpressed cyclophilin B suppresses apoptosis associated with ROS and Ca2+ homeostasis after ER stress. *J Cell Sci* **121**, 3636-48 (2008).

90.   Colgan, J. et al. Cyclophilin A regulates TCR signal strength in CD4+ T cells via a proline-directed conformational switch in Itk. *Immunity* **21**, 189-201 (2004).

91.   Jin, Z.G. et al. Cyclophilin A is a secreted growth factor induced by oxidative stress. *Circ Res* **87**, 789-96 (2000).

92.   Yurchenko, V., Constant, S., Eisenmesser, E. & Bukrinsky, M. Cyclophilin-CD147 interactions: a new target for anti-inflammatory therapeutics. *Clin Exp Immunol* **160**, 305-17 (2010).

93.   Nigro, P., Pompilio, G. & Capogrossi, M.C. Cyclophilin A: a key player for human disease. *Cell Death Dis* **4**, e888 (2013).

94.   Du, H. et al. Cyclophilin D deficiency attenuates mitochondrial and neuronal perturbation and ameliorates learning and memory in Alzheimer's disease. *Nat Med* **14**, 1097-105 (2008).

95.   Schutkowski, M. et al. Role of phosphorylation in determining the backbone dynamics of the serine/threonine-proline motif and Pin1 substrate recognition. *Biochemistry* **37**, 5566-75 (1998).

96.   Ryo, A., Liou, Y.C., Lu, K.P. & Wulf, G. Prolyl isomerase Pin1: a catalyst for oncogenesis and a potential therapeutic target in cancer. *J Cell Sci* **116**, 773-83 (2003).

97.   Driver, J.A., Zhou, X.Z. & Lu, K.P. Pin1 dysregulation helps to explain the inverse association between cancer and Alzheimer's disease. *Biochim Biophys Acta* **1850**, 2069-76 (2015).

98.   Eichner, T., Kutter, S., Labeikovsky, W., Buosi, V. & Kern, D. Molecular Mechanism of Pin1-Tau Recognition and Catalysis. *J Mol Biol* **428**, 1760-75 (2016).

99.   Abrahamsen, H. et al. Peptidyl-prolyl isomerase Pin1 controls down-regulation of conventional protein kinase C isozymes. *J Biol Chem* **287**, 13262-78 (2012).

100.   Kutter, S., Eichner, T., Deaconescu, A.M. & Kern, D. Regulation of Microtubule Assembly by Tau and not by Pin1. *J Mol Biol* **428**, 1742-59 (2016).

101.   Ibanez, K., Boullosa, C., Tabares-Seisdedos, R., Baudot, A. & Valencia, A. Molecular evidence for the inverse comorbidity between central nervous system disorders and cancers detected by transcriptomic meta-analyses. *PLoS Genet* **10**, e1004173 (2014).

102.   Bao, L. et al. Prevalent overexpression of prolyl isomerase Pin1 in human cancers. *Am J Pathol* **164**, 1727-37 (2004).

Chapter 2

Design of naturally inspired bifunctional molecules

2.1   *Abstract*

Inspired by the natural product FK506, we designed a series of bifunctional molecules composed of an FKBP ligand and HIV protease inhibitor to explore ways of engineering cyto-selectivity. Similar to cyto-selective targeting of bi-specific antibodies that rely on co-expression of two cell-surface proteins, we demonstrate that these small molecules possess affinity for two cytoplasmic proteins. We envisioned a model in which coincident, high-level expression of both protein targets - such as in HIV-infected lymphocytes - would drive selective compound targeting and sequestration. One end of the bifunctional molecules consisted of a ligand for FKBP12, either FK506 itself or a Synthetic Ligand for FKBP (SLF), to provide either tight or weak binding, respectively. On the opposite end of the molecule, we attached the core of the FDA-approved, HIV protease inhibitor, amprenavir. We chose this starting point because the core of amprenavir has modest efficacy against HIV protease but its affinity is highly variable depending on substitution at the nearby amine. Thus, by making substitutions in this linker region, we envisioned "tuning" the affinity for HIV protease while linking each end

of the bifunctional molecule. Amino acid linkers were incorporated to readily introduce functional groups with different hydrophobicities, flexibilities, geometries and chain lengths. Using biochemical assays, we characterized our library of bifunctional molecules and demonstrated that they possess a range of affinities for both FKBP12 and HIV protease. In Chapter 3, we demonstrate their ability for cyto-selective, intracellular targeting.

2.2   Introduction

2.2.1   Cyto-selective Targeting via Bifunctional Molecules

Bi-specific antibodies differentiate between cells by exploiting the target's expression of two proteins that are not co-incident on other cells.[1] Optimization of these drugs often hinges on maximizing their avidity, while reducing interactions with bystander cells.[2] Here, we wondered whether a similar approach might be used to drive the cyto-selectivity of a small molecule. One potential advantage of this idea would be that small molecules can access intracellular proteins, expanding the choices for discriminating between cell types. To this end, we were inspired by the natural product, FK506. This molecule is naturally bi-specific; it binds FK506-binding protein (FKBP12) with one chemical "face" and calcineurin with the other. FKBP has high affinity ($K_D \sim 0.6$ nM)[3] for FK506 and this drug-protein pair recruits calcineurin into a remarkably stable, ternary complex ($K_{app} \sim 6$ to 30 nM).[3, 4] This unusual binding mode may also impart cyto-selectivity because FK506 is principally sequestered into lymphocytes and red blood cells after oral administration,[5, 6] perhaps because these cell types express relatively

high concentrations of the two target proteins. To better understand this natural mechanism and explore ways of possibly engineering bi-specific small molecules, we chose a model system based on the human immunodeficiency virus (HIV) protease.

2.2.2 HIV Protease Inhibitors have Poor Pharmacological Properties

Although they are clinically effective, HIV protease inhibitors are poorly cell penetrant and rapidly metabolized.[7] Critical for the life cycle and replication of HIV virion particles, HIV protease cleaves synthesized Gag-Pol polyprotein into newly formed mature proteins.[8] Without active protease, HIV is unable to replicate and therefore unable to infect new cells.[9] Thus, HIV protease has been a critical target for antiretroviral therapies. HIV protease is an aspartyl protease that exists as a small homodimer consisting of 99 amino acids per monomer. Effective inhibitors of this protease have typically been peptidomimetics that mimic the binding conformation of native substrates.[10] The efficacy of the HIV protease inhibitors has resulted in their integral role in Highly Active Anti-Retroviral Therapy (HAART), a cocktail therapy approach to reduce viral load. Despite their utility, use of HIV protease inhibitors is often complicated by their relatively poor ADME properties.[7] In general, the protease inhibitors are often plasma bound (~99%) and are extensively degraded by first pass metabolism; they are excellent substrates for multiple cytochrome P450 enzymes (primarily 3A4, also 2D6 and 2D9) and the P-glycoprotein efflux pump. For these reasons, maximizing sequestration and tissue distribution has been essential. Low intracellular

concentration often limits efficacy and allows for rapid accumulation of resistance-conferring mutations.[11] Numerous approaches have been attempted to increase intracellular concentration and bioavailability of these drugs, some of which include prodrug strategies, PEGylation and ritonavir co-administration to inhibit metabolic enzymes and minimize first pass metabolism.[12]

We hypothesized that an "FK506-like" molecule capable of simultaneously binding FKBP12 and HIV protease might be selectively retained in cells that express both targets. To test this idea, we synthesized bifunctional molecules composed of an FKBP12 ligand and an HIV protease inhibitor attached by a modular linker. In this collection, we systematically varied the affinity of the molecules for FKBP12 and HIV protease, creating a suite of tools that were validated biochemically. Later, we discuss these molecules and ask how bivalency correlates with cyto-selectivity.

2.3   Results

2.3.1   General Overview of Bifunctional Approach

We envisioned the synthesis of compounds **9a-f** and **10a-f** using a general strategy composed of three major components (Figure 2.1). On one end would be a ligand
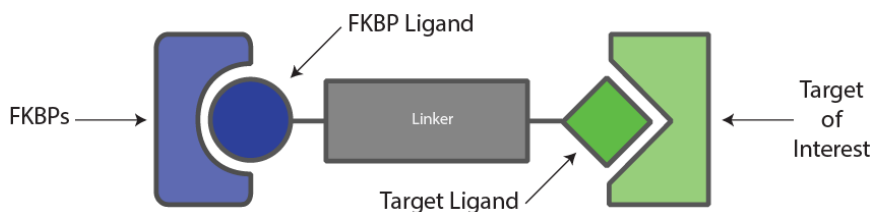

Figure 2.1) Schematic representation of bifunctional molecules. Ligands targeting FKBPs are connected to a small molecule targeting a protein of interest and connected via a short linker.

for FKBP12, either FK506 itself or SLF. On the other end is the ligand of interest, in this case an HIV protease inhibitor. Connecting the two is a short linker allowing for additional tuning of the affinity for each respective target.

For FKBP ligands, we chose to use FK506 and SLF. SLF is composed of only one half of FK506 and it is known to have a significantly weaker affinity for FKBP12.[13] Thus, using FK506 or SLF as one "end" of the molecule would be expected to provide either tight or weak binding to FKBP12, respectively. To avoid the immunosuppressive effects of using FK506, we took advantage of observations that modification of the extra-cyclic alkene destroys its affinity for calcineurin, but does not alter its tight binding to FKBP12.[14]

2.3.2 Synthesis of Bifunctional Molecules

To synthesize the FK506 building block **2**, microwave-assisted Grubbs' cross metathesis chemistry[15] was used to install 4-pentenoic acid at the terminal alkene in one step with modest yield (3hr, 80°C, 60%). Likewise, we modified SLF at the aniline with excess succinic anhydride in anhydrous DCM to produce a modified SLF (**4**) intermediate containing a terminal carboxylic acid in quantitative yield (Figure 2.2). These two compounds provided FKBP12-binding motifs for further coupling. On the opposite end of the molecule, we first assembled the 4-methoxy derivative of the core (**8**) of the FDA -approved, HIV protease inhibitor, amprenavir. We chose this starting point because the core of amprenavir has modest efficacy against HIV protease ($K_i \approx 180$ nM) but its affinity is highly tunable
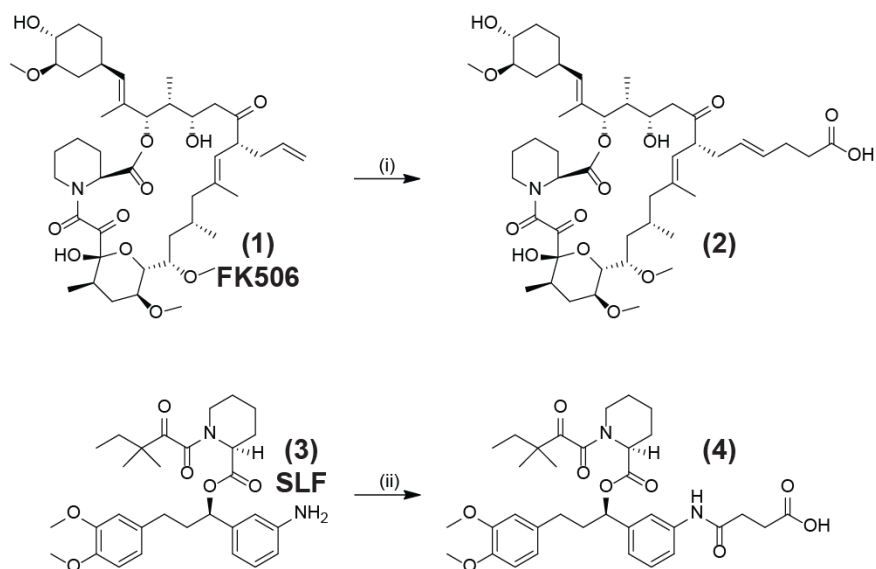
Figure 2.2) Synthesis of the FKBP-Binding Motif for Bi-Specific Library Generation (i) 4-pentenoic acid (3 eq), Grubbs 2nd Generation Catalyst (0.1eq), DCM, N_2, microwave irradiation for 3hr at 80°C. (ii) Succinic anhydride (3 eq), DIEA (1eq), DCM.

by substitution at the nearby amine.[16-18] Accordingly, the core of amprenavir

was synthesized by a known route starting from the epoxide (Figure 2.3)[19] then

functionalized at the pseudo N-terminus. Thus, by making substitutions in this

region, we envisioned "tuning" the affinity for HIV protease. Amino acids were

chosen for the linker because the side chains could be used to readily introduce

functional groups with different hydrophobicities, flexibilities, geometries and chain

lengths (Figure 2.4). Based on well-established structure-activity relationships
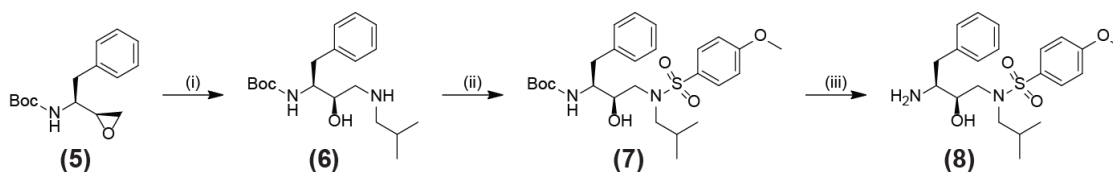

Figure 2.3) Synthesis of the Amprenavir Core (i) (2S,3S)-1,2-Epoxy-3-(Boc -amino)-4-phenylbutane (1 eq), isobutylamine (5 eq), isopropanol. (ii) 4-methoxybenzene sulfonyl chloride (1.1 eq), cesium carbonate, 1:1 DCN:water. (iii) 50% TFA /DCM.
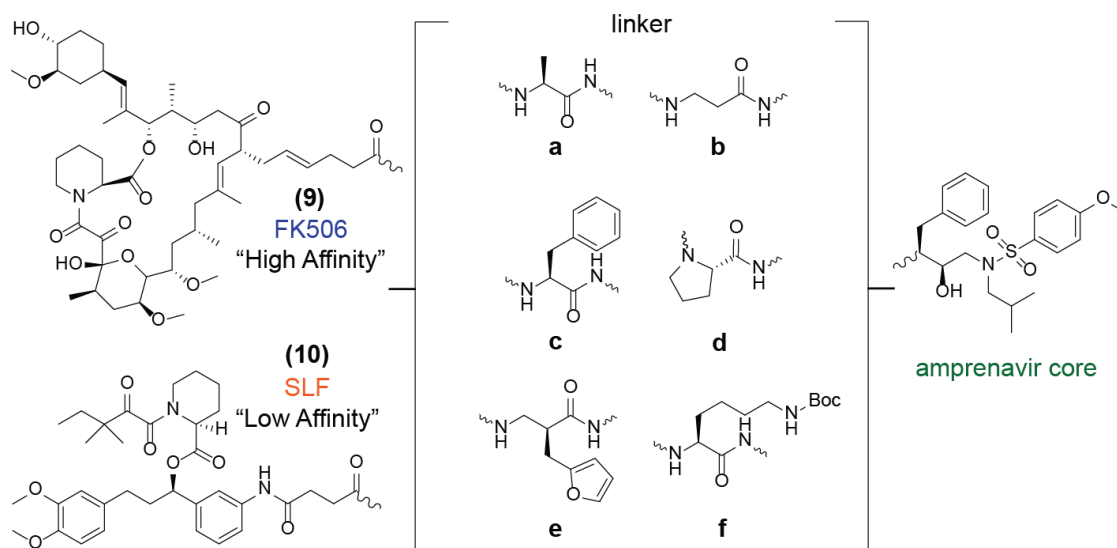
31

Figure 2.4) Focused Libary Design of Bifunctional Molecules. Modular methods were used to assemble molecules containing either FK506 (series 1) or SLF (series 2) attached to an Amprenavir core.

(SAR) for HIV protease inhibitors,[16-18] we hypothesized that small alkyl and benzyl substitutions would be tolerated, while the proline and lysine analogues might not. Finally, the modified amprenavir derivatives were coupled to the free acid of the modified FK506 or SLF motifs and the final products purified by HPLC to yield twelve bifunctional molecules (**9a-f** and **10a-f**) in 20 to 40% overall yield. As a control for later experiments, we synthesized 4-methoxy-amprenavir (herein amprenavir) that contains a tetrahydrofuranyl urethane moiety in the place of our linker (Figure 2.5). In part, we chose to use this variant of amprenavir rather than
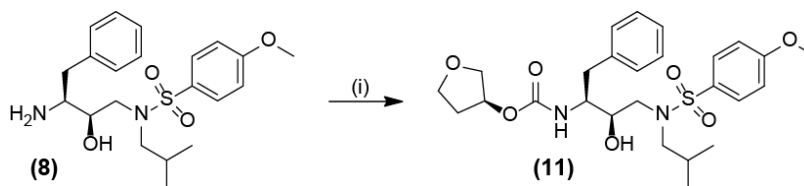

Figure 2.5) Synthesis of Amprenavir. (i) (S)-(+)3-hydroxytetrahydrofuran (1eq), disuccinimidyl carbonate(1.5eq), DIEA (2eq), DCM.

the FDA-approved compound because it has been shown to be equivalent in cell-based assays and is synthetically tractable.

2.3.4 *Biochemical Characterization of the Bifunctional Library*

With this library in-hand, we first measured the affinity of the compounds for purified FKBP12 *in vitro*. We adapted a previously reported fluorescence polarization (FP) assay based on the SLF scaffold shown in Figure 2.2. Amide coupling to 4'-(aminomethyl)-fluorescein resulted in the fluorescent tracer (**12** Figure 2.6A), which bound to FKBP12 with a K_D = 9.6 ± 1.6 nM (Figure 2.6B). To ensure the fluorescent tracer was binding to FKBP12 without significant affinity difference due to the fluorescein modification, the interaction was competed against unmodified FK506 and SLF, and calculated K_i values (5.1 ± 2.4 nM and 25 ± 14 nM, respectively) were found to be in good agreement with the literature

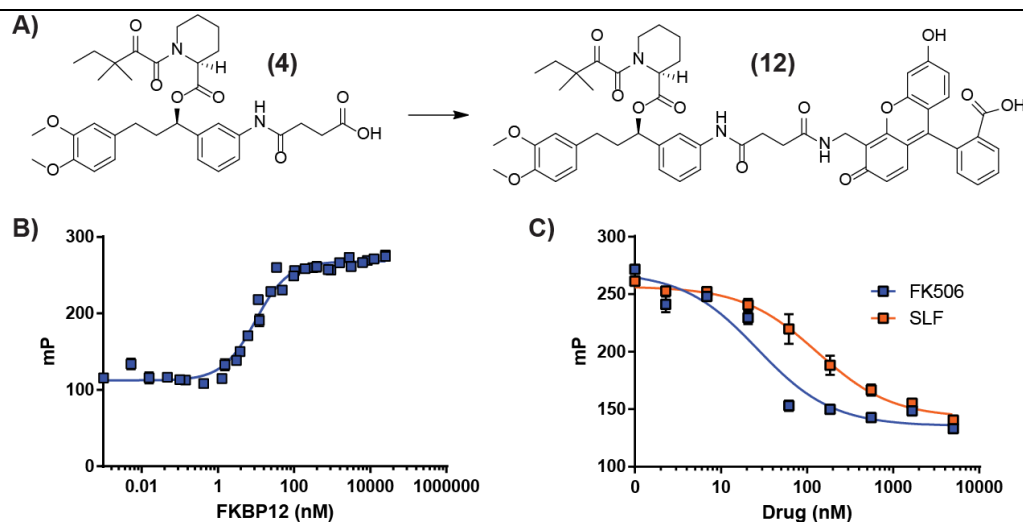Figure 2.6) Development of a Fluorescence Polarization Assay for FKBP12 Binding. A) 4'-(aminomethyl)-fluorescein (1.1 eq), HATU (1.3 eq), DIEA (3 eq), DMF. B) Fluorescent tracer binds with high affinity to FKBP12. C) FK506 and SLF compete with the fluorescent tracer for binding to FKBP12. Results are the average of at least three independent experiments performed in triplicate. Error bars are SEM.

(Figure 2.6C).[20, 21] Subsequent determination of K_i values for the library were likewise performed by competition assays in the FP platform. We found that the K_i values were principally determined by the identity of the FKBP12 ligand, either FK506 or SLF (Figure 2.7). Specifically, compounds **9a-f** had K_i values ranging between 19 and 29 nM, while **10a,b,d-f** had values ranging from 40 to 93 nM. These affinities were similar to those of unmodified FK506 or SLF (Figure 2.6C), suggesting that neither the linker nor the pendant HIV protease inhibitor dramatically impacted apparent affinity. This result might be expected because the binding site on FKBP12 is highly exposed[22, 23] and many studies on bifunctional FKBP12 ligands have shown similar modularity.[24-27] Because of non-specific tracer binding, we had to measure the affinity of **10c** for FKBP12 using a surface-plasmon resonance (SPR) platform instead of FP. FKBP12 was immobilized with traditional amide coupling and the rate of ligand association followed by dissociation was monitored across a range of concentrations. Using this approach
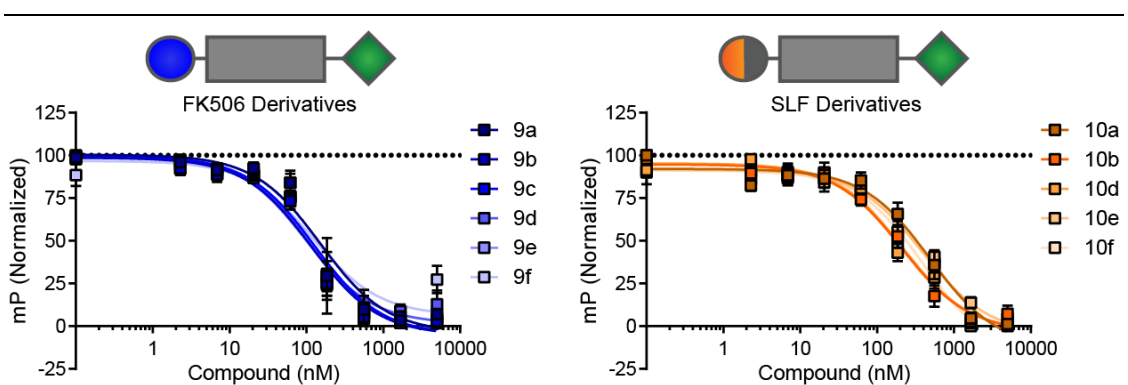

Figure 2.7) Competition for binding of an SLF tracer to human FKBP12. FK506 derivatives (blue, full circle representation) bind approximately 5-fold higher than their SLF counterparts (orange, half-circle representation). Results are the average of at least three independent experiments performed in triplicate. Error bars are SEM.

we found that **10c** had a similar affinity for FKBP12 as the other molecules in the series (K_D = 51 ± 50 nM, Figure 2.8).
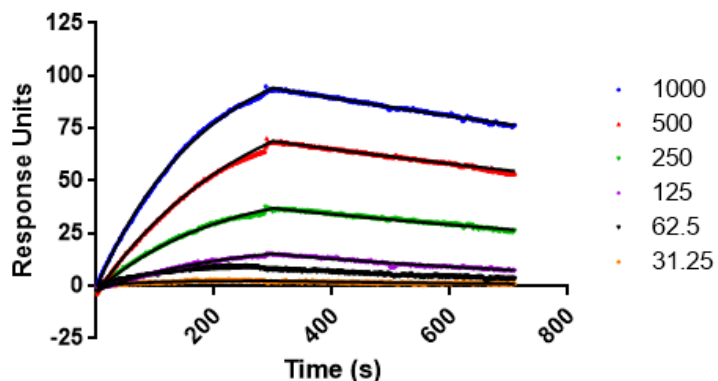

Figure 2.8) Binding of **10c** to FKBP12 Using Surface Plasmon Resonance. Compound **10c** was titrated across immobilized FKBP12 (legend in nM). Rate of association then dissociation was calculated to determine the K_D (51 ± 50 nM).

To analyze binding of the full compound collection to HIV protease, we employed a standard enzymatic cleavage assay.[28] We first tested our control amprenavir derivatives, **8** and **11**, which were incubated with HIV protease and a FRET-labelled substrate and inhibition curves generated from endpoint measurements (Figure 2.9) during the linear phase of the assay. As expected, the tetrahydrofuranyl urethane moiety provided a significant increase in potency (over 300-fold). This suggested that the linkers we chose could dramatically alter affinity for HIV protease. We then tested compounds **9a-f** and **10a-f** in the assay (Figure 2.10). Consistent with previous SAR,[16-18] we found that the identity of the linker had a substantial impact on activity. Specifically, the K_i values varied by more than two orders-of-magnitude; compound **10a** had a K_i of 1.3 ± 0.3 nM, while compound **9d** had a K_i of 170 ± 39 nM. Replacing FK506 with SLF did not seem to significantly
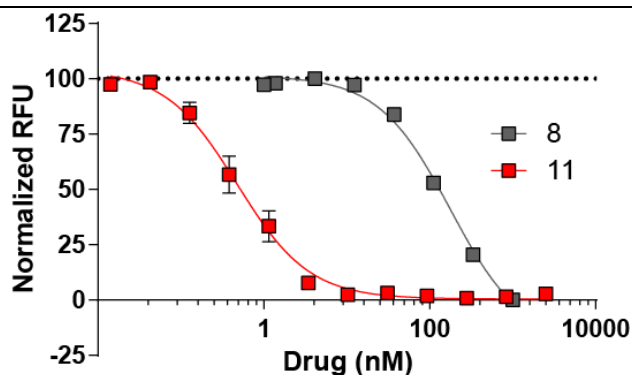
Figure 2.9) Derivatives of Amprenavir potently inhibit HIV protease in the FRET cleavage assay. The Amprenavir core **8** inhibits HIV protease with a K_i = 180±20 nM, while Amprenavir (**11**) inhibits HIV protease with a K_i = 0.48±0.06 nM. Results are the average of at least three independent experiments performed in triplicate. Error bars are SEM.

impact anti-protease activity, likely because that portion of the molecule is too far from the active site. The inhibitory activity of protease inhibitors is known to correlate with binding affinity,[29] thus, compounds **9a-f** and **10a-f** appear to provide a range of affinity values for each protein target. To further confirm the affinity range of the library for HIV protease, we again used the SPR platform as a secondary binding assay (Figure 2.11). In this case, HIV protease was immobilized
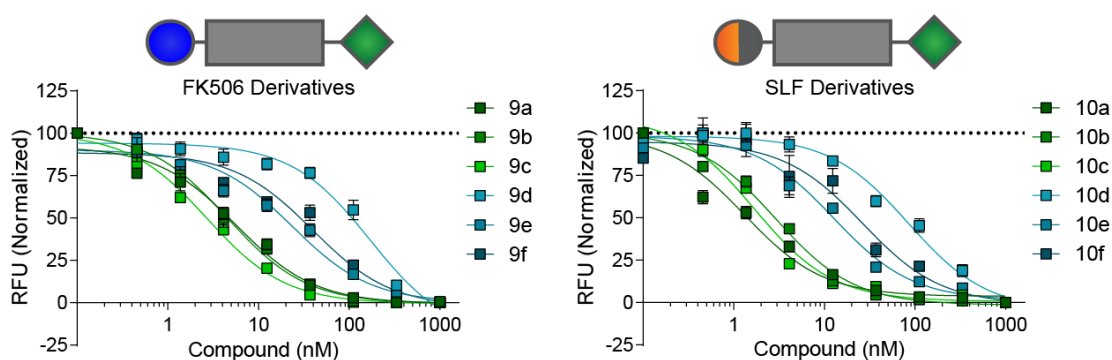

Figure 2.10) Apparent Affinity of the Library for HIV Protease. Identity of the linker of each bifunctional molecule impacts the compounds affinity for HIV protease by over 10-fold, while the FKBP ligand (FK506 – blue circle, SLF – orange half-circle) did not seem to have an effect. Results are the average of at least three independent experiments performed in triplicate. Error bars are SEM.
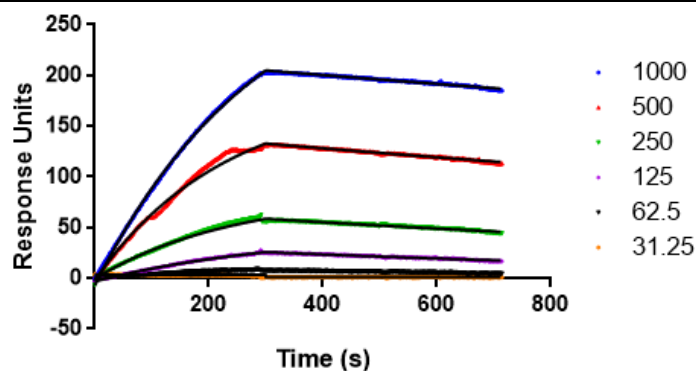
Figure 2.11) Binding of **10c** to HIV protease. Compound **10c** was titrated across immobilized HIV protease (legend in nM). Rate of association then dissociation was calculated to determine the K_D (42 ± 28 nM).

and compound **10c** was titrated across the chip surface. As expected, compound

10c bound with tight affinity to HIV protease (K_D = 42 ± 28 nM), confirming the

affinities determined in the protease cleavage assay. The affinities calculated for

each ligand for both FKBP12 and HIV protease are summarized in Table 2.1.

		a	b	c	d	e	f
				Ki Values (nM)			
FKBP12 Binding	Series 1	29 ± 9	22 ± 4	24 ± 5	19 ± 5	21 ± 5	23 ± 11
	Series 2	93 ± 24	40 ± 9	51 ± 50*	41 ± 9	75 ± 17	75 ± 28
HIVp Inhibition	Series 1	5.6 ± 1.0	4.6 ± 0.7	2.7 ± 0.3	170 ± 40	23 ± 5	40 ± 9
	Series 2	1.3 ± 0.3	2.9 ± 0.3	1.7 ± 0.2 / 42 ± 28*	84 ± 15	13 ± 2	26 ± 9

* Determined by SPR

Table 2.1) Summary of the biochemical characterization of the bifunctional library

2.3.5 Formation of a Ternary Complex Using Synthetic Bifunctional Molecules

To ensure that simultaneous binding to both FKBP and HIV protease does not

impair the ability of the ligands to effectively bind each target, FKBP12 was

introduced into the protease cleavage assay. A set of compounds from the library
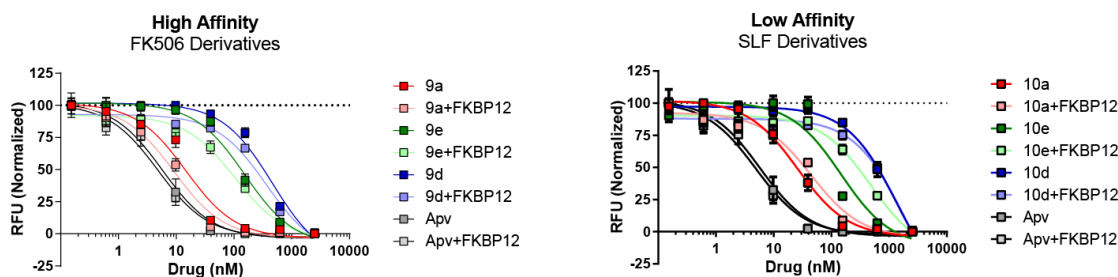
Figure 2.12) Simultaneous Binding to FKBP12 and HIV Protease does not impair anti-protease activity. Addition of FKBP12 (1µM) does not impact the apparent K_i of the library against HIV protease. Results are the average of at least two independent experiments performed in triplicate. Error bars are SEM.

was chosen to span a wide range of affinities and tested with the addition of

FKBP12 (1µM) at a concentration sufficient for binding. As expected, binding to

FKBP12 did not significantly impact the inhibitory activity of these ligands against

HIV protease (Figure 2.12). The parent HIV protease inhibitor amprenavir was also

included as a control to show that FKBP12 does not affect the assay. While the

addition of FKBP12 into the HIV protease cleavage assay provided evidence that

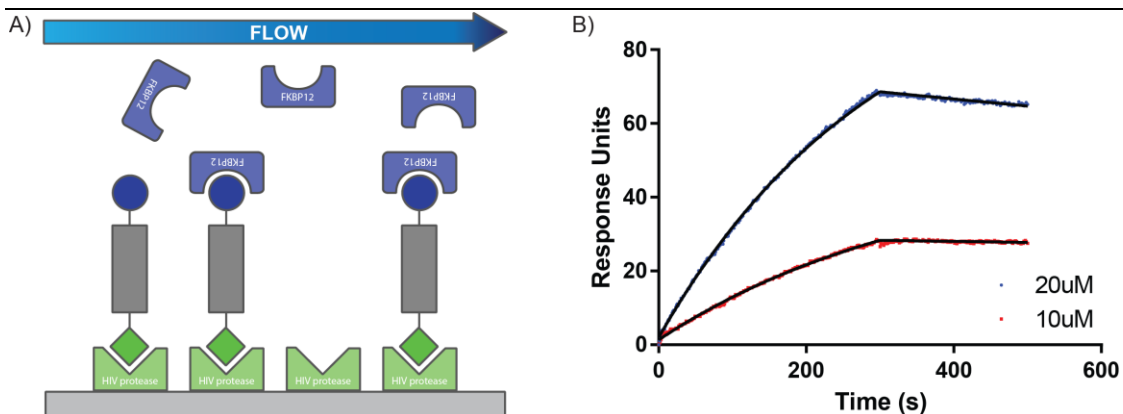these ligands could bind both protein partners without effecting their activity, we

Figure 2.13) Ternary complex formation between HIV Protease and FKBP12. A) Schematic for ternary complex formation mediated by bifunctional ligands. B) FKBP12 association and dissociation after addition of **9b** to the immobilized HIV protease surface.

38

still desired to show their ability for form a ternary complex like other CIDs. We again turned to the SPR platform, this time using the immobilized HIV protease surface, first injecting the bifunctional ligand **9b** (which possesses high affinity for both FKBP12 and HIV protease) then injecting FKBP12. Binding of **9b** to HIV protease followed by addition of FKBP12 allows for formation of the ternary complex on the chip surface. Rapid, subsequent injections are required so that HIV protease is occupied with ligand and can then bind FKBP12, before dissociation can occur. Including **9b** in the buffer instead would saturate both FKBP12 and HIV protease with ligand before the ternary complex is able to form (Figure 2.13A). Adding a combination of FKBP12 and **9b** to immobilized HIV protease showed that FKBP12 doesn't bind to HIV protease in the absence of **9b**, but that a stable ternary complex is formed in the presence of the molecule (Figure 2.13B). We also observed a significantly increased response on binding due to the large increase in apparent molecular mass from ternary complex formation as compared to ligand alone binding to protein.

2.4   *Discussion*

Inspired by FK506, we wanted to explore the design principles that might govern cyto-selectivity. Accordingly, we synthesized bifunctional inhibitors in which the affinities for two target proteins, HIV protease and FKBP12, were systematically varied. We gained control over the FKBP12 binding by using either FK506 or the weaker ligand, SLF, while affinity for HIV protease was tuned by installing linkers at a region that was known to impact binding. Using *in vitro* assays, we confirmed

that the affinities sampled a wide range, which allow us to ask how affinity correlates with cellular permeability in Chapter 3. These bifunctional ligands are additionally able to bind both FKBP12 and HIV protease, as observed in our *in vitro* assays.

We anticipate that this strategy may be beneficial in other situations in which therapeutics possess poor pharmacodynamic properties or need to be guided to a specific cell type with precision. The clear disadvantages of this approach are that the resulting molecules are large and complex, with predicted physical properties that do not correlate well with oral bioavailability.[30] Like the original inspiration, FK506, effective bi-specific molecules may require cyclization[31, 32] or further engineering to incorporate the favorable valency features into a more amenable scaffold.

2.5   Methods

2.5.1 Plasmid Generation and Protein Purification

Wild-type FKBP12 cDNA was obtained from Addgene (#20211) and cloned into the pMCSG7 vector using ligation independent cloning (Fwd: 5'-TAC TTC CAA TCC AAT GCT ATG GGA GTG CAG GTG GAA ACC ATC TCC-3', Rev: 5'-TTA TCC ACT TCC AAT GTT ATC ATT CCA GTT TTA GAA GCT CCA CAT CGA A G-3') for bacterial expression and purification. For cell-based studies, FKBP12 was cloned into the pcDNA3 mCherry ligation independent cloning vector (Fwd: 5'-TAC TTC CAA TCC AAT GCC ACC ATG GGA GTG CAG GTG GAA ACC ATC TCC-

3', Rev: 5'-CTC CCA CTA CCA ATG CCT TCC AGT TTT AGA AGC TCC ACA TCG AAG-3'). The GFP-HIV protease fusion construct was originally purchased from Addgene (#20253) and subcloned into the pcDNA5/FRT/TO vector with BamHI/XhoI restriction sites (Fwd: 5'- ATA GGA TCC ATG GTG AGC AAG GGC GAG GAG CT-3', Rev: 5'- CTT ACT CGA GTT AGG CCG CCA GTG TGA TGG A-3').

FKBP12 was transformed into E. coli BL21(DE3) cells and grown in Terrific Broth for six hours at 37 °C, followed by induction with 1 mM IPTG at 20 °C for 12 hours. Cells were collected, lysed by sonication (100 mM Tris, 100 mM NaCl, 30 mM Imidazole, pH 8.0) and 6xHis-FKBP12 was bound on Ni-NTA resin. Resin was washed once (100 mM Tris, 500 mM NaCl, 100 mM Imidazole, pH 8.0) and eluted (100 mM Tris, 500 mM NaCl, 300 mM Imidazole, pH 8.0) before subsequent TEV protease cleavage of the 6xHis-tag. Purified protein was dialyzed into 50 mM HEPES, 100 mM NaCl, pH 7.4 overnight.

HIV Protease Q7K expressed from the pET28a vector was purified from E. coli BL21(DE3) cells grown in Terrific Broth for six hours at 37 °C, followed by induction with 1 mM IPTG at 30 °C for 4 hours. Cells were collected, homogenized at 15,000 PSI in Extraction Buffer (20 mM Tris, 1 mM EDTA, 5 mM DTT, pH 7.5) and centrifuged to obtain HIV Protease as pelleted inclusion bodies. Pellet was re-suspended in Extraction Buffer + 2M Urea, centrifuged and the remaining inclusion bodies were solubilized in 1:1 Extraction Buffer:Acetic Acid (40 mL/L of initial

culture). The mixture was centrifuged to remove insoluble lipids and the supernatant was applied to SP-Sephadex resin and stirred for 30 minutes at 4 °C. Resin was washed with Buffer A (20 mM MES, 1 mM Glycine-glycine, 6 M Urea, pH 6.5), Buffer B (20 mM Tris, 1 mM Glycine-glycine, 6 M Urea, pH 9) until pH 7 and eluted with Buffer C (20 mM MES, 1 mM Glycine-glycine, 6 M Urea, 500 mM NaCl, pH 6.5). Eluted protein was bound to Ni-NTA Resin, washed with Buffer A, Buffer B and Buffer C and then eluted with Buffer D + 300 mM Imidazole. Elution was acidified with a small volume of acetic acid to pH 2 and DTT was added to 5 mM. Unfolded protein was concentrated and then refolded by rapid dilution into 10 mM formic acid, slowly adjusted to pH 7.5 with sodium acetate and NaCl was added to 1 M to precipitate inactive protease. Folded protein was dialyzed into Refolding Buffer (50 mM sodium acetate, 5 mM DTT, 10% Glycerol, 5% Ethylene Glycol, pH 5.5) overnight.

2.5.2   *FKBP12 Fluorescence Polarization Assay*

Binding to FKBP12 was measured by fluorescence polarization. The assay was performed at 60 µL final volume in PBS (Gibco) with 0.01% Triton X-100 using Corning 384-well flat-bottom black plates. For initial binding analysis of the fluorescent compound, recombinant FKBP12 was serially diluted 2-fold from 80 µM initial concentration and then 15 µL added to each well for a top concentration of 20 µM. Fluorescent ligand **6** was initially dissolved in DMSO at 100 µM then dissolved 1000-fold into assay buffer and 15 µL of this solution was added to each well to give a final concentration of 25 nM. Finally, 30 µL of assay buffer with 4%

DMSO was added to each well to give a final volume of 60 µL with 2% DMSO. The plate was covered and equilibrated at room temperature for 30 minutes then read on a SpectraMax M5 at wavelength 488/515 ex/em.

Competition experiments were performed under similar conditions. Separate solutions of FKBP12 and fluorescent ligand **6** at 100 µM were prepared and then 15 µL of both was added to each well. Under these conditions, the majority of the fluorescent ligand would be bound to FKBP12. Compounds were initially dissolved in DMSO to 250 µM, serially diluted 3-fold, then diluted to 10 µM with assay buffer and 30 µL was added to each well to a final top concentration of 5 µM and 2% DMSO. The assay was equilibrated at room temperature for 30 minutes and then read as before.

2.5.3 HIV Protease Enzymatic Cleavage Assay

The HIV protease cleavage assay was performed as previously described.[28] Protease Substrate 1, RE(edans)SQNYPIVQK(dabcyl)R, was purchased from Sigma and Corning Low Volume Round-Bottom Black plates were used. In brief, recombinant HIV protease was diluted into Buffer P (100 mM sodium acetate, 1 M NaCl, 1 mM EDTA, 1 mM DTT, 20% Glycerol, 0.1% w/v CHAPS, pH 4.7) to an initial concentration of 60 nM and 5 µL was added to each well. Compounds were 4-fold serially diluted from 1 mM in DMSO and then diluted 100-fold with assay buffer to 10 µM top concentration before 2 µL was added to each well. After compound addition, either 1 µL ddH$_2$O or PEG-400 (final concentration 0.2% v/v

43

to improve solubility) was added to each well and plates were incubated for 30 minutes at room temperature. After incubation, a fluorescent substrate solution (5 µM) was prepared in assay buffer and 12 µL was rapidly added to each well. The assay plate was immediately shaken for 5 seconds in a SpectraMax M5 plate reader and monitored at 340/490 nm with a 475 cutoff filter for 30 minutes. Inhibition curves were plotted from the final timepoint after background subtraction of the fluorescent signal at assay initiation.

2.5.4 Surface Plasmon Resonance

SPR studies were conducted on a Biacore T100 instrument using a CM5 sensor chip. The nucleotide-binding domain of Hsp72 was used as a non-binding reference protein for background subtraction. Protein immobilization was performed using standard amine-coupling strategies and approximately 1500 RU was immobilized on each channel. PBS (Gibco) with 1% DMSO was used as a running buffer at a flowrate of 50 µL/min. Compounds were 2-fold serially diluted in DMSO and diluted 1000-fold in PBS for a final DMSO concentration of 1%. Each compound concentration was injected across the chip surface in duplicate with a 5 minute association then dissociation phase. Between injections the protein surface was regenerated with two rapid 15 second injections of 20% ethanol in ddH$_2$O. Blank injections of PBS plus 1% DMSO were performed at the beginning and end of each run to ensure adequate regeneration conditions and for background correction. Data was background corrected and blank injections were subtracted before importing into GraphPad Prism 6 and fit to the nonlinear

'Association then dissociation' algorithm with a robust fit setting. Affinities were calculated as the mean K_D value of all fits across the dosing scheme and the error represented as the difference between the calculated K_D and the value of the most extreme single fit.

2.5.5 Synthetic Methods

(E)-5-[(1R,9S,12S,13R,14S,17R,21S,23S,24R,25S,27R,E)-12-[(E)-2-[(1R,3R,4R)-4-Hydroxy-3-methoxycyclohexyl]-1-methylethenyl]-1,14-dihydroxy-23,25-dimethoxy-13,19,21,27-tetramethyl-2,3,10,16-tetraoxo-11.28-dioxa-4-azatricyclo[22.3.1.0^{4,9}]octacos-18-en-17-yl]-3-pentenoic acid (2)

FK506 **(1)** was modified at the pendant alkene as previously described.[15] **(i) 1** (20 mg, 0.025 mmol, 1 eq., LC Chemicals) and 4-pentenoic acid (7.5 mg, 0.075 mmol, 3 eq., Sigma) in 0.5 mL anhydrous dichloromethane were added in a microwave vial, capped and sparged with dry N_2. A solution of Grubbs 2nd Generation Catalyst (2.1 mg, 0.0025 mmol, 0.1eq., Sigma) was prepared in 0.5 mL anhydrous dichloromethane and added under nitrogen. The mixture was placed in a microwave (Biotage) and irradiated with stirring for 3 hours at 80 °C. Afterwards, the vial was uncapped and ISOLUTE Si-Thiol was added (200mg, Biotage) to scavenge residual catalyst. The solution was filtered, solvent removed and purified by HPLC (40%-60% yield). ^{1}H NMR (400 MHz, DMSO) δ 6.98 (s, 1H), 6.57 (s, 1H) 5.63 (ddd, J = 16.8, 10.5, 5.9 Hz, 1H), 5.19 (d, J = 4.5 Hz, 1H), 5.15 – 4.85 (m, 4H), 4.69 (dd, J = 38.0, 9.9 Hz, 2H), 4.41 (s, 1H), 4.19 (b, 1H), 4.18 (d, J = 13.4 Hz, 2H), 3.83 (s, 1H), 3.63 – 3.36 (m, 3H), 3.36 – 3.12 (m, 11H), 2.88 (s,

1H), 2.18 (dt, J = 14.0, 7.5 Hz, 4H), 2.11 – 1.96 (m, 3H), 1.85 (d, J = 14.3 Hz, 2H), 1.78 – 1.44 (m, 12H), 1.45 – 1.34 (m, 2H), 1.31 – 1.07 (m, 9H), 0.91 – 0.63 (m, 12H). Expected MW: 875.5, Found M+Na$^+$: 898.67.

4-((3-((R)-3-(3,4-dimethoxyphenyl)-1-(((S)-1-(3,3-dimethyl-2-oxopentanoyl)piperidine-2-carbonyl)oxy)propyl)phenyl)amino)-4-oxobutanoic acid (4)

To a solution of SLF **(3)** (50 mg, 0.095 mmol, 1eq., Cayman Chemical) in dichloromethane, succinic anhydride (28.6 mg, 0.285 mmol, 3 eq., Sigma) and DIEA (12.3 mg, 0.095 mmol, 1 eq., Sigma) were added and stirred overnight. After reaction, solvents were removed and purified by HPLC (48mg, 96% yield). ^{1}H NMR (400 MHz, DMSO) δ 12.16 (s, 1H), 10.07 (d, 1H), 7.80 – 7.01 (m, 4H), 6.89 (dd, J = 8.3, 1.3 Hz, 1H), 6.84 – 6.78 (m, 1H), 6.72 (dd, J = 8.1, 2.0 Hz, 1H), 5.67 (dd, J = 8.7, 5.0 Hz, 1H), 5.19 (dd, J = 13.1, 5.5 Hz, 1H), 3.76 (s, 3H), 3.75 (s, 3H), 3.62 (s, 1H), 3.3 (s, 1H), 3.27 – 3.08 (m, 1H), 2.67 – 2.56 (m, 4H), 2.25 (d, J = 13.8 Hz, 1H), 2.12 (d, J = 51.0 Hz, 2H), 1.79 – 1.56 (m, 5H), 1.44 – 1.29 (m, 1H), 1.26 (d, J = 13.0 Hz, 1H), 1.21 (s, 3H), 1.17 (s, 3H), 1.08 (dd, J = 7.3, 4.8 Hz, 1H), 0.84 (td, J = 7.5, 1.0 Hz, 3H). Expected MW: 624.30, Found M+H$^+$: 625.41.

N-((2R,3S)-3-amino-2-hydroxy-4-phenylbutyl)-N-isobutyl-4-methoxybenzenesulfonamide (8)

The core of amprenavir was purified as previously described.[19] **(i)** (2S,3S)-1,2-Epoxy-3-(Boc-amino)-4-phenylbutane **(5)** (1 g, 3.8 mmol, 1 eq.,

Sigma) was dissolved in isopropanol followed by dropwise addition of isobutylamine (1.39 g, 19 mmol, 5 eq., Sigma) and stirred overnight. Isopropanol was removed and the crude mixture was brought up in dichloromethane, washed with ddH$_2$O and brine, dried over Na$_2$SO$_4$ and the solvent evaporated. Crude product was recrystallized in 1:1 Ethyl Acetate:Hexanes as a white solid **(6)** (930 mg, 72.7%). **(ii)** Without further purification, **(6)** was dissolved in 1:1 dichloromethane:water, chilled on ice and cesium carbonate was added. 4-methoxybenzene sulfonyl chloride (627 mg, 3.03 mmol, 1.1 eq, Sigma) was dissolved in 5 mL dichloromethane and added dropwise over 1 hour and the reaction was stirred until completion as monitored by TLC. After reaction, the product was extracted with a large volume of dichloromethane and purified by column chromatography (25:75 EtOAc:Hexanes) as a white, waxy solid **(7)** (1259 mg, 90%). **(iii)** The final amprenavir core **(8)** was deprotected in 50% TFA/DCM, monitored until completion by TLC and solvents were removed under vacuum to afford a yellow oily solid (quantitative yield). ^{1}H NMR (400 MHz, DMSO) δ 7.85 (d, J = 5.4 Hz, 3H), 7.73 – 7.65 (m, 2H), 7.39 – 7.24 (m, 5H), 7.28 – 7.03 (m, 3H), 5.61 (s, 1H), 3.97 (s, 1H), 3.83 (s, 3H), 3.32 (dd, J = 14.7, 5.6 Hz, 1H), 3.02 (dd, J = 14.3, 5.4 Hz, 1H), 2.90 (dd, J = 13.7, 8.6 Hz, 1H), 2.84 – 2.61 (m, 3H), 1.86 (tt, J = 12.9, 6.7 Hz, 1H), 0.80 (d, J = 6.5 Hz, 3H), 0.74 (d, J = 6.6 Hz, 3H).

*General synthetic scheme for bifunctional compounds **(9a-f, 10a-f)***

A routine amine-coupling strategy was employed in all cases to synthesize diverse linkers to the amprenavir core. Boc- or Fmoc-protected amino acids

(0.246mmol, 1eq.) were dissolved in anhydrous DMF, followed by addition of HATU (103mg, 0.27mmol, 1.1eq.) and DIEA (38.1mg, 0.29mmol, 1.2eq.) under nitrogen. The mixture was allowed to stir for 30 minutes, after which time a solution of **(8)** (100mg, 0.246mmol, 1eq.) was added dropwise and allowed to stir overnight. After reaction, the crude product was brought up in dichloromethane, washed once with ddH$_2$O and once with brine, dried with Na$_2$SO$_4$ and solvents were removed. The Boc or Fmoc protecting groups were removed with 50% TFA/DCM or 30% 4-methylpiperdine/DMF, respectively. After deprotection, solvents were removed and each amino acid-amprenavir derivative was purified by HPLC. (Yield 50-80%)

To a solution of **2** or **4** in anhydrous DMF (0.011mmol, 1eq.) was added HATU (5mg, 0.013mmol, 1.3eq.) and DIEA (3.7mg, 0.029mmol, 2.5eq.) under nitrogen and stirred for 30 minutes. A solution of amino acid-amprenavir derivative (0.011mmol, 1eq.) was added dropwise and stirred overnight in nitrogen atmosphere. The reaction was brought up in dichloromethane, washed once with brine and purified by HPLC to afford the final bifunctional molecules in modest yield (30-50%). After pooling fractions, purified compounds were run again by HPLC to ensure purity, which was conservatively estimated as peak area to baseline with should omitted.

(S)-tetrahydrofuran-3-yl-((2S,3R)-3-hydroxy-4-((N-isobutyl-4-methoxyphenyl)sulfonamido)-1-phenylbutan-2-yl)carbamate **(11)**

A solution of (S)-(+)3-hydroxytetrahydrofuran (100mg, 1.13mmol, 1eq) was prepared in dichloromethane followed by addition of disuccinimidyl carbonate

(436mg, 1.70mmol, 1.5eq.) and DIEA (292mg, 2.26mmol, 2 eq.) and stirred until completion by TLC. To this solution of mixed carbonate, amprenavir core (**5**; 0.5eq) was added and the reaction was stirred overnight. Solvent was removed and the product was purified twice by HPLC. Expected MW: 520.22, Found M+H^{+}: 521.16.

2-(4-((4-((3-((R)-3-(3,4-dimethoxyphenyl)-1-(((S)-1-(3,3-dimethyl-2-oxopentanoyl)piperidine-2-carbonyl)oxy)propyl)phenyl)amino)-4-oxobutanamido)methyl)-6-hydroxy-3-oxo-3H-xanthen-9-yl)benzoic acid **(12)**

To a solution of **2** (6.2 mg, 0.010 mmol, 1eq.) was added HATU (4.7 mg, 0.013 mmol, 1.3 eq.) and DIEA (3.9 mg, 0.030 mmol, 3eq.) in anhydrous DMF. The mixture was stirred for 30 minutes and a solution of 4'-(aminomethyl)-fluorescein (4.4 mg, 0.011mmol, 1.1eq.) was added dropwise. The crude product was purified by HPLC (4.5 mg, 46% yield). Expected MW: 967.39, Found M+H^{+}: 968.61.

2.6 Notes

This chapter represents a portion of the work published in "Dunyak, B.M., Nakamura, R.L., Frankel, A.D. & Gestwicki, J.E. Selective Targeting of Cells via Bispecific Molecules That Exploit Coexpression of Two Intracellular Proteins. *ACS Chem Biol* **10**, 2441-7 (2015)." Bryan M. Dunyak and Jason E. Gestwicki designed the experiments and synthetic schemes. Bryan M. Dunyak performed the experiments.

2.7 Appendix

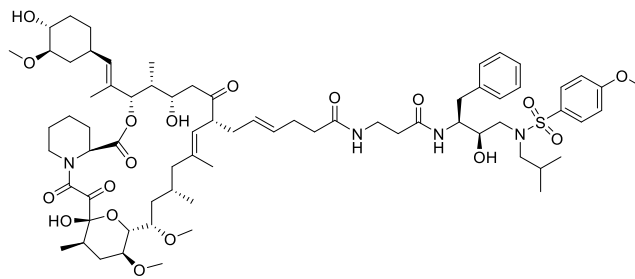Full molecular structure and characterization of bifunctional compounds used in Chapters 2 and 3.
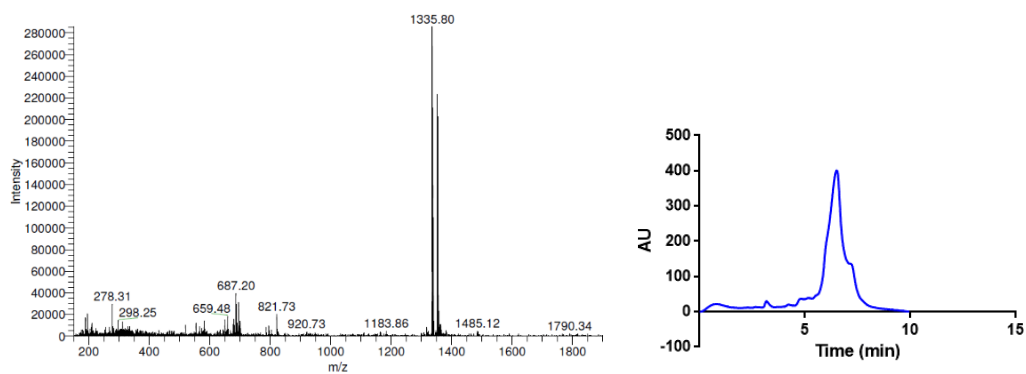
Compound 9a:
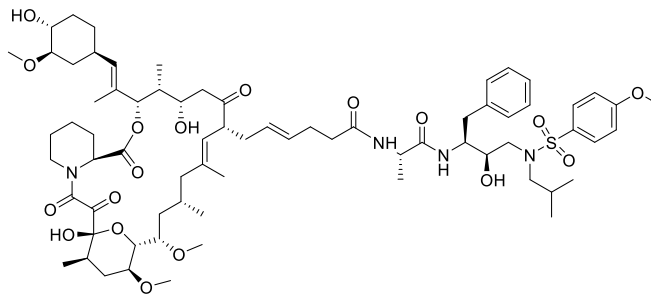
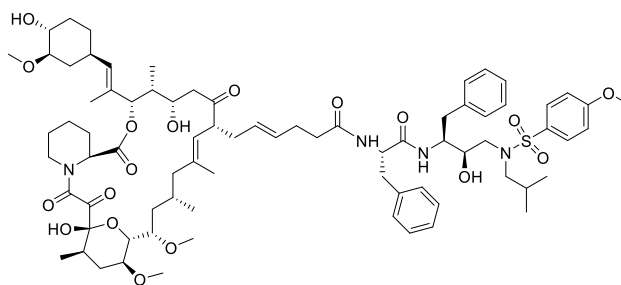Expected MW: 1334.72, Found M+H$^+$: 1335.90. Minimum purity 97.5%.
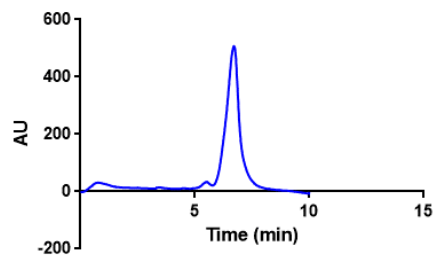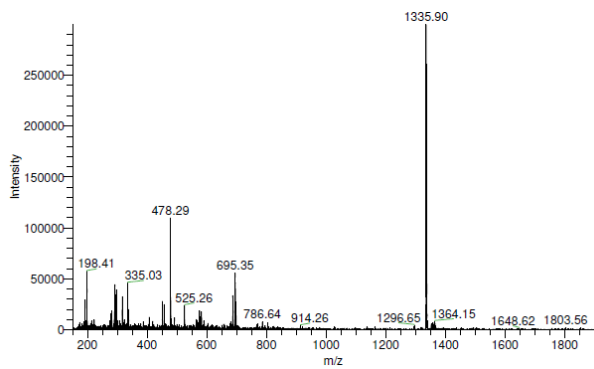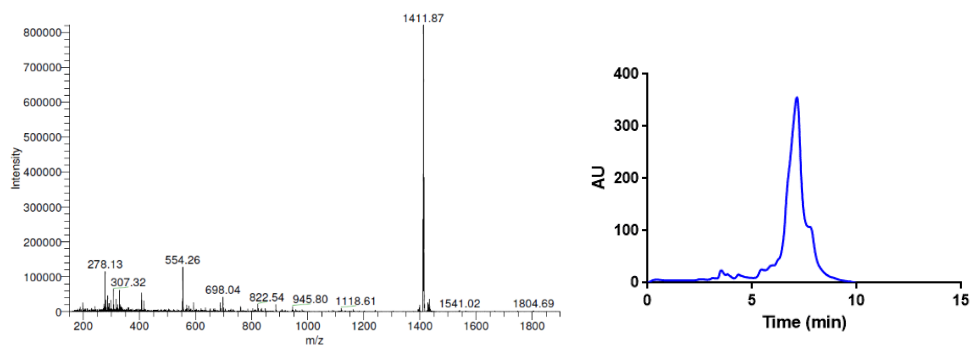
*Compound **9b**:*

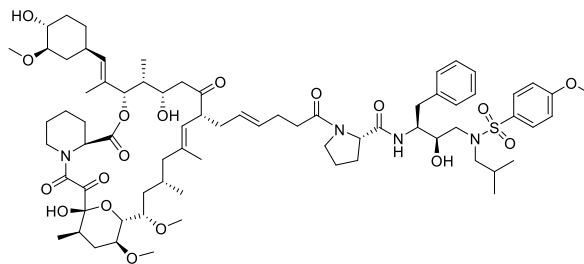Expected MW: 1334.72, Found M+H$^+$: 1335.80. Minimum purity 85.5%.
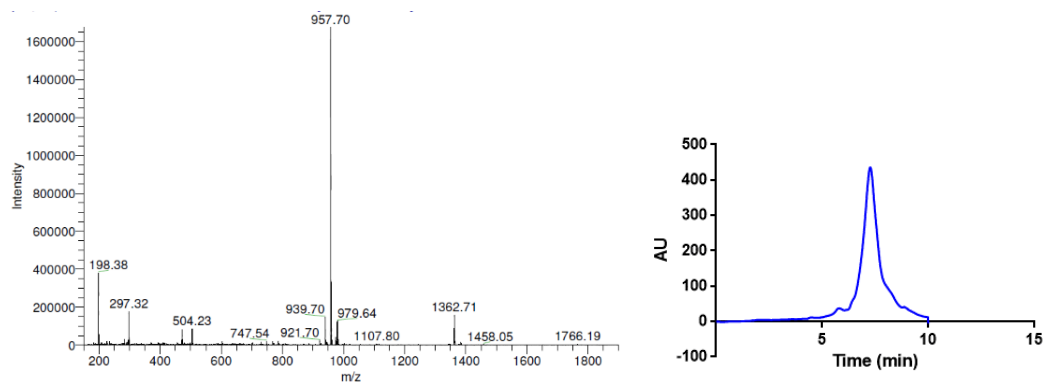

*Compound **9c**:*

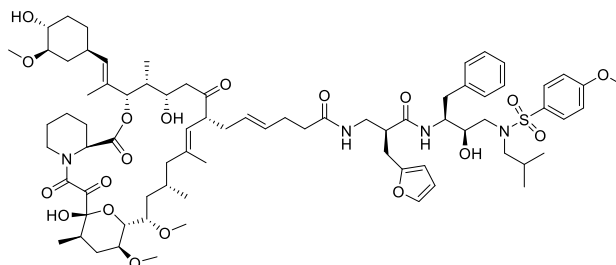Expected MW: 1410.75, Found M+H$^+$: 1411.87. Minimum purity 85.6%.
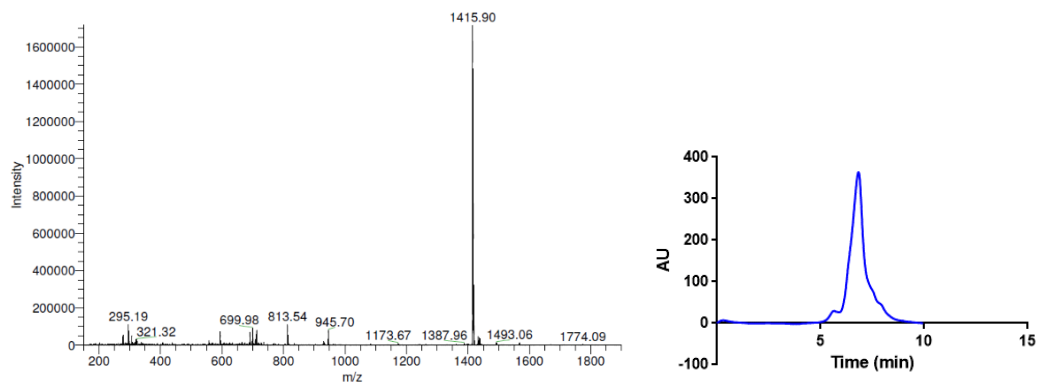
*Compound **9d***:

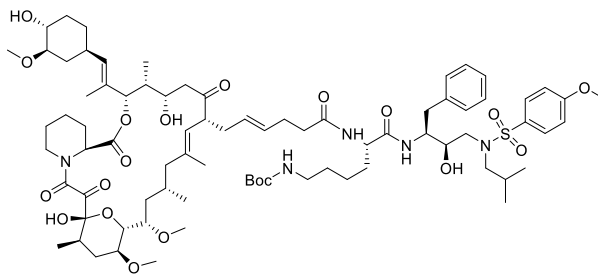Expected MW: 1360.74, Found M+2H$^+$: 1362.71. Minimum purity 91.5%.
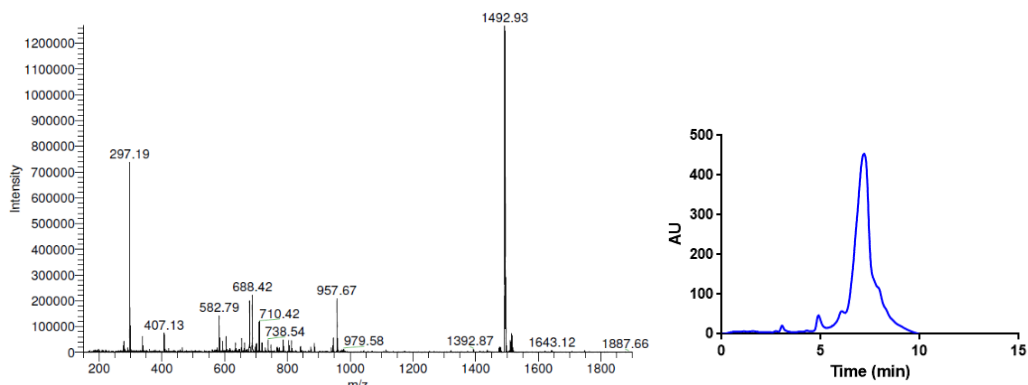

*Compound **9e***:

Expected MW: 1414.75, Found M+H$^+$: 1415.90. Minimum purity 92.3 %.
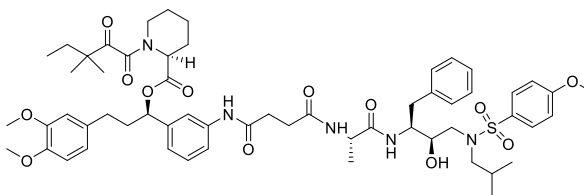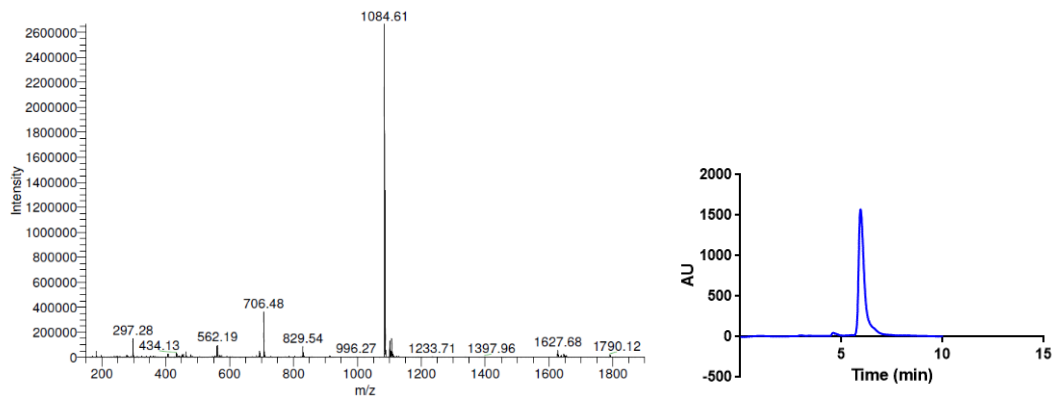
*Compound **9f**:*

Expected MW: 1491.83, Found M+H$^+$: 1492.93. Minimum purity 95.1%.

*Compound **10a**:*

Expected MW: 1083.52, Found M+H$^+$: 1084.61. Minimum purity 95.5%.
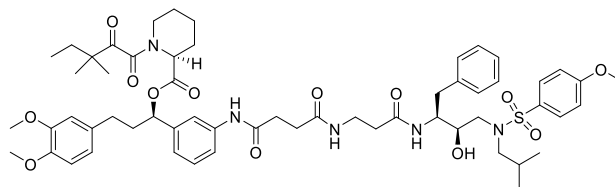
*Compound **10b**:*

Expected MW: 1083.52, Found M+H⁺: 1084.64. Minimum purity 94.6%.
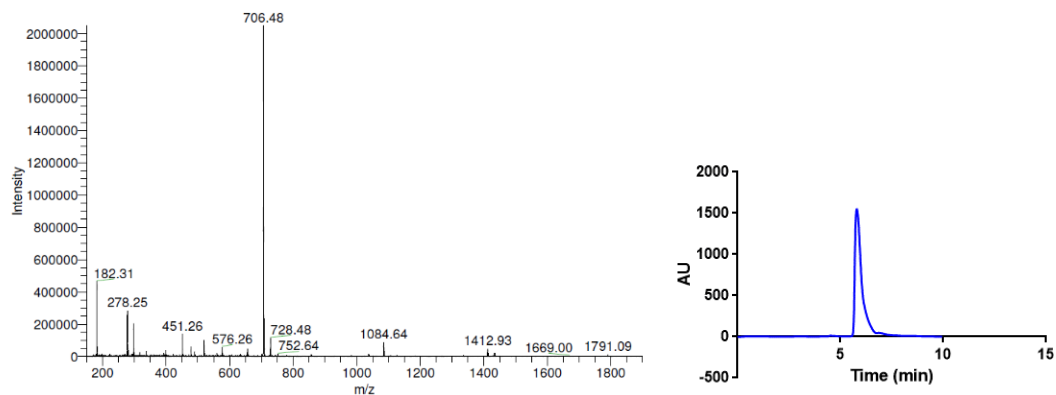
*Compound **10c**:*
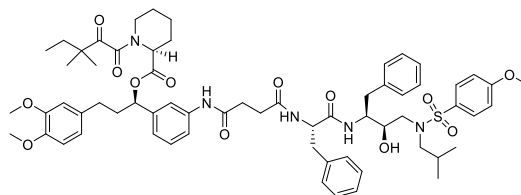
Expected MW: 1159.56, Found M+H⁺: 1160.64. Minimum purity 89.1%.
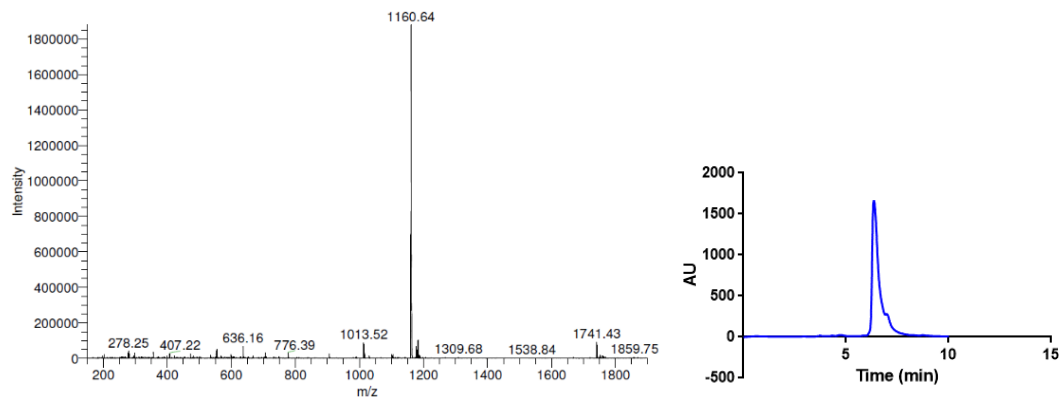
*Compound **10d***:
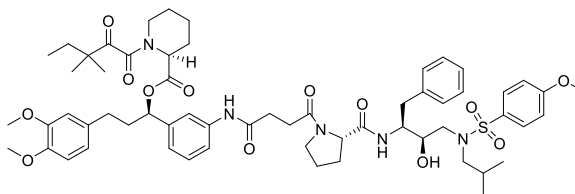
Expected MW: 1109.54, Found M+H$^+$: 1110.64. Minimum purity 98.0%.
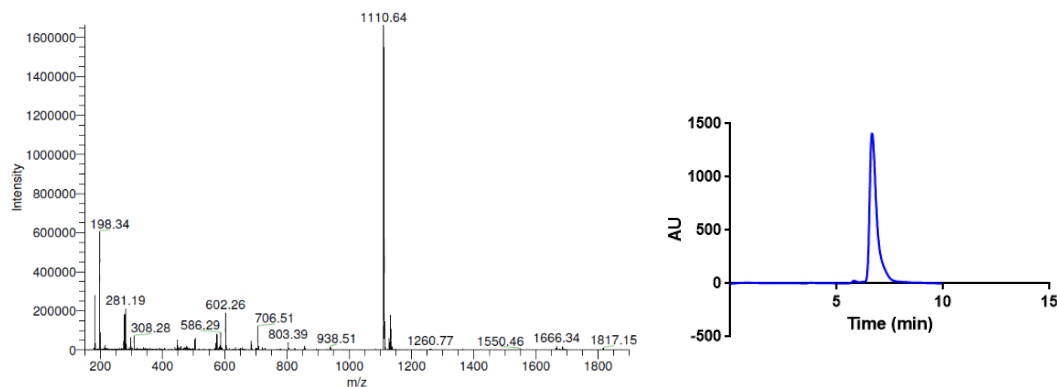
*Compound **10e***:

Expected MW: 1163.55, Found M+H$^+$: 1164.64. Minimum purity 83.0%.
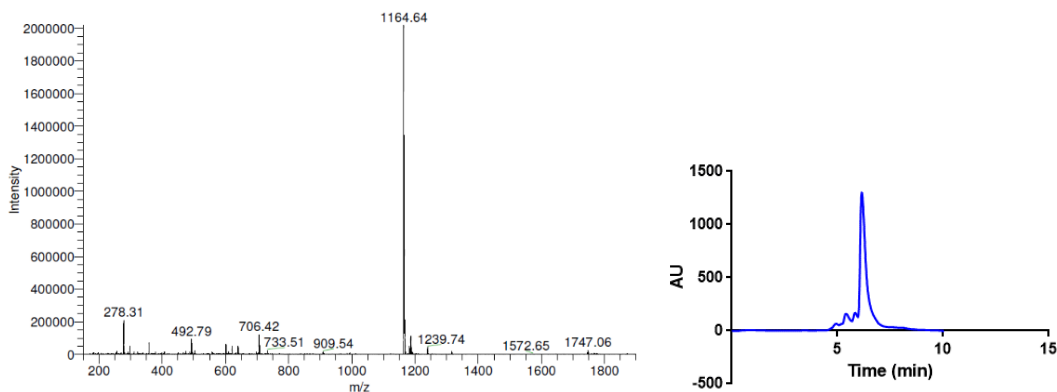
*Compound **10e**:*
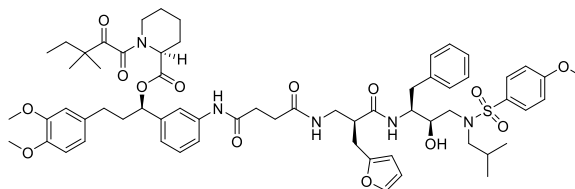
Expected MW: 1163.55, Found M+H$^+$: 1164.64. Minimum purity 83.0%.
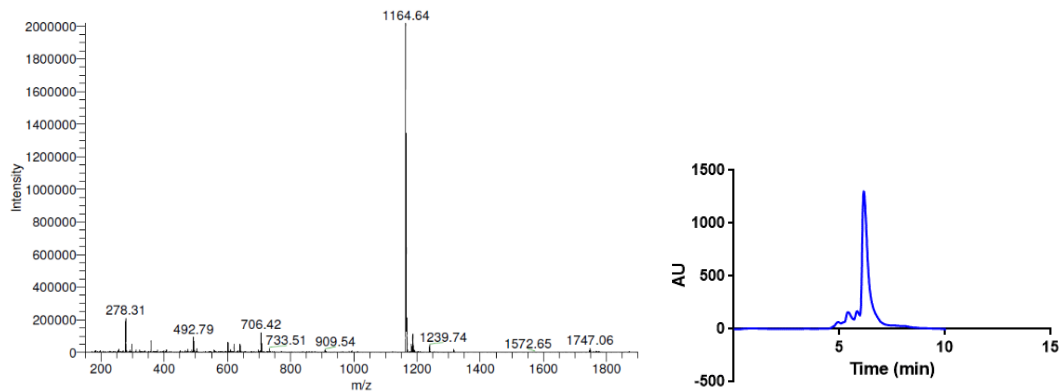
*Compound **10f**:*
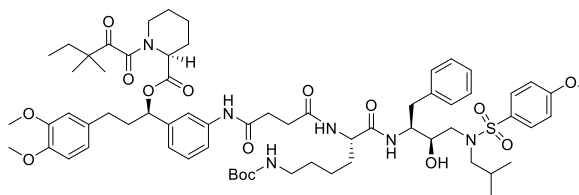
Expected MW: 1240.63, Found M+H$^+$: 1241.71. Minimum purity 87.0%.
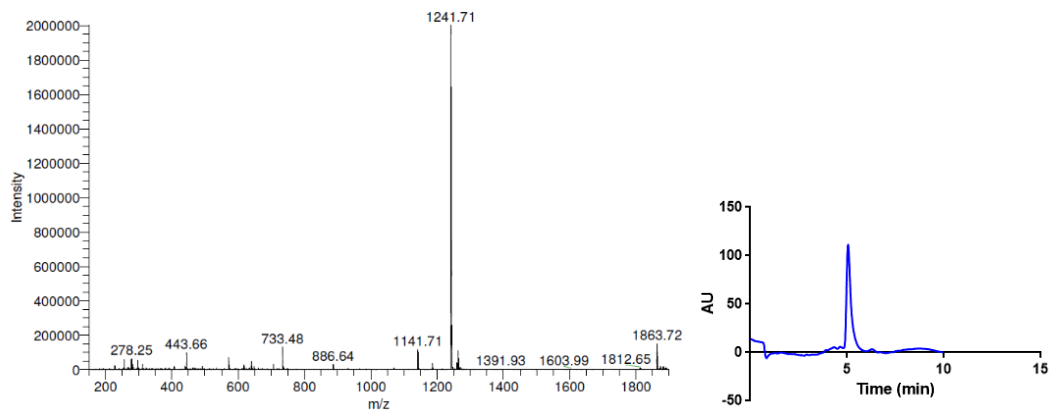
*Compound **10f***:

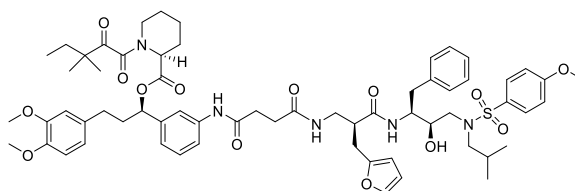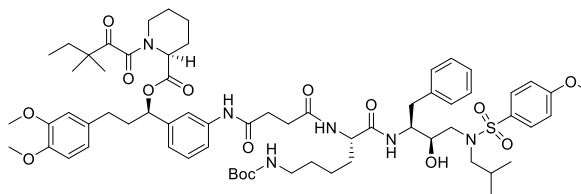Expected MW: 1240.63, Found M+H$^+$: 1241.71. Minimum purity 87.0%.
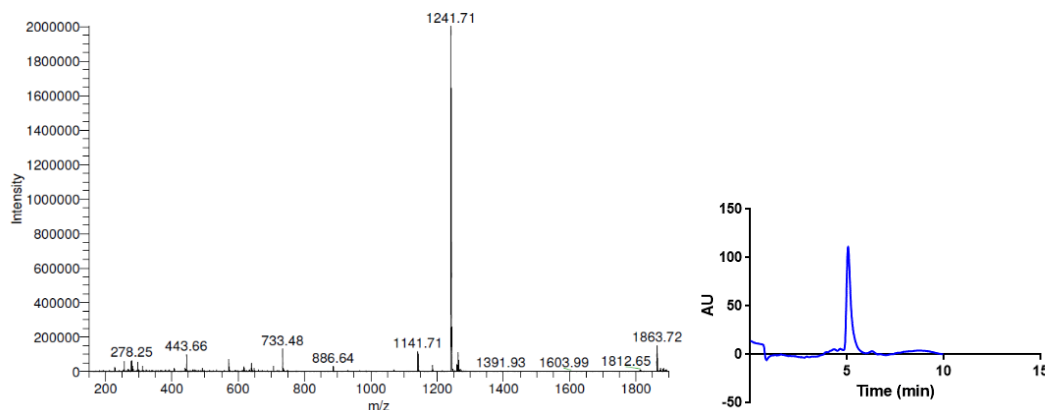
2.8   References

1.   Byrne, H., Conroy, P.J., Whisstock, J.C. & O'Kennedy, R.J. A tale of two specificities: bispecific antibodies for therapeutic and diagnostic applications. Trends Biotechnol 31, 621-32 (2013).
2.   Fitzgerald, J. & Lugovskoy, A. Rational engineering of antibody therapeutics targeting multiple oncogene pathways. MAbs 3, 299-309 (2011).
3.   Aldape, R.A. et al. Charged surface residues of FKBP12 participate in formation of the FKBP12-FK506-calcineurin complex. J Biol Chem 267, 16029-32 (1992).
4.   Liu, J. et al. Inhibition of T cell signaling by immunophilin-ligand complexes correlates with loss of calcineurin phosphatase activity. Biochemistry 31, 3896-901 (1992).
5.   Su, A.I. et al. A gene atlas of the mouse and human protein-encoding transcriptomes. Proc Natl Acad Sci U S A 101, 6062-7 (2004).
6.   Marinec, P.S. et al. FK506-binding protein (FKBP) partitions a modified HIV protease inhibitor into blood cells and prolongs its lifetime in vivo. Proc Natl Acad Sci U S A 106, 1336-41 (2009).

7.   Hoggard, P.G. & Owen, A. The mechanisms that control intracellular penetration of the HIV protease inhibitors. Journal of Antimicrobial Chemotherapy 51, 493-496 (2003).

8.   Freed, E.O. HIV-1 gag proteins: diverse functions in the virus life cycle. Virology 251, 1-15 (1998).

9.   Sundquist, W.I. & Krausslich, H.G. HIV-1 assembly, budding, and maturation. Cold Spring Harb Perspect Med 2, a006924 (2012).

10. Ghosh, A.K., Osswald, H.L. & Prato, G. Recent Progress in the Development of HIV-1 Protease Inhibitors for the Treatment of HIV/AIDS. J Med Chem 59, 5172-208 (2016).

11. Spaltenstein, A., Kazmierski, W.M., Miller, J.F. & Samano, V. Discovery of next generation inhibitors of HIV protease. Curr Top Med Chem 5, 1589-607 (2005).

12. Palombo, M.S., Singh, Y. & Sinko, P.J. Prodrug and conjugate drug delivery strategies for improving HIV/AIDS therapy. J Drug Deliv Sci Technol 19, 3-14 (2009).

13. Holt, D.A. et al. Design, synthesis, and kinetic evaluation of high-affinity FKBP ligands and the X-ray crystal structures of their complexes with FKBP12. Journal of the American Chemical Society 115, 9925-9938 (1993).

14. Clemons, P.A. et al. Synthesis of calcineurin-resistant derivatives of FK506 and selection of compensatory receptors. Chem Biol 9, 49-61 (2002).

15. Marinec, P.S. et al. Synthesis of orthogonally reactive FK506 derivatives via olefin cross metathesis. Bioorg Med Chem 17, 5763-8 (2009).

16. Freskos, J.N. et al. (Hydroxyethyl) sulfonamide HIV-1 Protease inhibitors: Identification of the 2-methylbenzoyl moiety at P-2. Bioorganic & Medicinal Chemistry Letters 6, 445-450 (1996).

17. Cheng, T.J., Brik, A., Wong, C.H. & Kan, C.C. Model system for high-throughput screening of novel human immunodeficiency virus protease inhibitors in Escherichia coli. Antimicrob Agents Chemother 48, 2437-47 (2004).

18. Ghosh, A.K. et al. Structure-based design of non-peptide HIV protease inhibitors. Farmaco 56, 29-32 (2001).

19. Ali, A. et al. Discovery of HIV-1 protease inhibitors with picomolar affinities incorporating N-aryl-oxazolidinone-5-carboxamides as novel P2 ligands. J Med Chem 49, 7342-56 (2006).

20. Nikolovska-Coleska, Z. et al. Development and optimization of a binding assay for the XIAP BIR3 domain using fluorescence polarization. Anal Biochem 332, 261-73 (2004).

21. Kozany, C., Marz, A., Kress, C. & Hausch, F. Fluorescent probes to characterise FK506-binding proteins. Chembiochem 10, 1402-10 (2009).

22. Clackson, T. et al. Redesigning an FKBP-ligand interface to generate chemical dimerizers with novel specificity. Proc Natl Acad Sci U S A 95, 10437-42 (1998).

23. Van Duyne, G.D., Standaert, R.F., Karplus, P.A., Schreiber, S.L. & Clardy, J. Atomic structure of FKBP-FK506, an immunophilin-immunosuppressant complex. Science 252, 839-42 (1991).

24. Inoue, T., Heo, W.D., Grimley, J.S., Wandless, T.J. & Meyer, T. An inducible translocation strategy to rapidly activate and inhibit small GTPase signaling pathways. Nat Methods 2, 415-8 (2005).

25. Keenan, T. et al. Synthesis and activity of bivalent FKBP12 ligands for the regulated dimerization of proteins. Bioorg Med Chem 6, 1309-35 (1998).

26. Spencer, D.M., Wandless, T.J., Schreiber, S.L. & Crabtree, G.R. Controlling signal transduction with synthetic ligands. Science 262, 1019-24 (1993).

27. Spencer, D.M., Graef, I., Austin, D.J., Schreiber, S.L. & Crabtree, G.R. A general strategy for producing conditional alleles of Src-like tyrosine kinases. Proc Natl Acad Sci U S A 92, 9805-9 (1995).

28. Ung, P.M., Dunbar, J.B., Jr., Gestwicki, J.E. & Carlson, H.A. An allosteric modulator of HIV-1 protease shows equipotent inhibition of wild-type and drug-resistant proteases. J Med Chem 57, 6468-78 (2014).

29. Matayoshi, E.D., Wang, G.T., Krafft, G.A. & Erickson, J. Novel fluorogenic substrates for assaying retroviral proteases by resonance energy transfer. Science 247, 954-8 (1990).

30. Lipinski, C.A., Lombardo, F., Dominy, B.W. & Feeney, P.J. Experimental and computational approaches to estimate solubility and permeability in drug discovery and development settings. Adv Drug Deliv Rev 46, 3-26 (2001).

31. Rezai, T., Yu, B., Millhauser, G.L., Jacobson, M.P. & Lokey, R.S. Testing the conformational hypothesis of passive membrane permeability using synthetic cyclic peptide diastereomers. J Am Chem Soc 128, 2510-1 (2006).

32. Hewitt, W.M. et al. Cell-permeable cyclic peptides from synthetic libraries inspired by natural products. J Am Chem Soc 137, 715-21 (2015).

Chapter 3

Selective Targeting of Cells that Exploit Coexpression of Two

Intracellular Proteins

3.1   *Abstract*

In Chapter 2, I developed a small library of bifunctional molecules composed of an FKBP ligand and HIV protease inhibitor. These molecules were designed to provide a way of systematically varying the affinity for both protein targets. Next, we characterized our library *in vitro* to show that, as designed, these bifunctional molecules bind both FKBP12 and HIV protease with a range of affinities. In this Chapter, we explore whether bifunctional molecules might be capable of cyto-selective targeting. Each of the compounds retained passive membrane diffusion and the best molecules inhibited FKBP12 and HIV protease activity in cells. Most excitingly, the molecules with tight affinity for FKBP12 and HIV protease were selectively taken up into cells that express both proteins. Treatment with competitive FKBP12 inhibitors partially blocked the partitioning of the compounds, while overexpression of FKBP12 enhanced it. Together, our data suggests that bifunctional molecules selectively accumulate in cells that express high levels of both protein partners and that this activity is driven by avidity effects. This result

has implications on the design of synthetic, bifunctional molecules, such as those that are nearing clinical trials. Further, these results suggest that the natural products, FK506 and rapamycin, might exploit this mechanism to gain potent pharmacological activity.

3.2   Introduction

3.2.1   Model for Selectively Targeting Cells via Intracellular Proteins

Bi-specific antibodies offer the advantage of high selectively. Can bi-specific small molecules share this feature (Figure 3.1)? In part, we chose the HIV protease and FKBP12 model system because HIV infection commonly occurs in lymphocytes. As mentioned in Chapter 1, lymphocytes are a major tissue target of FK506,[1]
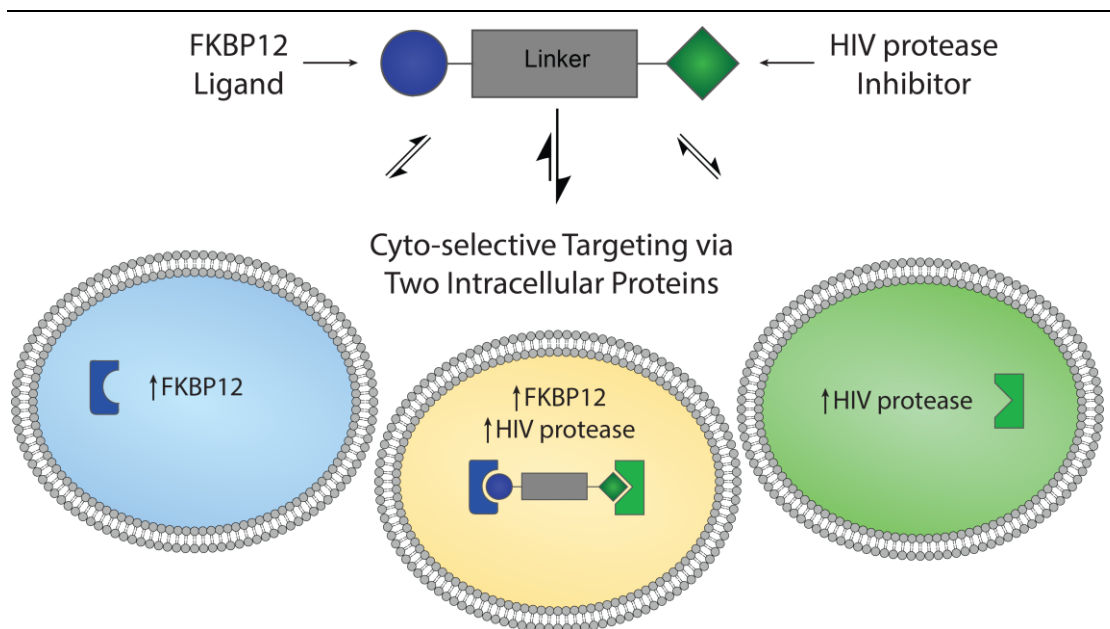
Figure 3.1) Bifunctional molecules are cyto-selective and accumulate in cells highly expressing both protein targets. Molecules possessing high affinity for both FKBP12 and HIV protease accumulate in cells that express both proteins in mixed cell populations.

likely because of the unusually high concentration of FKBP12 in these cells.[2]

Thus, we envisioned that the selectivity of HIV protease inhibitors might be improved by directing them to the relevant cell population – cells expressing both HIV protease and FKBP12. Such a strategy might improve activity by concentrating the active molecule into the relevant cell subpopulation, which in this case would be HIV-infected lymphocytes.

3.2.2 Enhanced Pharmacology of a Bifunctional HIV Protease Inhibitor

As mentioned in Chapter 2, HIV protease inhibitors are clinically effective but poorly cell penetrant and rapidly metabolized.[3] Their efficacy is often limited by low intracellular concentration, which may allow for rapid accumulation of resistance-conferring mutations.[4] To address these shortcomings, our group previously developed a bifunctional HIV protease inhibitor based on SLF and the amprenavir core as a proof of concept that intracellular FKBP targeting may be successful (Figure 3.2).[5] Specifically, this molecule was designed to test whether sequestering an HIV protease inhibitor in blood cells might partially protect it from
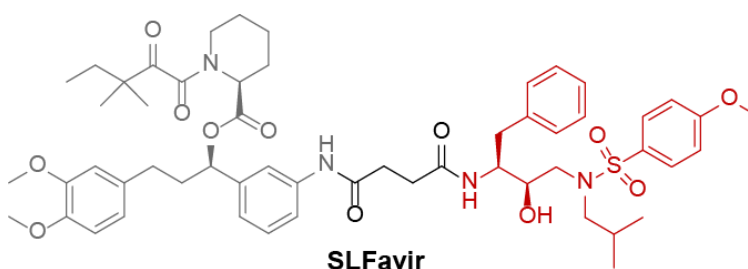

SLFavir

Figure 3.2) SLFavir is a first generation bifunctional HIV protease inhibitor with enhanced pharmacological properties. Anti-protease activity is retained *in vitro* and SLFavir is able to effectively partition into cells.
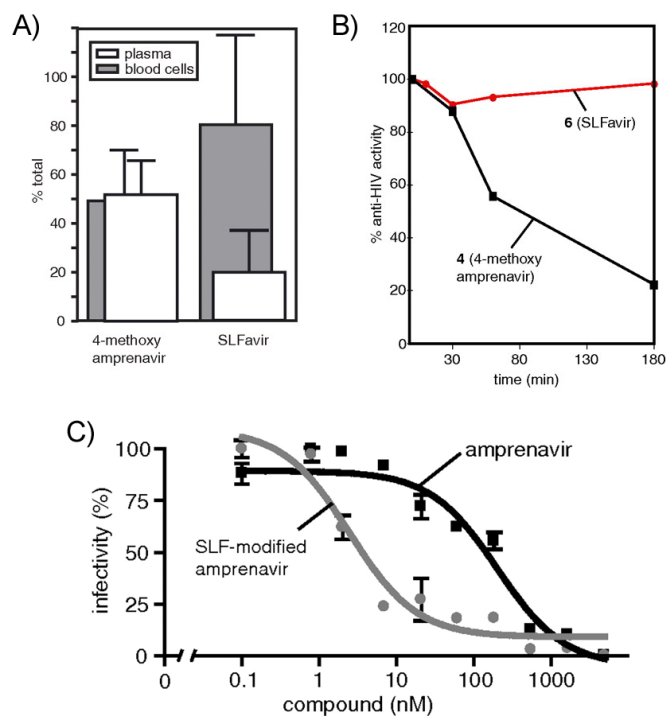
Figure 3.3) SLFavir preferentially accumulates in the cellular compartment, enhancing local drug concentration and improving efficacy. A) SLFavir primarily partitions into the cellular compartment, unlike the parent Amprenavir. B) Accumulation in the cellular compartment protects SLFavir from rapid first pass metabolism. C) SLFavir is more effective than the unmodified Amprenavir core in a model of live virus HIV infection. This is attributed to enhanced permeability and cellular accumulation of SLFavir.

metabolism and extend its half-life *in vivo*. Like other SLF-based CIDs, a short

linker was appended off the phenyl motif and coupled to amprenavir. The

compound (**SLFavir**) retained anti-HIV protease activity *in vitro* and was

investigated for *in vivo* efficacy.

Blood samples taken from mice treated with **SLFavir** were fractionated into cellular

or plasma components and analyzed for whole drug content by LC-MS. While the

parent amprenavir compound was found to be equally sequestered in cellular and

plasma fractions, **SLFavir** accumulated into the cellular compartment (Figure

3.3A), consistent with their design. Recovery and extraction of the HIV protease

inhibitor followed by determination of *in vitro* anti-protease activity suggested that **SLFavir** was protected from metabolism and degradation, unlike the parent amprenavir compound (Figure 3.3B). Using a cell model for HIV infectivity with live virus in CEM T lymphocytes, **SLFavir** was tested against unmodified amprenavir core and found to be approximately 80-fold more potent at preventing virion replication and subsequent infection (Figure 3.3C). Together, these studies show that FKBP12 binding can be used to "hide" a bifunctional HIV protease inhibitor to improve its poor pharmacological properties. However, the underlying mechanism for this improvement was unknown. Put another way, it wasn't clear how this activity might be "tuned" to increase accumulation of the HIV protease inhibitor in blood cells. This feature is important because eventual clinical use of such molecules may require adjusting lifetime and potency. For my thesis project, I wanted to understand the properties governing this effect and show whether bifunctional HIV protease inhibitors might be selectively targeted to relevant cell populations.

3.3 Results

3.3.1 Bifunctional Molecules Retain Passive Membrane Permeability

Before progressing into cellular models, we first explored the membrane permeability of the compounds using a standard parallel artificial membrane permeability assay (PAMPA). PAMPA assays are routinely used to quickly measure membrane permeability of drugs for a first approximation of bioavailability.[6] In this case, we used a newly-designed lipid-oil-lipid tri-layer
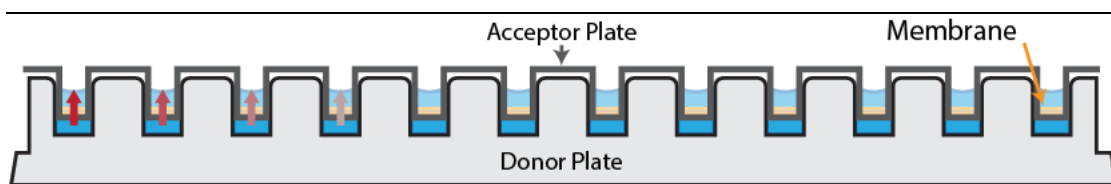
Figure 3.4) Design of artificial permeability assay. Compound is placed in a donor well and allowed to passively permeate into the acceptor wells. Depending on the compound composition, different permeability constants can be measured (illustrated as red to gray arrows).

system that is able to more accurately predict membrane permeability of non-canonical small molecules like our bifunctional library. Compound is added to a "donor well", then a filter plate containing buffer alone is added. After incubation, compound concentration is quantified on each side of the membrane (Figure 3.4).Consistent with their large size, the bifunctional molecules exhibited modest passive diffusion rates (1-2x10^{-6} cm/s, Figure 3.5). In comparison, the permeability

Figure 3.5) Artificial membrane permeability of the bifunctional library. In comparison to control compounds, the bifunctional molecules retained modest permeability despite their size. Results are the average of at least three independent experiments performed in triplicate. Error bars are SEM.
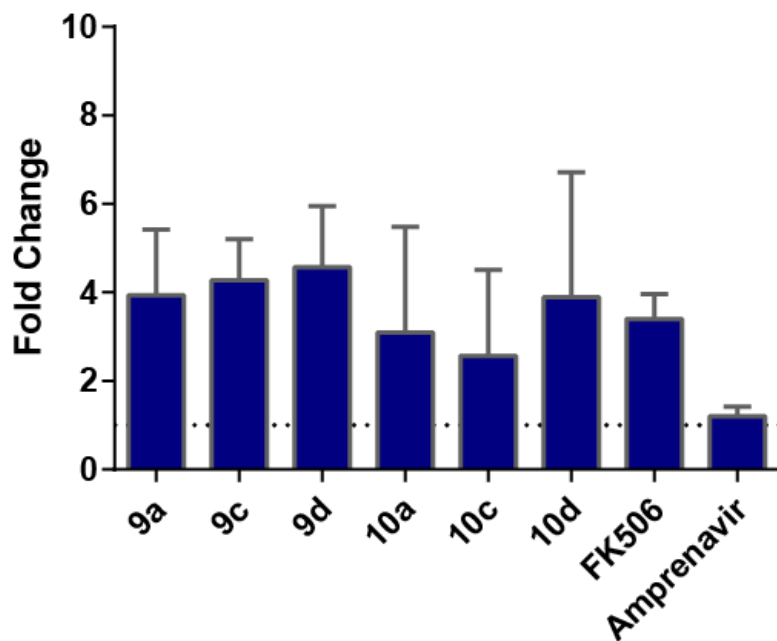
Figure 3.6) Addition of FKBP12 enhances partitioning of the bifunctional molecules but not Amprenavir. Recombinant FKBP12 added to the acceptor well sequesters compounds containing a FKBP-binding moie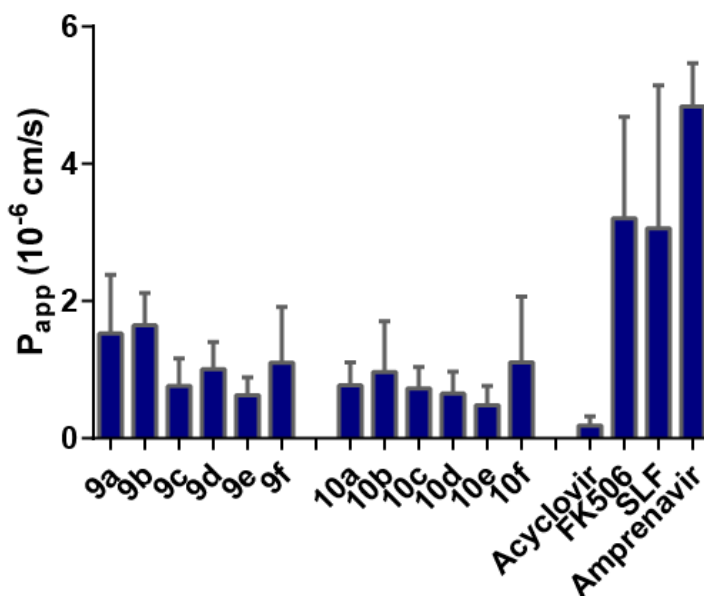ty. This effect is not observed with Amprenavir, which does not have FKBP-binding activity. Results are the average of at least three independent experiments performed in triplicate. Error bars are SEM.

rates for FK506 (3.2×10^{-6} cm/s) and amprenavir (4.8×10^{-6} cm/s) are considered fairly low, with the standard control compound acyclovir being impermeable. Thus, the permeability values of the bifunctional molecules are only 2- to 5-fold less than the parent compounds, suggesting that the modifications had relatively modest effects on permeability. With these baselines established, we added recombinant human FKBP12 to one side of the PAMPA membrane and measured the partitioning of a subset of compounds. Ideally, FKBP12 binding would sequester free compound on one side of the membrane, acting as a sink for free drug in solution, driving the equilibrium towards enhanced permeability. As we anticipated, FKBP12 enhanced partitioning by 2- to 5-fold compared to control wells (Figure 3.6), providing proof-of-concept that protein binding could retain the molecule on

one side of a membrane. Additionally, the partitioning of amprenavir – which is not able to bind to FKBPs - was unaffected by FKBP12. We desired to see if HIV protease could enhance partitioning in a similar fashion, but found that the buffers tolerated in the PAMPA system were not compatible with HIV protease solubility. Thus, we turned to a cellular assay.

3.3.2 Design of a Cell-Based GFP-HIV Protease Reporter System

To measure HIV protease binding in cells, we adapted an assay that uses a GFP-HIV protease reporter (Figure 3.7).[7, 8] This method relies on the observation that expression of HIV protease culminates in rapid cytotoxicity and cell death in mammalian cells.[9, 10] In this system, active HIV protease first cleaves GFP before cell death occurs, thus GFP stability is a proxy for anti-HIV protease activity. When a protease inhibitor is added, the cells become fluorescent and are able to proliferate. In this way, the extent of partitioning and HIV protease binding can be estimated from the stabilization of GFP and measured fluorescence levels. To further control the expression of the GFP-HIV protease fusion construct, we
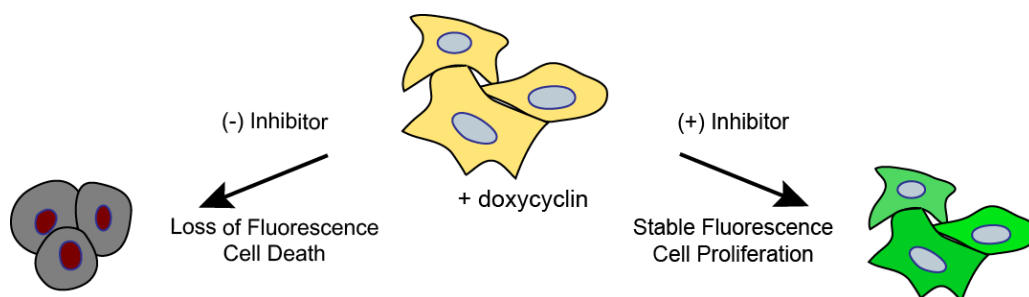

Figure 3.7) Cell-based reporter system for HIV protease inhibition using a GFP-HIV protease fusion protein. Inhibition of HIV protease stabilizes GFP fluoresence and rescues cell viability. Lack of inhibition of HIV protease results in cytotoxicty and cell death.

generated stable HEK293 T-REx cell lines under the control of a Tet repressor. This cell system has been developed to stably incorporate a gene of interest at a known flippase recombination target (FRT) site. Transient transfection of the pCDNA5 vector containing the gene of interest alongside Flp recombinase allows for intermolecular DNA recombination at the FRT site. Successful integration incorporates a Hygromycin B resistance cassette, and monoclonal populations can be selected. Since expression of the GFP-HIV protease fusion construct is closely regulated by the Tet repressor, little background expression occurs and cell viability is not impacted.
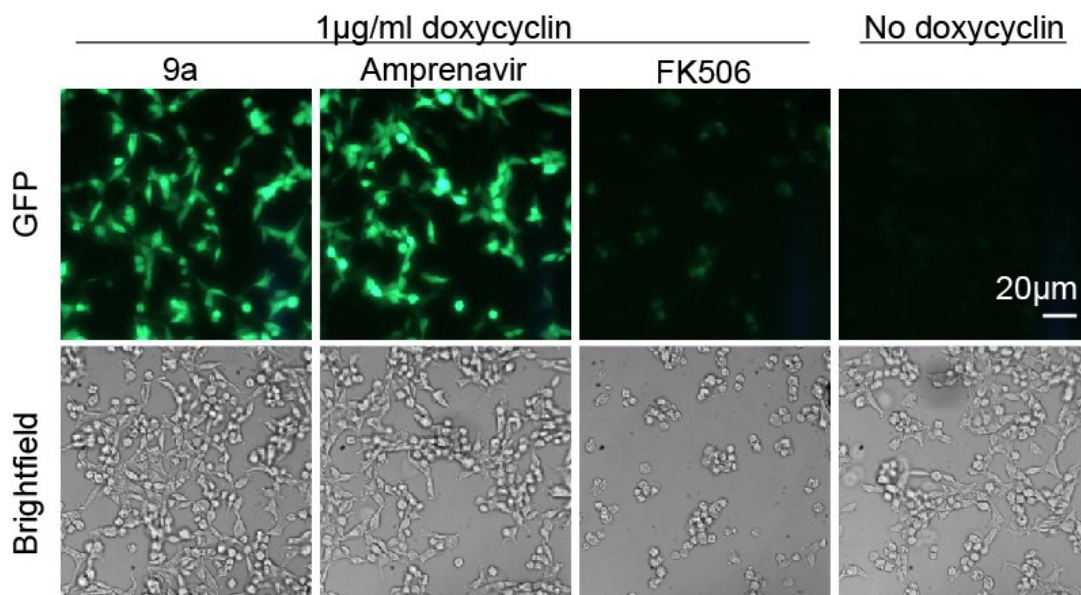
Figure 3.8) Protease inhibitors stabilize GFP fluorescence, but FK506 does not. Doxycyclin induces expression of the GFP-HIV protease fusion construct, which is stabilized by inhibition via HIV protease inhibitor. The FK506 control does not inhibit the active HIV protease and stablize GFP fluorescence, which ultimately leads to cell death as seen in the brightfield image.

3.3.3 Protease Inhibitors Stabilize the GFP-HIV Protease Reporter

Using fluorescence microscopy, we found that HIV protease was auto-proteolyzed

following doxycycline induction in the absence of HIV protease inhibitor, leading to

cell death (Figure 3.8). However, treatment with amprenavir or **9a** (5 µM), but not

FK506 or DMSO, could rescue cell viability and increase fluorescence, as

observed by fluorescence and brightfield microscopy. To validate these findings,

we used western blots to examine protein expression levels (Figure 3.9). After

induction with doxycycline, we saw robust expression of the GFP-HIV fusion
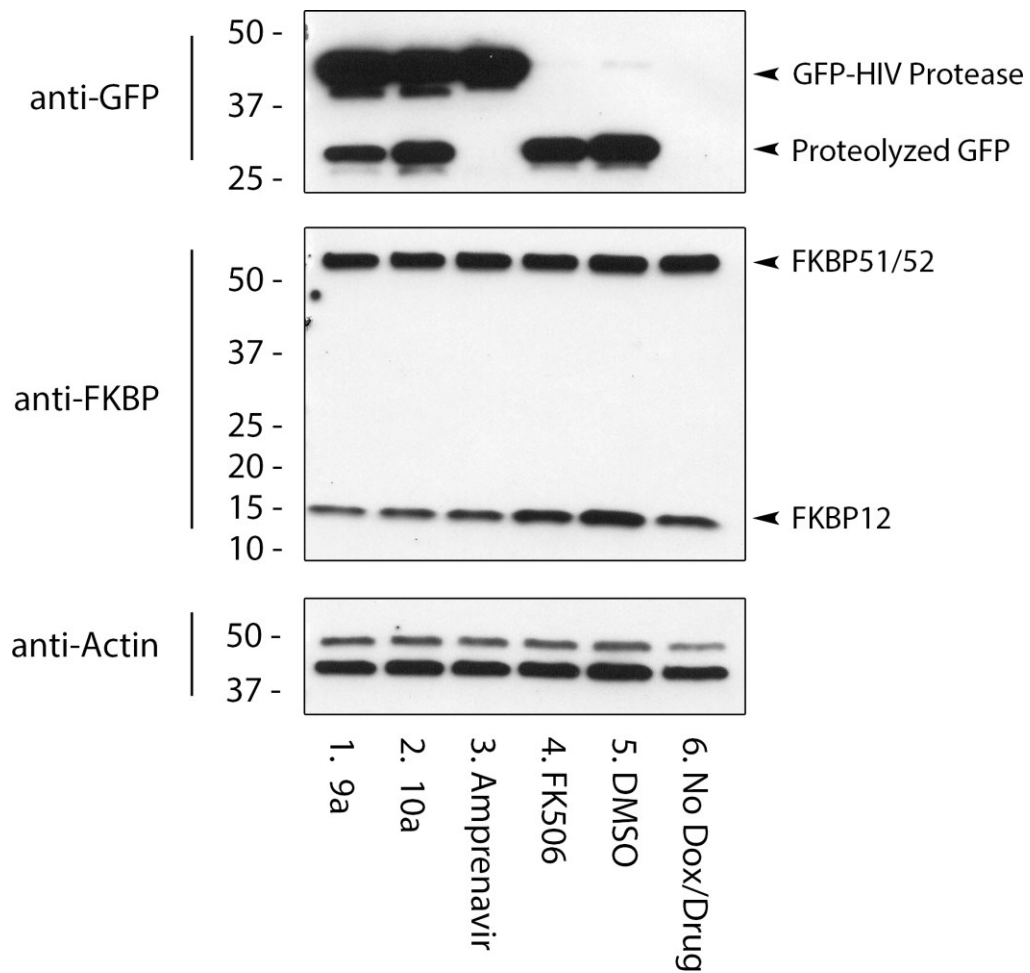

Figure 3.9) GFP-HIV protease is abundantly expressed and stabilized by the addition of protease inhibitor. Both **9a** and **10a** lead to some degradation of the GFP-HIV protease construct, while the control Amprenavir does not. Both FK506 and DMSO allow for the active protease to cleave GFP in to a smaller, inactive form, ultimately leading to cell death.

construct. Treatment with **9a**, **10a** and amprenavir stabilized the full fusion protein, while DMSO and FK506 did not. Interestingly, we saw some slight degradation of the GFP-HIV protease fusion construct with **9a**, but not with amprenavir. This suggested that the bifunctional molecules were less effective than amprenavir to stabilize the GFP-HIV protease fusion construct. However, amprenavir is a highly optimized drug that has reached regulatory approval and includes addition of the tetrahydrofuranyl urethane group where we install the linker of our molecules. This group dramatically enhances affinity for HIV protease, and amprenavir is approximately 10-fold higher affinity than the most effective bifunctional molecule in our library. Therefore, we were pleased to see that our compounds were nearly as effective as the approved drug. We next desired to analyze our library using a higher-throughput, more quantitative approach. To do so, we measured the effects of compounds **9a-f** and **10a-f** on GFP expression by flow cytometry. Populations of cells were gated and the median fluorescence of each population was analyzed (Figure 3.10A). Titrating compound shows a shift in the fluorescent population with a decrease in the median fluorescence intensity, which could then be quantified to
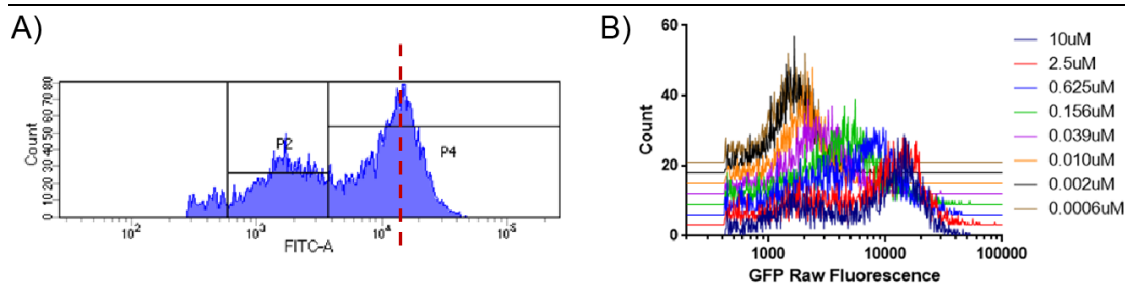
Figure 3.10) Flow cytometry analysis of fluorescent GFP-HIV protease cells. A) Treatment with protease inhibitor results in two populations of cells, one with high fluorescence intensity in the FITC channel and one without fluorescence. Each population of cells is gated and the median fluorescence (red dotted line) of the high intensity population is quantified. B) Titration of compound shifts the median of the high intensity fluorescent population.
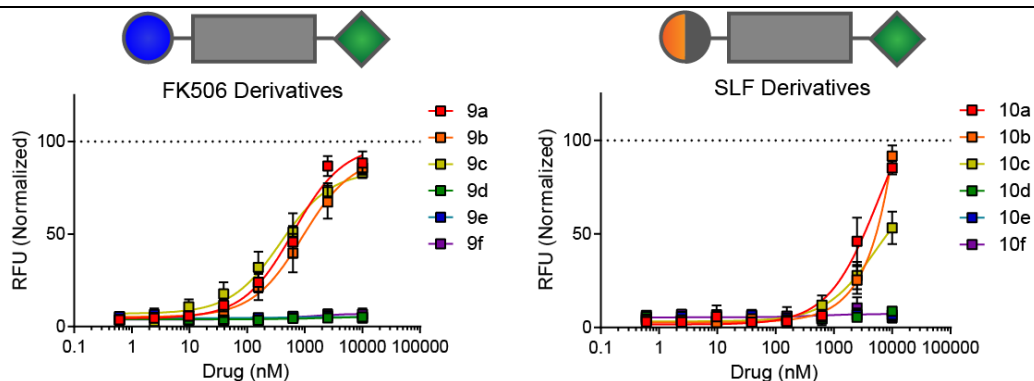
Figure 3.11) Quantification of anti-HIV protease activity using the cell-based GFP reporter. FK506-based bifunctional molecules exhibited higher activity against the GFP-HIV protease reporter, despite relatively similar permeability. Some compounds with low activity against HIV protease had no efficacy in this assay. Results are the average of at least three experiments in which fluorescence from 10,000 cells per concentration were quantified. Error bars were calculated from the three independent experiments.

determine EC_{50} values for each compound (Figure 3.10B). These studies showed that the best compounds, such as compounds **9a-c** or **10a-c**, also had potent anti-protease activity in the cells. Satisfyingly, the most potent molecules from this experiment were also those with the best anti-protease activity in the biochemical assays. For example, compound **9a** was significantly better than **9f** (Figure 3.11). We also noticed that there was an apparent "activity cliff" in the results. In other words, compounds **9a-c** were active in the GFP-HIV protease assay, while **9d-f** were largely inactive rather than simply weaker. This type of threshold response has been observed previously for HIV protease inhibitors and is likely due to an inability to stabilize the active site.[11] The second observation from our studies was that compounds **9a-c**, bearing the FK506 group, were significantly more potent than the equivalent compounds with the SLF moiety, **10a-c** (all $IC_{50} > 5000$ nM). These results suggest that the affinity for FKBP is critical to cellular partitioning. FKBP12 is more abundantly expressed (concentration estimated to

71

be high micromolar)[12] than HIV protease, consistent with FKBP12 being a major determinant of compound retention in the cytosol.

3.3.4 FKBP12 Drives Partitioning of the Bifunctional Molecules

These results suggested that the availability of FKBP12 may tune partitioning. As a test of this idea, we saturated available FKBP12 sites using free FK506 or SLF as direct competitors and tested the efficacy of **9a**. Competitive ligand modestly reduced fluorescence in the GFP-HIV reporter cells, with FK506 being more potent than the weaker binding SLF (Figure 3.12). This is to be expected, as **9a** is based on FK506 and is significantly more potent than SLF. To test this idea in the opposite direction, we increased the available pool of FKBP12 through transient overexpression of an mCherry-FKBP12 construct (Figure 3.13). After the transfected cells were allowed to recover, we treated with **9a** and used microscopy
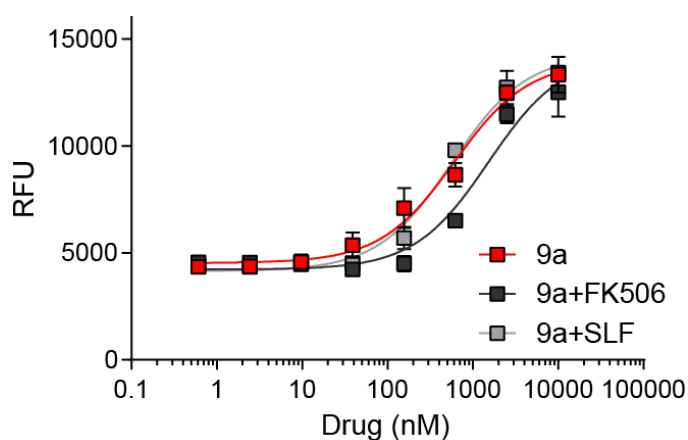
Figure 3.12) Competition of intracellular FKBP binding sites with FK506 reduces efficacy of the bifunctional molecule 1a. Pre-treatment with the high-affinity competitive ligand FK506, but not SLF, is capable of reducing the anti-HIV protease activity of FK506 derivative **9a**. Results are the average of at least three experiments in which fluorescence from 10,000 cells per concentration were quantified. Error bars were calculated from the three independent experiments.

Figure 3.13) GFP-HIVp stabilization is enhanced in **9a** treated mCherry-FKBP12 cells. Cells expressing increased FKBP12 had higher coincident stabilization of GFP-HIV protease in **9a** treated cells but not in cells treated with Amprenavir (merge).

to reveal that GFP fluorescence was concomitantly increased in cells that also had high levels of mCherry-FKBP12 (merge, Figure 3.13). Amprenavir did not show this dependence on mCherry-FKBP12 expression, showing that bivalency was required. To ensure the mCherry-FKBP12 construct was being over-expressed, we analyzed treated cells by Western blot. 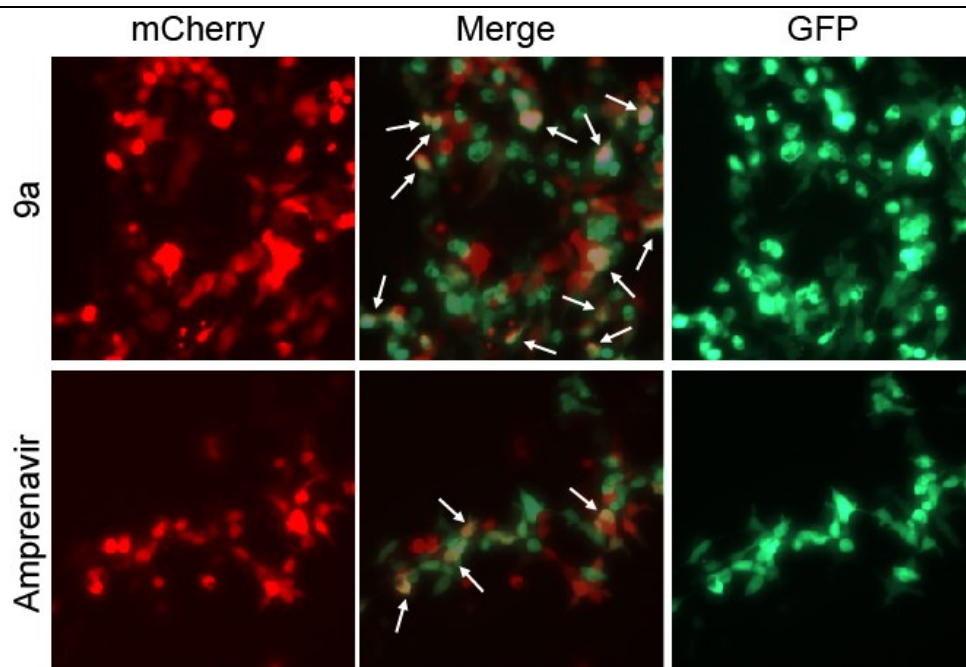As in Figure 3.9, we saw that protease inhibitor stabilized the GFP-HIV protease fusion protein. However, the additional expression of mCherry-FKBP12 enhanced the activity of both **9a** and **10a** (Figure 3.14, lanes 1 and 2), emphasized by the reduction of cleaved GFP in the anti-GFP blot. Under these conditions, the activity of **9a** was enhanced to the level of the control Amprenavir. Using flow cytometry, we then quantified the effect of FKBP12 on partitioning. Specifically, we isolated the subpopulation of cells (approximately 50%) that had high levels of mCherry expression. In these cells, the EC_{50} for **9a**

24 hour
2µM Compound

48 hour
2µM Compound

anti-GFP

50 -
37 -
25 -

◄ GFP-HIV Protease

◄ Proteolyzed GFP

anti-FKBP12

50 -
37 -
25 -
20 -
15 -
10 -

◄ FKBP51/52
◄ mCherry-FKBP12

◄ FKBP12

anti-Actin

50 -
37 -

1. 9a
2. 10a
3. Amprenavir
4. FK506
5. DMSO
6. No Dox/Drug
1. 9a
2. 10a
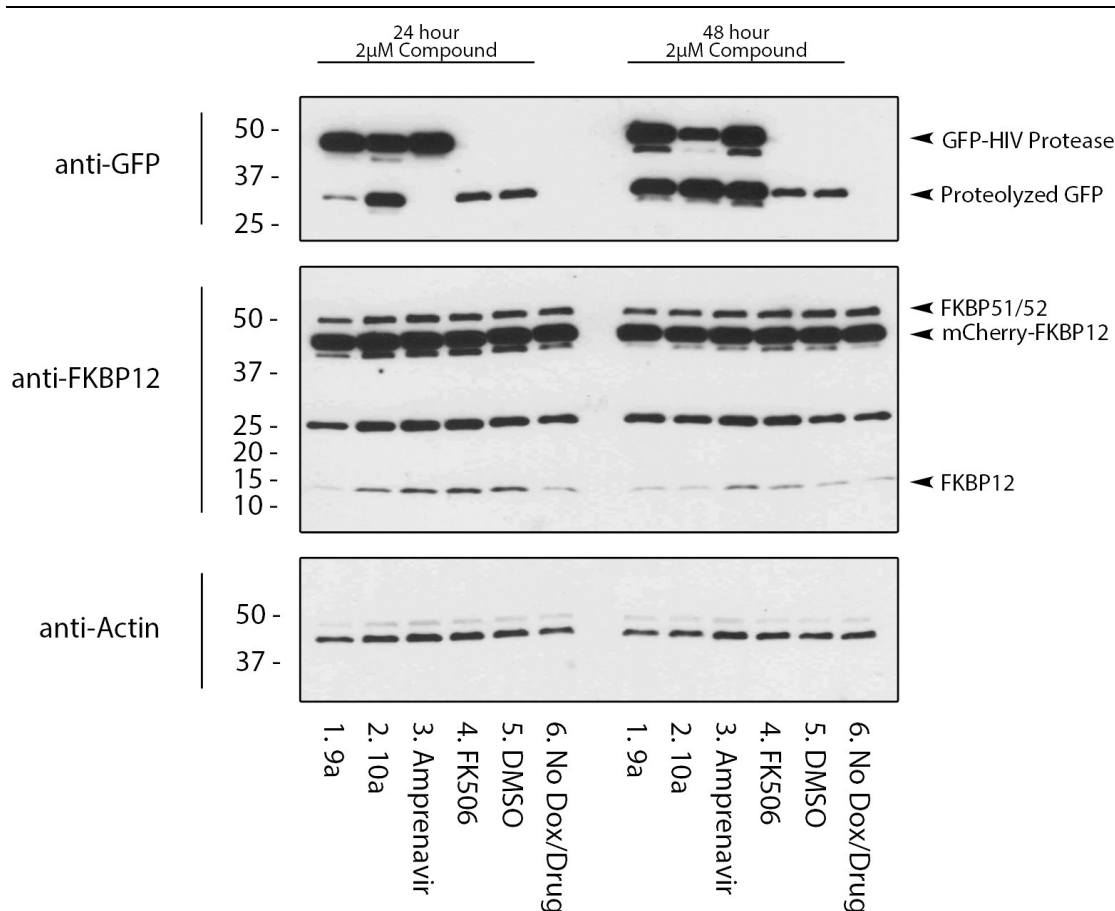3. Amprenavir
4. FK506
5. DMSO
6. No Dox/Drug

Figure 3.14) Overexpression of FKBP12 enhances activity of the bifunctional HIV protease inhibitors. Both **9a** and **10a** had reduced levels of GFP cleavage, suggesting increased activity of the compounds via enhanced partitioning.

was substantially improved (Figure 3.15A, EC_{50} = 600 nM in the FKBP12^{low} cells vs. EC50 = 105 nM in the FKBP12^{high} cells). Interestingly, cells negative for mCherry-FKBP12 in this experiment had apparent EC50 values that were slightly worse than cells that were never transfected (~ 380 nM vs 600 nM). We interpret this result as being consistent with the FKBP12 over-expressing cells acting as a sink for compound **9a**, reducing its availability for other cells. Co-treatment with free FK506 reversed the enhanced partitioning effect in the over-expressing FKBP12 cells (Figure 3.15B), demonstrating that it is indeed due to the availability of FKBP12. Consistent with our model, overexpression of FKBP12 had no effect
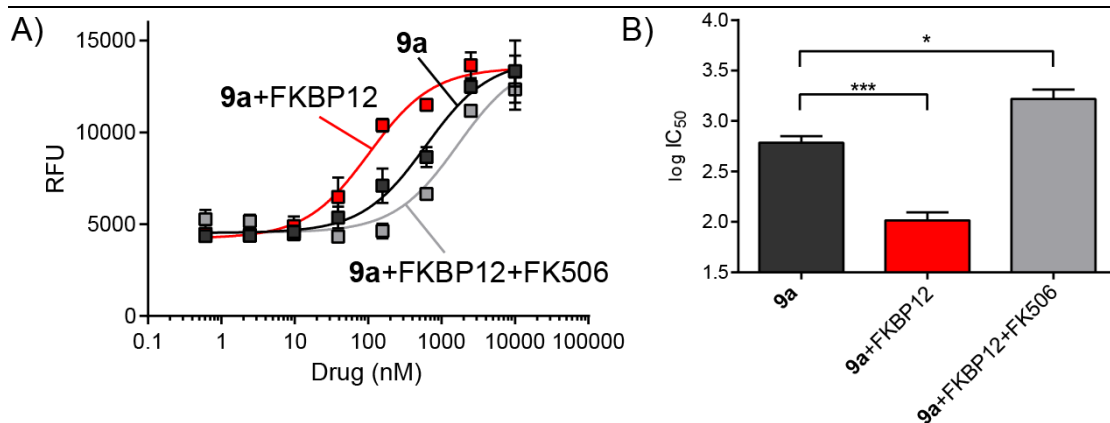
Figure 3.15) Partitioning of **9a** is "tuned" by the levels of free FKBP12. A) Shift in dose-response curves are dependent on the available FKBP12 for binding. B) Quantification of the ability of FKBP12 to tune partitioning, as judged by flow cytometry. Results are the average of at least three experiments in which fluorescence from 10,000 cells per concentration were quantified. Error bars were calculated from the three independent experiments. Statistical analysis was conducted using a one-way ANOVA ($p < 0.001$) and posthoc Dunnett's multiple comparisons test with 1a as a reference (*$p < 0.05$, ***$p < 0.001$).

on the partitioning of the control **11** (Figure 3.16A) and the IC_{50} was unchanged

(Figure 3.16B). Finally, we performed live virus HIV-infectivity assays. Consistent

with our cell-based reporter assay, we observed that **9a** was significantly more
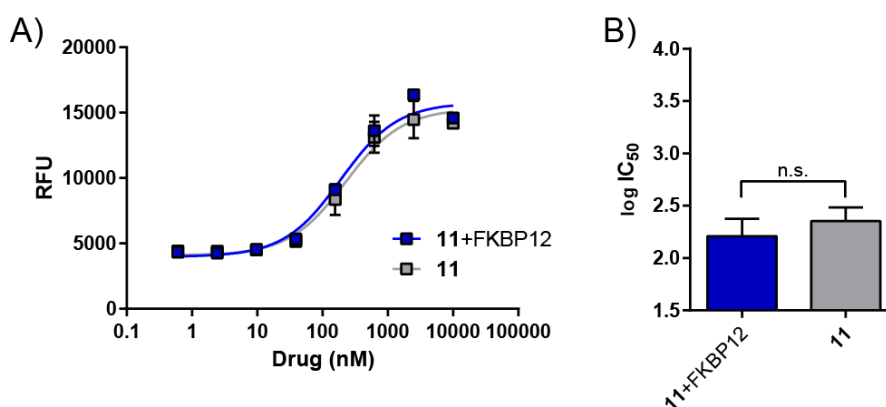
Figure 3.16) Overexpression of FKBP12 does not enhance the partitioning of **11**. A) Increasing the available FKBP12 for binding has no effect on the ability of **11** to stabilize GFP in the GFP-HIVp cells. B) Quantification of the ability of FKBP12 to tune partitioning, as judged by flow cytometry. Results are the average of two experiments in which fluorescence from 10,000 cells per concentration were quantified. Error bars are SD. Statistical analysis was conducted using a one-way ANOVA (not significant).

75

Figure 3.17) Affinity for each bivalent interaction mediates cellular anti-infectivity activity of bifunctional molecules. Viral replication is inhibited by **9a** and **10a** 6 and 8 days post-infection. **9a** exhibits greater efficacy due to the tighter affinity for FKBP12 despite identical protease inhibitor motifs. Infectivity curves are representative of experiments performed twice in triplicate. Error bars are SD.
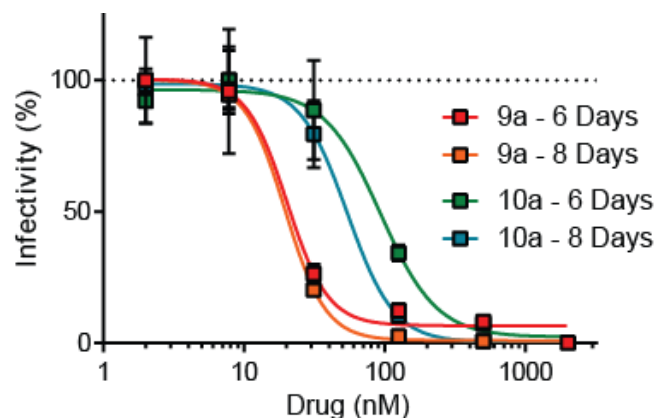
potent than **10a** (Figure 3.17), further supporting the idea that the affinity for FKBP

determines relative partitioning. Together, these results show that bi-specific

molecules take advantage of dual expression of two proteins to gain enhanced

cyto-selectivity. These results are summarized in Table 3.1.

	GFP-HIVp Reporter Assay			HIV Infectivity Assay	
	Standard	*FKBP12low*	*FKBP12high*	*6 Days*	*8 Days*
9a	610 ± 180	1700 ± 730	100 ± 40	20 ± 10	20 ± 2
9b	910 ± 350	3900 ± 6800	420 ± 120		
9c	380 ± 160	8600 ± 25000	79 ± 21		
10a	5900 ± 3000			93 ± 27	54 ± 12
10b	>10000				
10c	5300 ± 4200				

Table 3.1) Quantification of cell-based activity assays. Values are the IC_{50} in nM.

3.4   *Discussion*

The selectivity of a drug for its target cell in an animal helps determine its maximum safe dose by limiting damage to bystander cells. Using *in vitro* permeability assays, we found that the bi-specific molecules retained permeability despite their increased size and were sequestered on one side of a membrane by FKBP12. This partitioning partially overcame the poor permeability of the molecules, emphasizing that target engagement impacts equilibrium across membranes.[13] Then, using a modified version of a cell-based GFP reporter assay, we confirmed that interactions with FKBP12 and HIV protease also control partitioning in cells. Binding to FKBP12 dominated the cyto-selectivity effect, likely because it represents a greater pool of available binding sites. To further explore the role of FKBP12, we used pharmacological competitors and overexpression to systematically control the number of free binding sites. Consistent with a key role for this binding partner, overexpression of an mCherry-FKBP12 construct could further enhance partitioning (and anti-HIV protease activity), while competitors neutralized this effect. These results suggest that the key design principles in engineering cyto-selective small molecules are the abundance of the protein partners and the avidity of the interactions, reminiscent of what has been found for bi-specific antibodies

This concept is supported by the results of the live viral assays, in which compound **9a** was found to be much more potent than **10a**. However, we anticipate that this strategy may be beneficial in other situations in which therapeutics need to be guided to a specific cell type with precision. For example, many transformed cells

express high levels of at least two possible targets, such as oncoproteins, cell cycle proteins and molecular chaperones. Using bi-specific molecules might enhance selectivity for these cancer cells and reduce accumulation in healthy cells. Also, recent work has established ways of degrading target proteins, including FKBP12, by recruiting the cereblon E3 ligase.[14-16] Alternatively, this approach may be beneficial for the optimization of "cocktail" therapies, where multiple drugs are given to simultaneously target a particular disease. This is most common in HAART for HIV, in which four or five different drugs may be given in combination. This is necessary to ensure optimal inhibition of HIV replication, since targeting multiple drugs to the infected cells can be a challenge with low systemic accumulation. Using a bifunctional approach may be another strategy for delivery of two drugs to the same cell, guaranteeing a high local concentration of both therapeutics. The results presented here might inform ways of thinking about how these bi-specific molecules might take advantage of dual binding to generate cyto-selectivity.

3.5   Methods

3.5.1 Plasmid Generation and Protein Purification

For cell-based studies, FKBP12 was cloned into the pcDNA3 mCherry ligation independent cloning vector (Fwd: 5'-TAC TTC CAA TCC AAT GCC ACC ATG GGA GTG CAG GTG GAA ACC AT CT CC-3', Rev: 5'-CTC CCA CTA CCA ATG CCT TCC AGT TTT AGA AGC TCC ACA TCG AAG-3'). The GFP-HIV protease fusion construct was originally purchased from Addgene (#20253) and subcloned

into the pcDNA5/FRT/TO vector with BamHI/XhoI restriction sites (Fwd: 5'- ATAG GAT CCA TGG TGA GCA AGG GCG AGG AGC T-3', Rev: 5'- CTT ACT CGA GTT AGG CCG CCA GTG TGA TGG A-3').

3.5.2 *Parallel Artificial Membrane Permeability Assay*

Assay plates were purchased from Corning and stored at -30 °C until use. Plates were returned to room temperature and equilibrated for at least 30 minutes before opening. An acceptor well solution was prepared consisting of PBS (Gibco) and 5% DMSO. Compounds were diluted to 400 µM in DMSO and then added to PBS 1:20 to a final concentration of 20 µM. This initial solution was measured for UV absorbance at 280 nM and then added to the donor well of the PAMPA plate in triplicate. The acceptor plate containing the phospholipid membrane was slowly added into the donor plate and acceptor well solution was added. Plates were incubated at room temperature for 5 hours at room temperature before 100 µL aliquots were taken from both the donor and acceptor wells and analyzed by UV absorption to determine passive diffusion across the membrane. Permeability was calculated as follows:

$$P_e = \frac{-\ln(1 - C_A/C_{eq})}{S * \left(\frac{1}{V_D} + \frac{1}{V_A}\right) * t} \qquad C_{eq} = \frac{C_D * V_D - C_A * V_A}{V_D - V_A}$$

and,

$$C_D = C_0 * \frac{A_D - A_{buffer}}{A_0 - A_{buffer}} \qquad C_A = C_0 * \frac{A_A - A_{buffer}}{A_0 - A_{buffer}}$$

where P_e = permeability (cm/s), C_A = acceptor well final concentration, C_D = donor well final concentration, C_{eq} = equilibrium concentration, S = membrane surface

area, t = incubation time (seconds), V_D = donor well volume, V_A = acceptor well volume and $A_{0,A,D,buffer}$ = absorbance for initial solution absorbance, acceptor well final absorbance, donor well final absorbance and buffer background absorbance, respectively.

3.5.3 Generation of GFP-HIV Protease Cell Lines

HEK293 T-REx cells were grown in DMEM supplemented with 10% FBS at 37 °C in 5% CO_2. pcDNA5/FRT/TO containing the GFP-HIV protease fusion was transiently transfected into cells with different ratios of pOG44 (Invitrogen) with Lipofectamine 3000. Clones incorporating GFP-HIVp at the FRT site were selected with Hygromycin B (Roche) then checked for Zeocin sensitivity and expression levels after doxycyclin induction via fluorescent microscopy.

3.5.5 Transient Expression of mCherry-FKBP12

HEK293 T-Rex cells were transiently transfected with an mCherry-FKBP12 pcDNA3 expression plasmid. Expression levels were qualitatively analyzed by fluorescence microscopy. Media was replaced 12 hr after transfection and cells were grown for an additional 24 hours before plating for GFP-HIV Protease induction and compound treatment.

3.5.6 Flow Cytometry Analysis of Fluorescent Construct Expression

HEK293 cells incorporating the GFP-HIVp fusion construct were plated at 20,000 cells/well in clear 96-well TC-treated plates and grown for 24 hours. Compounds

were titrated down in DMSO, diluted to 5X final concentration with PBS and 10 µL was added to each well to a final volume of 200 µL and 1% DMSO. Doxycyclin was then added to each well at 1 µg/ml to induce GFP-HIVp expression. Cells were incubated for 36 hours at 37 °C in 5% CO_2, media aspirated, washed once with PBS and trypsinized. Cells were then re-suspended in ice-cold PBS and analyzed on a BD LSRii cytometer for GFP fluorescence. Median fluorescence for each well was determined. To analyze FKBP12 levels, cells positive for mCherry fluorescence were gated and median GFP fluorescence was measured.

3.5.7 Western Blot Analysis

Treated cells were washed twice with cold PBS and lysed with RIPA buffer at 4 °C for 30 minutes. Cell lysate was centrifuged for 25 min at 15,000 xg to pellet insoluble material and supernatant was collected. A BCA was performed and concentrations were corrected with RIPA buffer such that 2.5 micrograms total protein was loaded per well. SDS-PAGE was performed and the proteins transferred to nitrocellulose membrane, followed by subsequent washing and immunoblotting. Antibodies were obtained from Santa Cruz Biotechnology and detected with Amersham ECL Detection Kit.

3.6   Notes

This chapter represents a portion of the work published in "Dunyak, B.M., Nakamura, R.L., Frankel, A.D. & Gestwicki, J.E. Selective Targeting of Cells via Bispecific Molecules That Exploit Coexpression of Two Intracellular Proteins. *ACS*

Chem Biol **10**, 2441-7 (2015)." Figure 3.3 was adapted from previous work by Paul S. Marinec. Bryan M. Dunyak and Jason E. Gestwicki designed the experiments and synthetic schemes. Bryan M. Dunyak performed the experiments, with the exception of the live virus anti-HIV infectivity assay performed by Robert L. Nakamura and Alan D. Frankel in Figure 3.17.

3.7   References

1.   Takada, K., Katayama, N., Kiriyama, A. & Usuda, H. Distribution characteristics of immunosuppressants FK506 and cyclosporin A in the blood compartment. Biopharm Drug Dispos 14, 659-71 (1993).
2.   Su, A.I. et al. A gene atlas of the mouse and human protein-encoding transcriptomes. Proc Natl Acad Sci U S A 101, 6062-7 (2004).
3.   Hoggard, P.G. & Owen, A. The mechanisms that control intracellular penetration of the HIV protease inhibitors. Journal of Antimicrobial Chemotherapy 51, 493-496 (2003).
4.   Spaltenstein, A., Kazmierski, W.M., Miller, J.F. & Samano, V. Discovery of next generation inhibitors of HIV protease. Curr Top Med Chem 5, 1589-607 (2005).
5.   Marinec, P.S. et al. FK506-binding protein (FKBP) partitions a modified HIV protease inhibitor into blood cells and prolongs its lifetime in vivo. Proc Natl Acad Sci U S A 106, 1336-41 (2009).
6.   Kerns, E.H. & Di, L. Physicochemical profiling: overview of the screens. Drug Discov Today Technol 1, 343-8 (2004).
7.   Lindsten, K., Uhlikova, T., Konvalinka, J., Masucci, M.G. & Dantuma, N.P. Cell-based fluorescence assay for human immunodeficiency virus type 1 protease activity. Antimicrob Agents Chemother 45, 2616-22 (2001).
8.   Fuse, T., Watanabe, K., Kitazato, K. & Kobayashi, N. Establishment of a new cell line inducibly expressing HIV-1 protease for performing safe and highly sensitive screening of HIV protease inhibitors. Microbes Infect 8, 1783-9 (2006).
9.   Nie, Z. et al. HIV-1 protease processes procaspase 8 to cause mitochondrial release of cytochrome c, caspase cleavage and nuclear fragmentation. Cell Death Differ 9, 1172-84 (2002).
10.   Strack, P.R. et al. Apoptosis mediated by HIV protease is preceded by cleavage of Bcl-2. Proc Natl Acad Sci U S A 93, 9571-6 (1996).
11.   Lefebvre, E. & Schiffer, C.A. Resilience to resistance of HIV-1 protease inhibitors: profile of darunavir. AIDS Rev 10, 131-42 (2008).

12. Siekierka, J.J. et al. The cytosolic-binding protein for the immunosuppressant FK-506 is both a ubiquitous and highly conserved peptidyl-prolyl cis-trans isomerase. J Biol Chem 265, 21011-5 (1990).

13. Marinec, P.S., Lancia, J.K. & Gestwicki, J.E. Bifunctional molecules evade cytochrome P(450) metabolism by forming protective complexes with FK506-binding protein. Mol Biosyst 4, 571-8 (2008).

14. Corson, T.W., Aberle, N. & Crews, C.M. Design and Applications of Bifunctional Small Molecules: Why Two Heads Are Better Than One. ACS Chem Biol 3, 677-692 (2008).

15. Buckley, D.L. et al. HaloPROTACS: Use of Small Molecule PROTACs to Induce Degradation of HaloTag Fusion Proteins. ACS Chem Biol (2015).

16. Winter, G.E. et al. DRUG DEVELOPMENT. Phthalimide conjugation as a strategy for in vivo target protein degradation. Science 348, 1376-81 (2015).

Chapter 4

Novel Design of Inhibitors Targeting the PPIase Pin1

4.1   Abstract

Pin1 is unique among the PPIases because it only binds to prolines that directly follow phosphorylated serine or threonine residues (pS/T-P motif). This activity is important as the phosphate of the pS/T-P motif sterically hinders the local peptide backbone and dramatically slows the spontaneous *cis*-trans isomerization of the proline. Thus, Pin1 activity becomes essential for isomerization of this motif on a relevant physiological time scale. Moreover, Pin1's clients include multiple cell cycle regulators, modulators of stress responses, and transcription factors. In these clients, isomerization of pS/T-P motifs is used as an essential regulatory switch, often in tandem with proline-directed kinases. Accordingly, misregulation or overexpression of Pin1 is implicated in numerous diseases, including cancer and neurodegeneration, making Pin1 an especially attractive target. However, as introduced in Chapter 1, attempts to discover Pin1 inhibitors have had limited success. The requirement for a highly electronegative group in the Pin1 active site, mimicking the pS/T-P interaction, seems to render many potential inhibitors inactive in cell and animal models because of poor permeability. In this chapter,

our hypothesis is that the excellent pharmacological properties of FK506 might make it a suitable chemical scaffold for engineering Pin1 inhibitors. We reasoned that these molecules might take advantage of the mechanisms outlined in Chapters 1, 2, and 3, to yield potent, selective and long-lived inhibitors. However, FK506 itself has little affinity for Pin1, because it lacks the key, electronegative region essential for Pin1 binding. To overcome this hurdle, we have designed a novel semisynthetic strategy to modify FK506 at a position likely to improve affinity and selectivity for Pin1. We found that installing a sulfamic acid at the C10-position of the macrocyclic ring significantly improved the affinity for Pin1 (>100-fold) *in vitro*. This molecule is designed to yield the first high-affinity membrane-permeable inhibitors of Pin1, which should prove to be a powerful chemical probe of this PPIase.

4.2   Introduction

4.2.1 Pin1 Plays a Diverse Role in Cellular Homeostasis

Pin1 has a unique role among all of the PPIases in that it only recognizes prolines immediately following phosphorylated serine or threonine residues (known as the pS/T-P motif).[1] This unique feature of Pin1 bindings is mediated by a cationic groove formed by Lys-63, Arg-68 and Arg-69, which makes contact with the pS/T group (Figure 4.1).[2] In turn, isomerization of bound substrate is thought to be mediated by the nearby residue Cys-113.[3] Like other PPIases, Pin1 also has a hydrophobic "shelf" adjacent to the proline pocket that it uses to gain additional contacts (see Chapter 1).
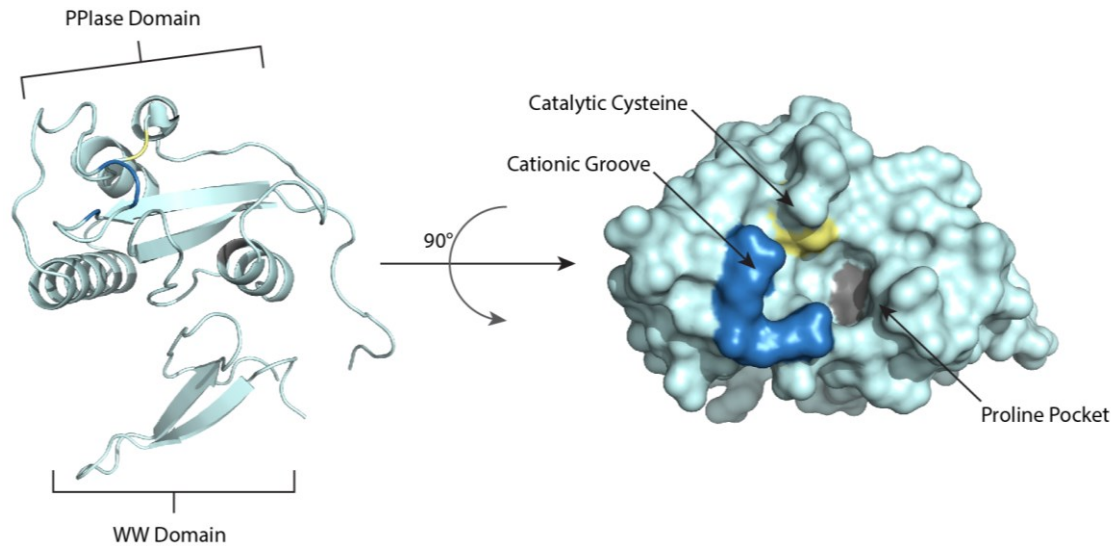
Figure 4.1) Structure of Pin1 with key features highlighted. A) Ribbon diagram. The active site pocket within the PPIase domain is composed of antiparallel β-strands that position a short α-helix. The WW domain consists of two, short antiparallel β-strands connected to the PPIase domain by a flexible linker (not resolved in this structure). B) Surface representation of the active site. The hydrophobic proline pocket (gray) orients substrate to interact with the catalytic cysteine (yellow) and the cationic groove that binds phosphate groups (blue). (PDB: 1PIN)

In addition to its PPIase domain, Pin1 has an N-terminal WW domain, that seems to contribute to the binding of phosphopeptide substrates. The WW domain does not possess intrinsic isomerase activity, and the reason for overlapping substrate preference with the PPIase domain is unclear. It is thought that the WW domain may initially localize with relevant clients, but the hand-off mechanism to the PPIase domain for isomerization is unknown.

Pin1 and its orthologs have been discovered in all eukaryotes and they are known to be critical for cell cycle regulation and cellular homeostasis. In *Saccharomyces cerevisiae*, the Pin1 homolog Ess1 is essential,[4] and complementation with

human Pin1 rescues viability.[1] One essential activity of Pin1 is in regulation of the cell cycle, through its activity on numerous phosphorylation-dependent regulatory pathways. Pin1 works in tandem with 'proline-directed' kinases and phosphatases, binding and isomerizing the peptide backbone of the pS/T-P motifs to alter the prolyl *cis*/trans conformation. This is especially important in the context of pS/T-P motifs, as they have been shown to isomerize 8-fold slower than their non-phosphorylated counterparts.[5] This slow rate is driven by specific contacts between the phosphate moiety and the amide backbone.[6] Since proline isomerization already represents a significant bottleneck in protein dynamics phosphoprotein substrates of Pin1 require the specific isomerase activity of this chaperone to function. Pin1-mediated conformational changes have been implicated in activating transcription factors, facilitating dephosphorylation or degradation of clients, stabilizing protein-protein interactions and targeting proteins for specific subcellular localization.[7]

4.2.1 The Role of Pin1 in Disease

The importance of Pin1 for cellular homeostasis and the progression through mitosis suggests that misregulation of this protein may lead to a variety of disease states. Indeed, Pin1 has been implicated in both cancer and neurodedgeneration. Pin1 interacts with multiple oncogenes, such as p53, and often enhances their oncogenic activity. Significant Pin1 overexpression has been found in numerous cancer types, including prostate, brain, breast, ovary, cervical and melanomas.[8] Conversely, low Pin1 expression has been correlated to increased neuronal

vulnerability and enhanced degeneration of neurons and neurofibrillary tangle formation during AD-like pathologies.[9] Pin1 is often sequestered into paired helical filaments (PHF) of hyperphosphorylated tau[10] while soluble Pin1 is deactivated by oxidative stress at its catalytic cysteine.[11] Thus, Pin1 expression and activity is often inversely correlated with disease; it is upregulated and highly active in cancer, or downregulated and inactive in neurodegenerative diseases.[12] For these reasons, Pin1 inhibitors are of significant interest as potential anti-cancer therapeutics, where modulation of Pin1 levels have been shown to be effective at preventing tumorigenesis. Further, Pin1 inhibition may have some therapeutic benefit in certain neurodegenerative diseases, such as in tauopathies where specific destabilizing mutations in tau have exhibited a decrease in pathogenesis when Pin1 levels are reduced.[13]

4.2.2 Natural Product Inhibitors of Pin1

Finding high affinity, cell permeable inhibitors has been an active and ongoing pursuit for many years.[14] Discovered as the first Pin1 inhibitor, Juglone (Figure 4.2) functions by covalent modification of Cys-113 in the active site.[15] Juglone is
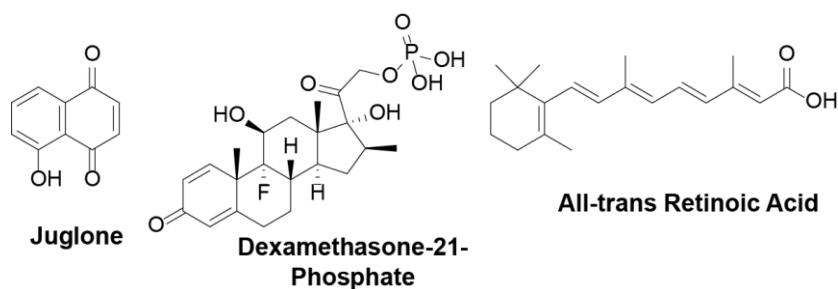
Figure 4.2) Natural product inhibitors of Pin1.

produced by the Black Walnut tree and its inhibition of Pin1 activity has been suggested to contribute to the toxicity of Black Walnuts. However, the exact binding interaction of Juglone is unclear and this compound has proven to have other cellular targets, possibly acting non-specifically.[16] To date, no inhibitors are known to mimic this mode of inhibition. Interestingly, Juglone does not inhibit the FKBPs or cyclophilins, whereas Pin1 has not been shown to have any appreciable affinity for the natural products, rapamycin, FK506 or cyclosporin. This observation is perhaps surprising, due to the similarity between active sites across the PPIases. However, Pin1 is unique among the PPIases because of its phospho-peptide binding activity through a positively charged surface. Thus, Pin1 inhibitors must navigate this feature of the pocket by including highly electronegative substituents. The challenge is that these same features often reduce membrane permeability. Other natural product derivatives (Figure 4.2) have been shown to inhibit Pin1 while also engaging the phosphate-binding region, providing an alternate approach towards novel scaffolds. Dexamethasone-21-phosphate is a synthetic corticosteroid prodrug found to modestly inhibits Pin1 activity (K_D = 2.2uM).[17] By NMR and X-ray crystallography, dexamethasone-21-phosphate was shown to bind across the proline pocket to the cationic groove formed by Lys-63, Arg-68 and Arg-69. Using a similar screening strategy, the vitamin A derivative all-trans retinoic acid (ATRA) was found to be a submicromolar inhibitor of Pin1 (K_D = 0.8uM) and bound similarly to dexamethasone-21-phosphate.[18] The cyclohexene ring is anchored into the proline binding pocket with the alkene chain extending the carboxylic acid into the cationic phosphate-binding region.

89

Treatment with ATRA suppresses proliferation of mouse embryonic fribroblasts and leads to Pin1 degradation but has no effect in Pin1 knockout cells or those harboring inactivating mutations in the binding site. In a model of acute promyelocytic leukemia (APL), ATRA facilitates degradation of the fusion oncoprotein promyelocytic leukemia-retinoic acid receptor α (PML-RAR-α) and was shown to be due to the inhibition of the stabilizing effect of Pin1. This was further demonstrated in a breast cancer model where Pin1 is highly expressed and possesses pro-oncogenic activity. Inhibition of Pin1 by ATRA limited tumorigenicity of MDA-MBA-231 cells injected into mice in a dose-dependent manner. Inhibitors based on these natural products may be a promising starting point.

4.2.3 *Peptidomimetics Demonstrate the Necessity for Charged Substituents in Pin1 Inhibitors*

Because of the challenges with the Pin1 site, early inhibitors were primarily based on peptides. Although these molecules haven't been useful as probes in cells or
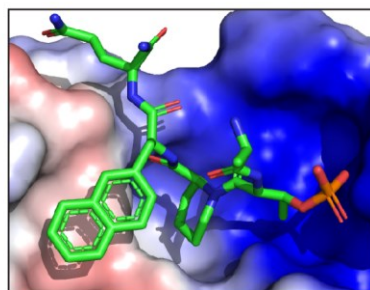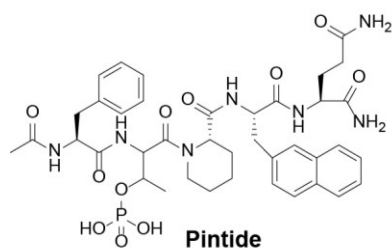
Figure 4.3) Representative pipecolic acid-based phosphopeptide inhibitor of Pin1. The phosphopeptide, pintide, is bound to Pin1 (shown as the surface electrostatic map). Significantly, the pipecolate ring is anchored in the proline binding pocket, positioning the phosphate group to interact with the cationic groove (blue). Further affinity is gained via the napthyl interaction with the hydrophobic shelf of the active site.

animals, they have illustrated the features of the active site. In one approach, a combinatorial library of 5-mer N-acetylated peptides incorporating unnatural amino acids surrounding a phosphothreonine residue was screened against the PPIase domain of Pin1. The strongest hit contained a pipecolate core not unlike those found to strongly inhibit FKBPs that is central to the binding region of FK506 and rapamycin. Optimization of the peptide resulted in "pintide" (Ac-Phe-D-Thr(PO_3H_2)-Pip-Nal-Gln-NH_2; Figure 4.3), which had a $K_i \approx 18$ nM. Switching the phosphothreonine residue to the L-isomer (*) resulted in a 30-fold loss in activity ($K_i \approx 550$ nM) and removing the phosphate group ablated the interaction. Addition of the WW domain in the full-length protein did not alter binding preference, which was perhaps unexpected due to the overlapping substrate specificity of the two domains.[19] Crystallization of the L- and D-peptide versions of pintide yielded surprising results, with nearly identical conformations of the stereoisomers. In both structures, the electronegative phosphate group was anchored into the phosphate recognition pocket, contacting Lys-63 and Arg-69. The pipecolate core rested in the proline-binding pocket, making hydrophobic contacts with Leu-122, Met-130 and Phe-134. The naphthylalanine side chain extends up and stacks on a hydrophobic shelf formed by Leu-122 and the top of the Met-130 side chain.[20] Based on these structures, the reasons for the large difference in binding affinity are not obvious. Strikingly, the Pin1 active site occupied by these peptides adopted a conformation that is reminiscent of FKBP when bound to rapamycin, with both pipecolic rings in nearly identical orientations. However, rapamycin has no

measureable affinity for Pin1 so the affinity of the peptides for Pin1 must originate through the phosphate-binding surface.

4.2.4 Early Design of Small Molecule Pin1 Inhibitors

Guided by the Pin1 crystal structure, FKBP ligands were modeled in the Pin1 active site to design novel small molecules. The first compound was found to be a low micromolar inhibitor ($K_i \approx 1.7$ μM), which was promising for a *de novo* lead (Figure 4.4). Attempts to optimize the charge by replacing the phosphate with a sulfate resulted in a significant drop in potency (9.5 μM). Re-installing the phosphate and appending a propylbenzene to the carbinol center improved potency to 0.8 μM and inhibited cell cycle progression of CA46 cells at 15 μM (**4.4a**). However, these compounds were not ligand efficient, so the scaffold was abandoned. The pipecolyl ester found in FK506 and rapamycin was replaced with a phenylalaninol phosphate as the minimum binding epitope. A pilot chemical screen identified a bi-aryl amide scaffold, which inhibited Pin at 100 nM (Figure 4.5). Derivatization and co-crystallization of (**4.5a**) revealed a new binding pose, with the compound rotated to allow the phenyl group to dock into the hydrophobic
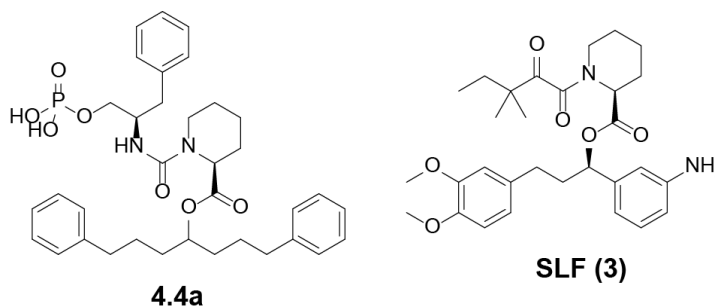
Figure 4.4) Small molecule Pin1 inhibitors based on pipecolic acid. Note the resemblance to FKBP inhibitors, such as SLF.
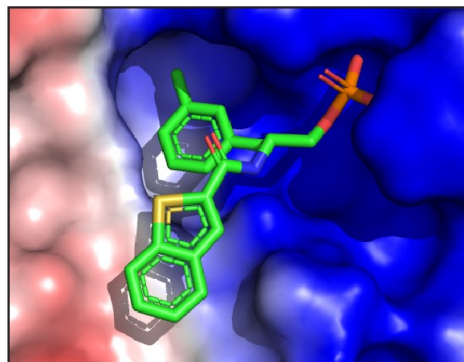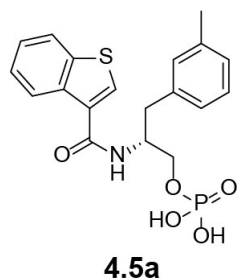
Figure 4.5) Bi-aryl amides potently bind Pin1.Bi-aryl amides potently bind Pin1. Co-crystallization with 65c (PDB: 3IKG) revealed a new binding orientation with the phenyl ring oriented in the proline-binding pocket and the phosphate group oriented between Arg-68 and Arg-69. (PDB: 3IKG)

proline pocket and placing the benzothiophene on the hydrophobic shelf formed by Leu-122 and Met-130.[21] The phosphate group was rotated slightly and bound in-between Arg-68 and Arg-69, losing the interaction with Lys-63 as in the previous phosphopeptide inhibitors. This suggests that there is some flexibility in orienting the phosphate group in these compounds, with the positive charge being spread throughout a large region of the active site. However, this series of compounds were inactive in whole cell assays, likely due to the poor permeability of the phosphate group. Subsequent derivatization to replace the phosphate group with either a primary alcohol or carboxylic acid (Figure 4.6) resulted in a significant drop in potency; the alcohol inactivated the compound while the carboxylate retained weak Pin1 inhibitory activity (**4.6a**, $K_i \approx 28$ µM). This was deemed suitable and the carboxylate-based scaffold was the subject of a limited SAR series.[22] In addition to modifications of the phenyl ring system, phosphate bioisosteres, such as tetrazoles, acylaminothiazols and acylsulfonamides, were tried in replacement of the carboxylic acid. Unfortunately, only the tetrazole retained the same activity as
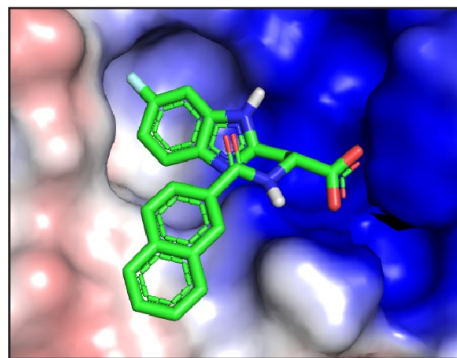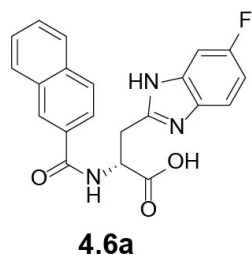
Figure 4.6) Optimization of the bi-aryl amide scaffold to enhance cellular permeability. The phosphate group was replaced with a carboxylic acid, which retained a similar binding pose as (**4.5a**) with the orientation of the carboxylate facing Lys-63 as in the phosphopeptide inhibitors. (PDB: 4TYO)

the carboxylate. It was hypothesized that export by P-glycoprotein efflux pumps may be responsible for the limited activity of this series. The amidyl carboxylate moiety in particular was implicated in recognition by P-glycoprotein, and it was concluded that further optimization of the scaffold was necessary to achieve cellular activity.

In an alternate approach, engagement of peripheral residues flanking the cationic phosphate-binding region was shown to be effective in the development of Pin1
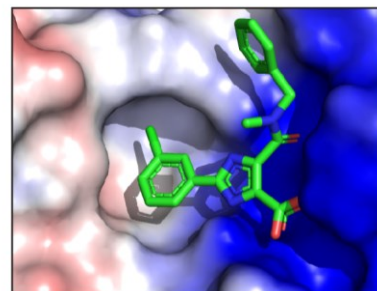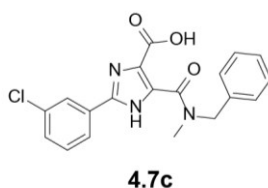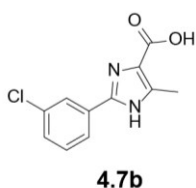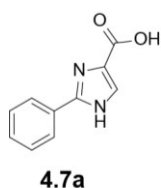
Figure 4.7) Alternative bi-aryl scaffold engages peripheral residues of the Pin1 cationic groove. Spanning the phosphate-binding region (Lys-63, Arg-68, Arg-69) enhances affinity for Pin1, even without engagement of the hydrophobic shelf.

inhibitors (Figure 4.7). An initial fragment-based screen was performed to inhibit Pin1 isomerase activity on a model substrate and confirmed in a follow-up NMR platform.[23] Optimization of the primary hit (**4.7a**) resulted in a phenyl-imidazole fragment substituted at the 3-position (**4.7b**; Figure 4.7), a site shown previously to be effective in engaging the proline pocket. Unfortunately, these compounds also lacked cellular activity. Subsequent modification of the central imidazole ring resulted in a series of amide substituted 3-chloro-phenyl-imidazole inhibitors with modest affinity for Pin1 (**4.7c**, $IC_{50} \approx 2.0$ µM) that were cell penetrant and able to inhibit cell division and Pin1-mediated cyclin D1 expression at micromolar levels. Furthermore, these compounds had a unique binding mode in Pin1, flanking Lys-63, Arg-68 and Arg-69 in the phosphate recognition pocket. It is worth noting that these fragments do not engage the hydrophobic shelf, as seen with other potent Pin1 inhibitors (**4.5a, 4.5b**).

Together, these small molecules are the first Pin1 inhibitors that possess cellular activity. Yet, cellular activity is relatively low, especially compared to the high affinity observed in the Pin1 *in vitro* assays. Attempting to optimize permeability by using phosphate bioisosteres has been unsuccessful. Furthermore, these compounds have not yet been shown to be effective in animal models. Critical to the design of these small molecules, they all engage the cationic phosphate-binding site. Additional affinity is gained from either interacting with the hydrophobic shelf or residues adjacent to the phosphate binding site. In general,

all of these compounds suffer from an inability to adequately partition and sequester into cells.

4.2.5 Remodeling FK506 and Rapamycin for Anti-Pin1 Activity

In Chapter 2 and 3, we showed that FK506 effectively drives the partitioning of HIV protease inhibitors into relevant cells. We wondered if a similar strategy may overcome the major problems that have plagued discovery of Pin1 inhibitors. As discussed above, early investigation into Pin1 inhibitors involved modifying the core scaffold of FKBP ligands based on the pipecolate core, which resulted in a series of compounds with good affinity. However, these molecules still suffered
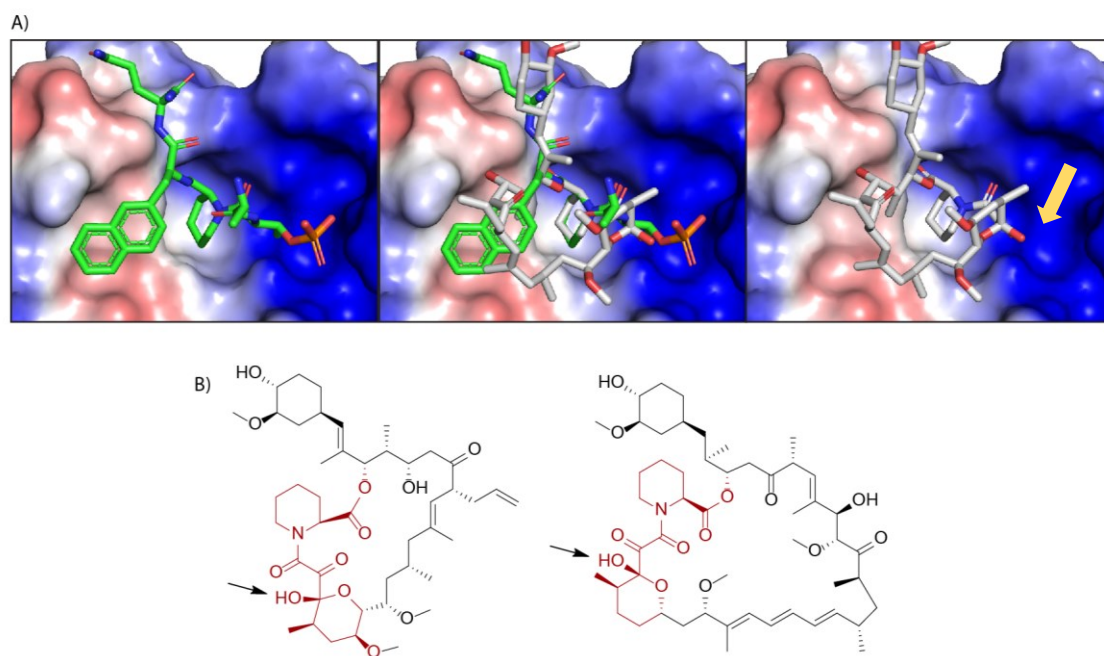
Figure 4.8) Overlay of the bound conformation of FK506 compared to the pintide phosphopeptide, highlighting the potential modification site. A) Aligning the pipecolate ring in FK506 to the pintide phosphopeptide demonstrates the binding pose similarity of each compound and proximity to the cationic phosphate binding site. B) FK506 and Rapamycin shown with the FKBP binding motif highlighted in red. The tertiary hydroxyl is highlighted (Yellow arrow in A, third panel. Black arrow in B).

from poor permeability. So, we wondered if the favorable properties of FK506 could be leveraged to drive the permeability of analogs containing electronegative groups.

To design an initial model, I created an overlay of the Pin1 active site with bound FK506 and compared it to the known co-crystal structures of Pin1 with inhibitors containing a pipecolate core. Analysis of these structures suggested that FK506 analogs might bind to Pin1 if the cationic groove could be sufficiently occupied (Figure 4.8). Likewise, modified analogs of rapamycin were predicted to have a similar interaction.

Analyzing the structure of both FK506 and Rapamycin highlighted the tertiary hydroxyl as being a potential point for modification. Unfortunately, initial attempts to derivatize the macrocycles at this position were not successful, likely due to the lack of reactivity of the hydroxyl. During our initial investigations into the feasibility of engineering Pin1-specific FK506/rapamycin derivatives, we rediscovered an obscure report on modifying the natural products at this position.[24] Specifically, the authors showed that treatment of either of these macrocycles with methanolic ammonia converts the tertiary hydroxyl into a primary amine by an undetermined mechanism (Figure 4.9). We predicted that the primary amine substitution at this position would create an orthogonally reactive handle for further derivatization. However, we first wanted to systematically explore the chemistry of this reaction, as it had remained underexplored.
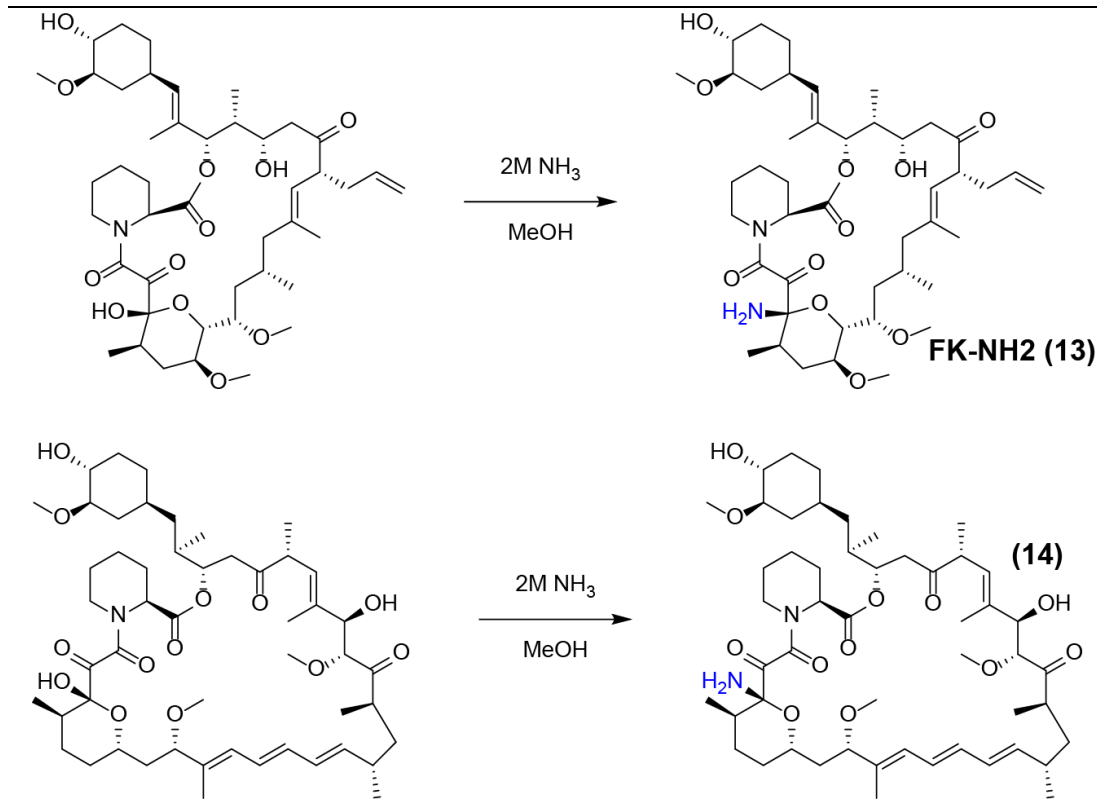
Figure 4.9) Semisynthetic modification of FK506 and rapamycin. Straightforward modification of the tertiary hydroxyl of FK506 and Rapamycin into a primary amine for further derivatization.

4.3   Results

4.3.1   Semisynthetic Modification of FK506 and Rapamycin

Using the previously reported conditions, FK506 was treated with methanolic ammonia (2M) and monitored by HPLC (Figure 4.10). Within 30 minutes, we saw conversion of FK506 into a more polar product (**13**, herein FK-NH2), which we attributed to the primary amine. At the same time, we noticed that the unreacted FK506 peak appeared to develop a slightly more polar shoulder and that a small number of minor side products were produced. It had previously been suggested
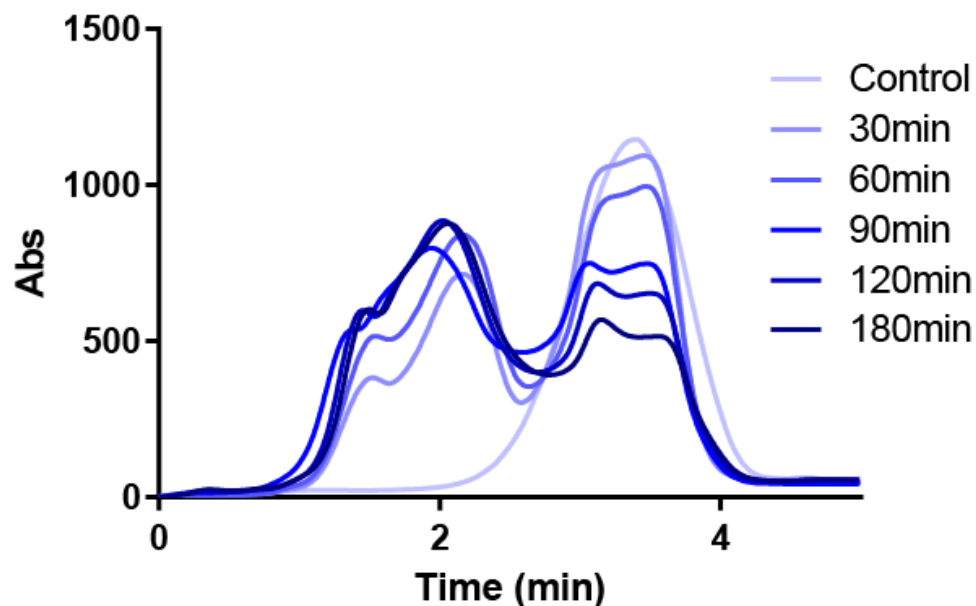
Figure 4.10) Conversion of FK506 into FK-NH2. Within 30 minutes, a significant portion of FK506 is converted into the amine-containing derivative.

that treatment of FK506 with ammonia could also result in formation of the imine

at the adjacent carbonyl, so we hypothesize that the "shoulder" might be the less

polar imine. However, we have not been able to isolate enough of this compound

for an in-depth characterization by NMR and MS. Similarly, we reasoned that the

excess ammonia could be modifying FK506 with both the amine and imine, which

Plateau	60.25
K	0.03853
Tau	25.95
Half-time	17.99
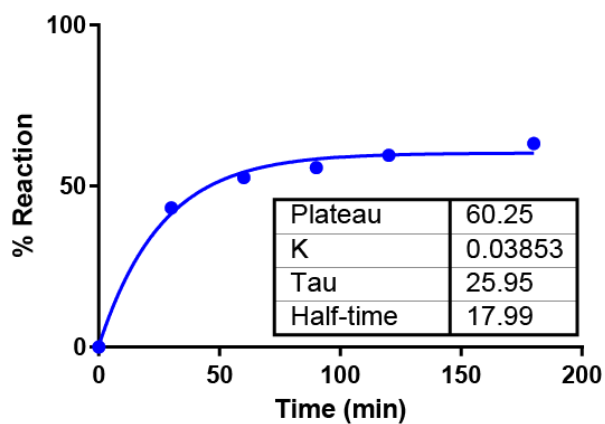
Figure 4.11) Reaction rate of the FK506 conversion. Data was fit to a one-phase exponential.

would explain the other trace product slightly more polar than the FK-NH2 peak. With these caveats, we quantified the HPLC traces to determine the amount of product formation and fit the data to a first order exponential (Figure 4.11). We only observed approximately 60% product formation, largely owning to the off-pathway side products. At longer time points, we did not see the reaction continue but
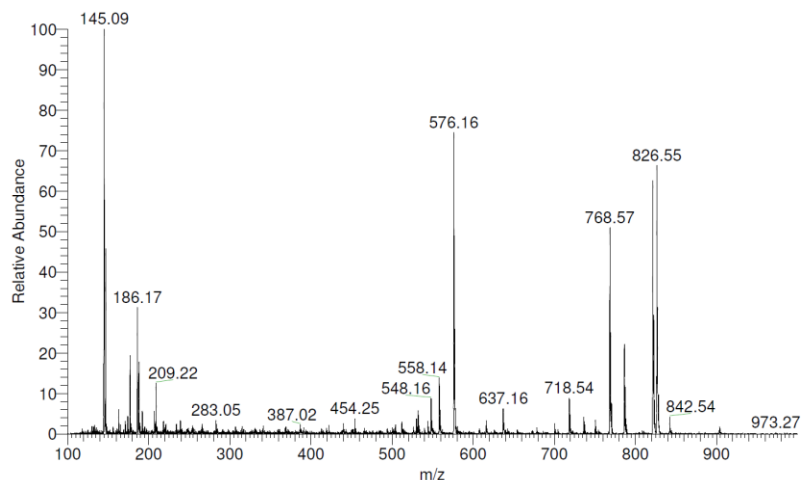
FK-NH2:
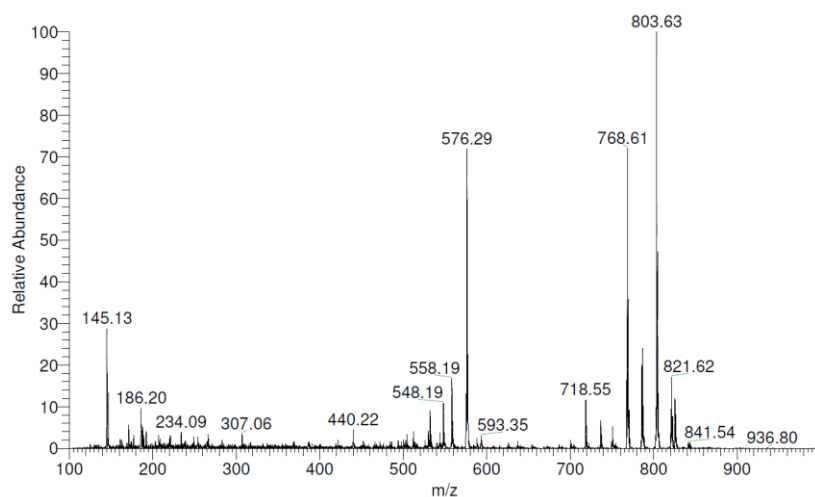
FK506:

Figure 4.12) Comparison of FK-NH2 and FK506 by MS. In the converted FK-NH2, the parent amine is readily ionized unlike in FK506.

instead saw significant degradation of both FK506 and the putative amine derivative.

Next, we characterized the presumed FK-NH2 product by MS and NMR. The molecular mass was readily observed by MS (Figure 4.12. M+H$^+$: 803.63, expected: 803.50), which is in contrast to the parent compound FK506. This represents a slight decrease in mass (~ 1 amu) compared to FK506. However, the imine would also exhibit the same mass loss, so we turned to NMR. Due to the complexity of the compound and the large number of hydrogens (70 in FK-NH2), we opted for ^{13}C NMR. Guided by previous peak assignments, we observed that
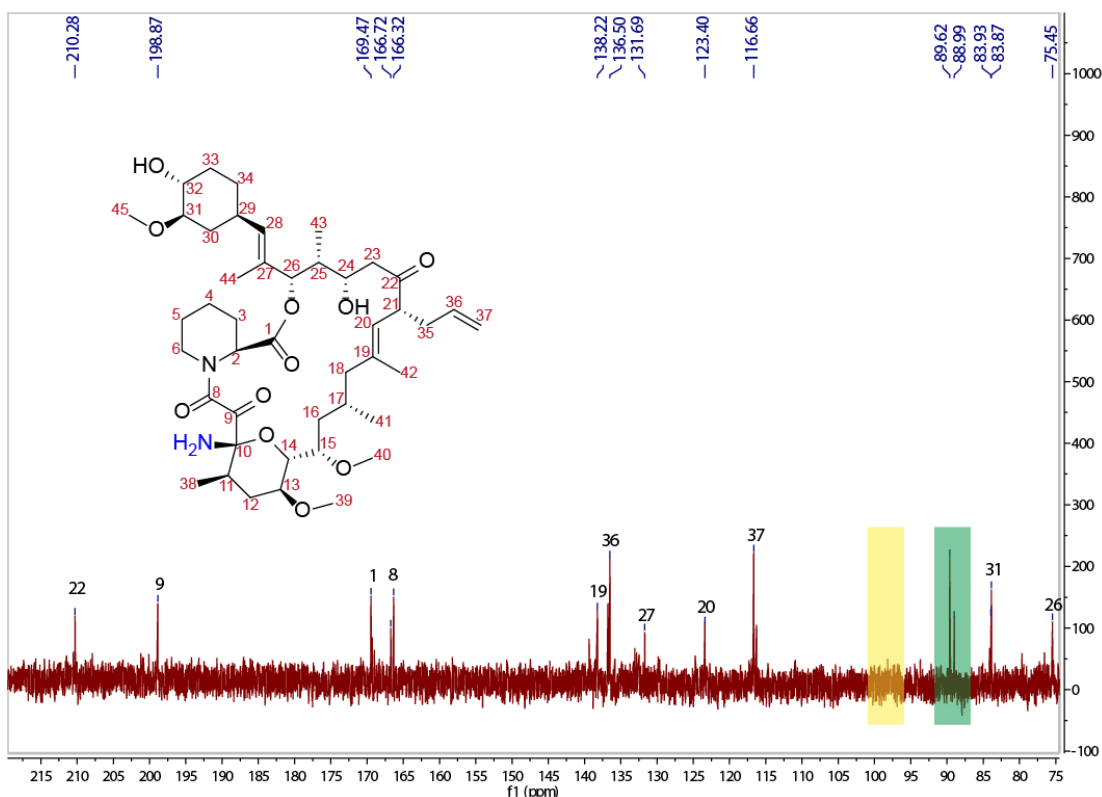
Figure 4.13) Downfield region of the FK-NH2 ^{13}C NMR spectrum. The C10 peak corresponding to the tertiary hydroxyl attachment point is typically at 97ppm (yellow highlight), but appears shifted after conversion to the amine (green highlight).

the C10 peak was significantly shifted (Figure 4.13).[25] Rather, this carbon was shifted upfield, consistent with attachment of an amine. Interestingly, we observed a slight double peak in the shifted spectrum, possibly due to tautomerization of FK506 in this region of the molecule. We are currently pursuing small molecule X-ray crystallography to further confirm the structure and its absolute stereochemistry as we continue the conversion of FK-NH2 to desired products.

4.3.2 Solvent Screen of the FK506 Substitution Reaction

During scale-up of FK-NH2, we noticed that preparative HPLC purification of the converted product led to reversion to FK506. We suspected that this decomposition may be due to the acidic mobile phase used (0.1% TFA in H_2O/ACN), so we decided to pursue a one-pot approach to carry forwards the FK-NH2 without purification. First, we attempted to optimize the concentration of ammonia to improve yield and minimize residual starting material in subsequent reactions. This led to a characteristic change in the observed peak shapes that
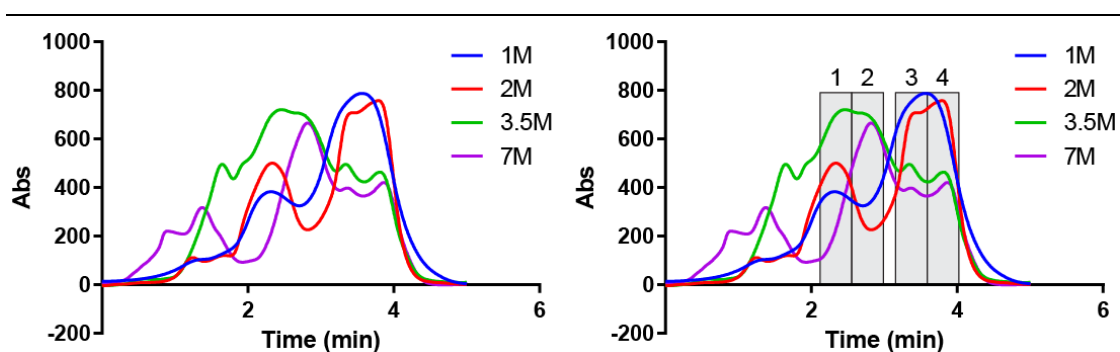

Figure 4.14) Determination of concentration effects on the conversion of FK506. HPLC traces are shown of the reaction after two hours in various concentrations of ammonia without and with peak highlighting (left and right, respectively). Increasing ammonia concentration seems to result in formation of a new species that is less polar than FK-NH2.

progressed as concentration was increased (Figure 4.14). At 1M ammonia, little reaction was observed that consisted of primarily unreacted FK506 and only a small amount of the FK-NH2 product forming (box 1). The 2M reaction progressed as normal, with increased formation of FK-NH2 (box 1) and appearance of the imine "shoulder" (box 3) that overlapped with the FK506 peak. Higher concentration 3.5M ammonia largely converted FK506 (box 4) with a mixture of FK-NH2 (box 1) and a previously not seen side product (box 2). Likewise, 7M ammonia produced only the new peak (box 2), with no FK-NH2 formation occurring. We suspect that the high concentration of ammonia causes some form of off-pathway rearrangement, possibly opening of the lactone after the initial formation of the converted FK-NH2. MS analysis of the products was inconclusive.

Using the 2M ammonia conditions, we proceeded to optimize solvent conditions. For these experiments, we chose a series of solvents to represent a range of properties from polar (DMPU) to nonpolar (DCM), as well as protic (methanol) to aprotic (DMPU, dioxane, DCM) solvents. Notably, to this point we were performing the reactions by first diluting a stock 7M ammonia in methanol solution, which is commercially available, to a final concentration of 2M. For the solvent screens we used the same strategy, which resulted in a solvent mixture consisting of the co-solvent plus residual methanol as a by-product of the dilution. Surprisingly, none of the solvent mixtures supported conversion to FK-NH2, even at longer reaction times (Figure 4.15). This result suggested that solvent effects were critical to the reaction. Because of the reasonable effectiveness of methanol, we next focused
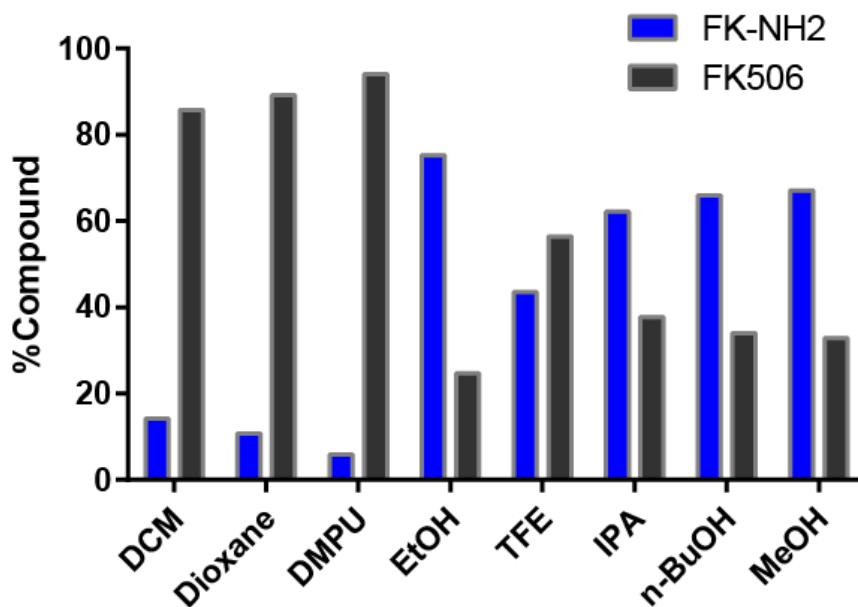
Figure 4.15) Solvent dramatically effects the conversion of FK506. Alcohols are heavily preferred in the conversion of FK506, with other polar and protic solvents leading to only minimal product formation after three hours.

on an additional series of alcohols. Interestingly, all of the alcohols supported

conversion to FK-NH2, with ethanol being slightly preferred (Figure 4.15).

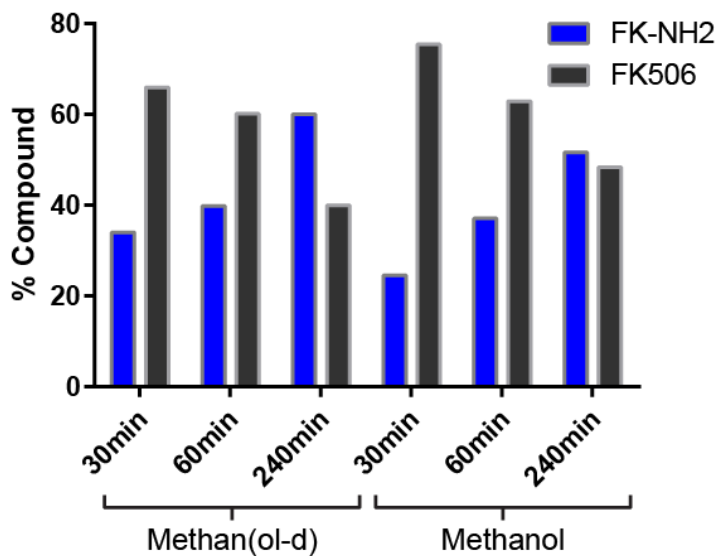Performing the reaction in trifluoroethanol did not lead to significant conversion,

Figure 4.16) Deuterated methanol slightly enhances the rate of reaction.

which we hypothesized could be due to the lower pKa of the free hydroxyl compared to ethanol (12.5 versus 15.9, respectively). Consistent for the role of the hydroxyl pKa, the reaction progressed slightly faster in methan(ol-d). From these optimization studies, we selected ethanol with 2M ammonia (75% yield) for subsequent experiments.

4.3.3 Investigating the Reactivity of amino-FK506 and amino-Rapamycin

Our first attempts at derivatization of FK-NH2 involved a simple alkylation of the amine using 3-chlorobenzyl bromide (product **15**; Figure 4.17). Unfortunately, the yield was very low, with optimization of the reaction resulting in approximately 10% product formation. In part, we chose to begin with the 3-chlorobenzyl bromide reagent because we feared that modification of the amine would be difficult and the 3-chlorobenzene group would act as a fingerprint. By ^{1}H NMR the 3-chlorobenzene ring was easily visible, as neither FK506 nor FK-NH2 have any aromatic protons, and the chlorine isotopic signature was observed by MS. This confirmed that the desired product was formed, albeit in low yield.
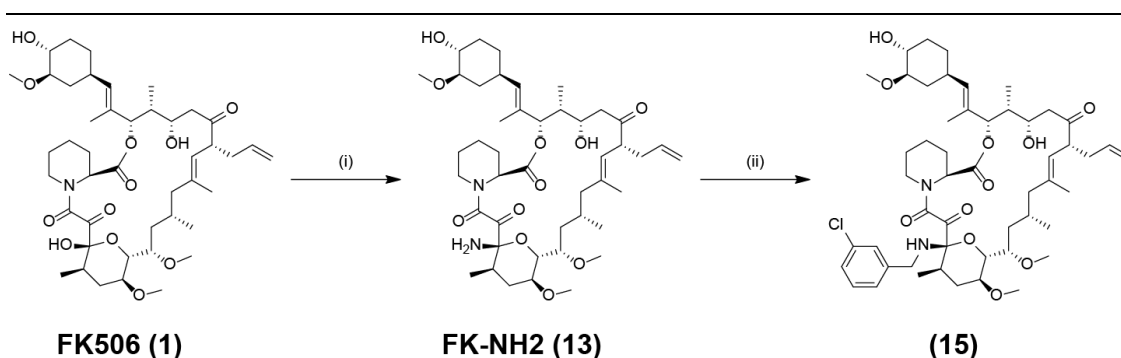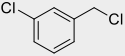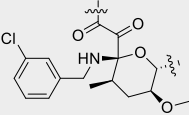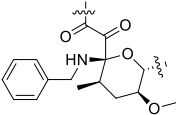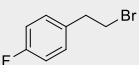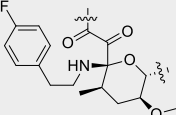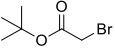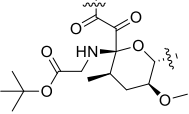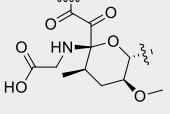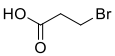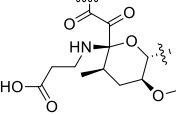

Figure 4.17) Semisynthetic scheme to derivatize FK-NH2. (i) 2M ammonia, ethanol. (ii) FK-NH2, 3-chlorobenzyl bromide (3eq), DIEA (6 eq), DMAP (0.1eq), DCM.

To test the scope of the reaction, we performed alkylations with benzyl (compounds **16** and **17**), alkyl (compounds **21** and **22**) and carboxyl-containing groups (compounds **18-20**; Table 4.1). However, we were only able to achieve low or trace product formation. Increasing temperature or reactant equivalents typically resulted in FK-NH2 degradation before reaction occurred. Increasing the leaving group propensity was likewise ineffective, with only low yield observed with the tosylate (compound **22**).

Based on these results, we explored amide formation as an alternative (compounds **23-26**; Table 4.2). However, traditional amide coupling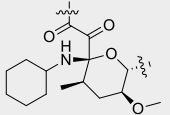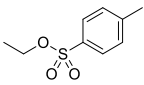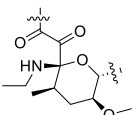 techniques (DIC/DIEA/DMAP) did not produce significant product. Even the use of HATU, a highly reactive coupling agent designed for peptide synthesis, was not sufficient for these reactions. However, some conversion was observed with the p-nitrophenol ester, a highly activated amide formation reagent that may be viable in future reactions.

Thus, we moved to progressively more reactive amide coupling conditions (Table 4.3). In neat acetic anhydride FK-NH2 proceeded to the desired product (**27**) in quantitative yield. Next, a series of other anhydrides were attempted. Initial attempts with succinic anhydride (**28**) were frustrated by addition of multiple succinates, but optimization of reaction conditions allowed for reduction in the number of equivalents that afforded the desired compound. Similar profiles were

Compound ID	Reactant	Desired Product	Yield	Attempted Conditions
15			12%	a,b,h
16			10%	a,b,e,f,g
17			trace	d,e,f
18			25%	a,b,h
19			N/A	a,g
20			N/A	a
21			N/A	a,c,e,h
22			5%	a,b,d,e,f,g

[a]DMF, DIEA
[b]DCM, DIEA, DMAP
[c]THF, DIEA
[d]Toluene, DIEA
[e]DMF, Pyridine
[f]DMF, DIEA, DMAP, 50°C
[g]DCM, DIEA, DMAP, 50°C
[h]DMF, Cs_2CO_3

Table 4.1) Attempted alkylations and conditions of FK-NH2. The pyranose fragment is shown where modification occurs. Yield is approximate as determined by product appearance in MS compared to residual starting material.

Compound ID	Reactant	Desired Product	Yield	Attempted Conditions
23			N/A	a,b
24			5%	a,b,c,d,e
25			trace	d,e
26			N/A	d,e

[a]DMF, DIEA, DMAP
[b]DCM, DIEA, DMAP
[c]DMF, Pyridine
[d]DMF, DIEA, DMAP, 50°C
[e]DCM, DIEA, DMAP, 50°
[f]DMF, DIEA, HATU
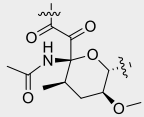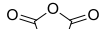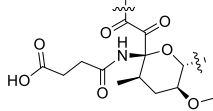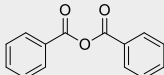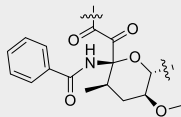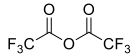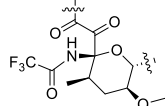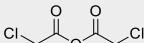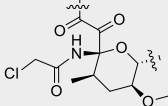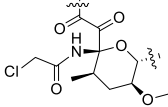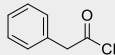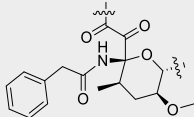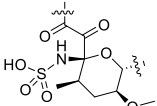
Table 4.2) Attempted amide formations and conditions of FK-NH2. The pyranose fragment is shown where modification occurs. Yield is approximate as determined by product appearance in MS compared to residual starting material.

observed with anhydride reactions yielding **29** and **31**. The one outlier was observed with trifluoroacetic anhydride (**30**), which did not yield any product. We are actively pursuing **31**, as installation of a reactive electrophile would be an additional strategy to append a variety of substituents to the molecule to create potential Pin1 inhibitors. Finally, a small series of acid chlorides are being explored as an alternate to the anhydrides. Neither **32** nor **33** resulted in sufficient product formation, but reaction conditions are continuing to be optimized. Lastly, the

Compound ID	Reactant	Desired Product	Yield	Attempted Conditions
27			100%	a,e,f
28			100%	b,c,d,e,f
29			100%	b,c,e,f
30			N/A	f
31			100%	f
32			trace	f
33			N/A	d,e,f
34			25%	c,d

aNeat
bDMF, DIEA
cDCM, DIEA
dDCM, DIEA, DMAP
eDMF, DIEA, 50°C
fDCM, DIEA, DMAP, 50°C

Table 4.3) FK-NH2 amide formation using anhydrides and acyl chlorides. The pyranose fragment is shown where modification occurs. Yield is approximate as determined by product appearance in MS compared to residual starting material.

reaction to produce **34** was chosen in an attempt to synthesize the sulfamic acid as a direct phosphate bioisostere and proceeded in low to modest yield (~25%). Further attempts to characterize this compound are underway.

In summary, a series of FK-NH2 derivatives have been prepared in modest yields. Reactions in nonpolar conditions seem to be heavily favored and the anhydrides were significantly more reactive than other approaches. This synthetic route provides an entry into FK506 analogs designed to bind Pin1

4.3.4 Binding of FK506 Derivatives to FKBP12 and Pin1 by Fluorescence

Polarization

To test binding to Pin1, we chose to employ a fluorescence polarization assay. This assay was based on our FP approach to measure binding to FKBP12 from Chapter 2. We found that a fluorescein-tagged substrate (WFYpSPFLE) bound with tight affinity to wild-type Pin1 (K_D = 10.1 ± 4.1 nM, Figure 4.18A), which was in good agreement with the known phosphopeptide substrates. Binding to the PPIase domain was considerably weaker (K_D = 427 ± 98 nM), although not unexpected, as the WW domain is known to contribute to binding. Purified compounds were titrated in a competition format against static tracer and Pin1 protein. Only one compound appeared to be active in this format, the sulfamic acid **34**, which possessed sub-micromolar activity for the wild-type construct (K_i^{WT} = 931nM, K_i^{PPIase} = 4350nM, Figure 4.1B). This was promising, as this compound
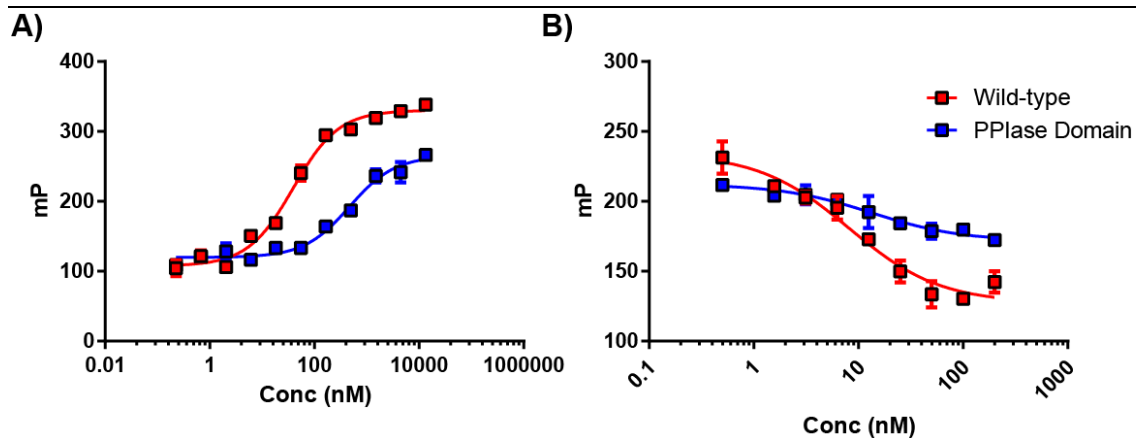
Figure 4.18) The phosphopeptide WFYpSPFLE binds to Pin1 and is competed by **34**. A) Wild-type Pin1 and the PPIase domain (see B legend) bind with good affinity to the phosphopeptide tracer. The smaller PPIase domain has a lower ΔmP corresponding to its smaller molecular mass. B) The phosphopeptide tracer is competed by **34**, which contains an electronegative sulfamic acid group that likely engages the Pin1 cationic groove. Experiments are the average of at least two experiments with duplicate measurements. Error is SEM.

would be most likely to engage the Pin1 cationic groove via electrostatic interactions with the charged sulfonate moiety.

Next, we tested the effects of our modification on FKBP12 binding. Based on the known FK506 binding interaction, we would expect many of these derivatives to have significantly impaired affinity for FKBP12. To test this, we used the FKBP12 binding assay (Chapter 2) to measure K_i values for the new FK506 analogs (Figure 4.19). We found that small alkyl substitutions, such as in **19**, were reasonably well tolerated. Larger functional groups (such as in compounds **15** and **24**) resulted in a significant drop in affinity, as expected. Lastly, the sulfamic acid substitution in **34** had nearly a 500-fold loss of potency. This result is encouraging, it shows that Pin1 binding can be favored at the expense of FKBP12 binding.
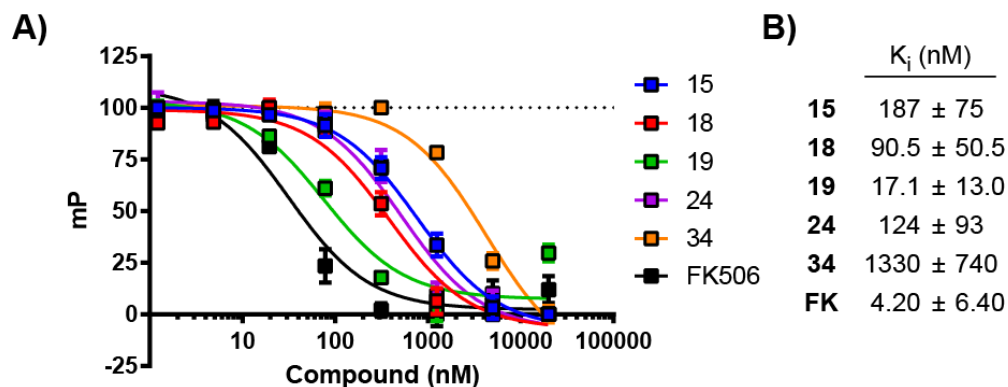
Figure 4.19) Competitive binding to FKBP12 of our FK506 derivatives. A) Modification of FK506 at this position dramatically reduces affinity for FKBP12 depending on the functional group properties. B) K_i calculations of the FK506 derivatives in comparison to FK506. Results are the average of triplicates and error is SEM.

4.4 Discussion

As discussed in Chapter 1, the discovery of effective, cell-permeable Pin1 inhibitors has remained a significant challenge. In this Chapter, we first discussed numerous strategies that have been designed to identify Pin1 inhibitors. The requirement for a strongly electronegative group typically precludes membrane permeability of these molecules, limiting their use. Some improvement has been made for small molecules where the phosphate group is substituted by a carboxylic acid, but the cellular activity of these ligands is weak. Other strategies, such as phosphate prodrugs and bioisosteres, have also been unsuccessful.

In my thesis work, I was inspired by the natural mechanisms of FK506 and rapamycin (Chapter 1). Despite their high molecular mass and chemical complexity, they possess excellent pharmacological properties, specifically membrane permeability. Early studies on bifunctional molecules (Chapter 2 and 3) took advantage of this trait, and our investigation into this mechanism found that

appending a PPIase ligand to HIV protease inhibitors could significantly improve its cellular partitioning (Chapter 2). Here, I wanted to see if these features could be exploited to create potent Pin1 inhibitors. The early small molecules of Pin1 were based on the pipecolate scaffold found in FK506 and rapamycin, suggesting that the core recognition motif might be conserved. In addition, I found that the bound conformation of pipecolate-containing Pin1 inhibitors is highly reminiscent of FK506 bound to FKBP12 (Figure 4.8). Despite these similarities, FK506 has no measurable affinity for Pin1, likely because it lacks the electronegative functional group that is unique to Pin1 binding. We decided to pursue the semisynthetic modification of FK506 to impart Pin1 binding. We found that FK506 could be converted to FK-NH2 at a region that is predicted to be in close proximity to the phosphate-binding region of the Pin1 active site. Indeed, compound **34** had affinity for Pin1 *in vitro* with FKBP12 binding considerably reduced. We are currently exploring the permeability of these analogs and creating more potent versions,

One of the goals of this study was to optimize the route for creation of FK-NH2. We found that the concentration of ammonia was critical; 1M ammonia resulted in the reaction stalling without significant conversion, while concentrations above 2M caused undesirable side-product formation. Dramatic solvent effects were also observed, with suitable conversion only occurring in alcohols. We found that FK-NH2 would revert to FK506 during purification, so we moved to a one-pot strategy for subsequent derivatization. It was immediately apparent that the installed amine of FK-NH2 had limited reactivity, because direct alkylation with alkyl halides or

amide coupling with activated carboxylic acids or acyl chlorides was only moderately effective. However, we found that anhydrides allowed robust product formation in excellent yields (~100% in most cases). These systematic studies are expected to facilitate the creation of a larger collection of potential Pin1 inhibitors, with the next series of FK-NH2 derivatives bearing substituents designed for Pin1 binding.

In the next stage of this project, it will be essential to understand the binding interaction and cellular activity of these molecules. In collaboration with the Fraser lab, we are pursuing crystal structures of the free molecules as well as co-crystallized with Pin1. Fortunately, Pin1 has been well validated as a target in a variety of cell lines, including its impact on cell viability in numerous human cancers, so we propose to use these established models to test the cellular activity of the molecules.

4.5   Methods

4.5.1 Plasmid Generation and Protein Purification

Wild-type Pin1 was obtained from the lab of Dr. Dustin Maly in the pMCSG7 vector for bacterial expression and purification. The PPIase domain (45-163) of Pin1 was cloned into the pMCSG7 vector using ligation independent cloning (Fwd: 5'-TAC TTC CAA TCC AAT GCA AAA AAC GGG CAG G-3', Rev: 5'-TTA TCC ACT TCC AAT GTT ACT CAG TGC GGA GGA TGA-3') for bacterial expression and purification.

The Pin1 constructs were transformed into E. coli BL21(DE3) cells and grown in Terrific Broth for six hours at 37 °C, followed by induction with 1 mM IPTG at 20 °C for 12 hours. Cells were collected, lysed by sonication (25 mM Tris, 500 mM NaCl, 10 mM imidazole, 10% glycerol, pH 8.0) and was bound on Ni-NTA resin. Resin was washed once with wash buffer 1 (25 mM Tris, 500 mM NaCl, 30 mM imidazole, 3% ethanol, 10% glycerol, pH 8.0), once with wash buffer 2 (25mM Tris, 100mM NaCl, 30mM imidazole, 3% ethanol, 10% glycerol, pH 8.0), once with wash buffer 3 (25mM Tris, 300mM NaCl, 30mM imidazole, 10% glycerol, pH 8.0) and eluted (25 mM Tris, 300 mM NaCl, 300 mM Imidazole, 10% glycerol, pH 8.0). Eluted protein was dialyzed overnight (10mM HEPES, 100mM NaCl, 5% glycerol, pH 7.5) and purified by Size Exclusion Chromatography using a SD75 column with the dialysis buffer.

4.5.2 Pin1 Fluorescence Polarization Assay

Binding to Pin1 was measured by fluorescence polarization. The assay was performed at 60 μL final volume in MOPS (pH 7.5) with 0.01% Triton X-100 using Corning 384-well flat-bottom black plates. For initial binding analysis of the fluorescent compound, recombinant Pin1 was serially diluted 3-fold from 80 μM initial concentration and then 30 μL added to each well for a top concentration of 40 μM. Fluorescent phosphopeptide WFYpSPFLE was initially dissolved in DMSO at 100 μM then dissolved into assay buffer and 30 μL of this solution was added to each well to give a final concentration of 75 nM. The plate was covered and

equilibrated at room temperature for 30 minutes then read on a SpectraMax M5 at wavelength 488/515 ex/em.

Competition experiments were performed under similar conditions. Separate solutions of Pin1 and fluorescent peptide at were prepared and then 15 μL of both was added to each well. The final concentrations used in the assay were 50nM and 1000nM for wild-type Pin1 and the Pin1 PPIase domain, respectively. Compounds were initially dissolved in DMSO to 10 mM, serially diluted 2-fold, then diluted to 400 μM with assay buffer and 30 μL was added to each well to a final top concentration of 200 μM and 2% DMSO. The assay was equilibrated at room temperature for 30 minutes and then read as before.

4.5.3 Synthetic Methods

(1R,9S,12S,13R,14S,17R,18E,21S,23S,24R,25S,27R)-12-[(1E)-1-[(1R,3R,4R)-4-hydroxy-3-methoxycyclohexyl]prop-1-en-2-yl]-1-amino-23,25-dimethoxy-14-hydroxy-13,19,21,27-tetramethyl-17-(prop-2-en-1-yl)-11,28-dioxa-4-azatricyclo[22.3.1.0^{4,9}]octacos-18-ene-2,3,10,16-tetrone (13)

To a solution of FK506 **(1)** (25mg, 0.031mmol, 1eq) in 2.5mL ethanol was added 1mL 7M ammonia in methanol to a final concentration of 2M (excess). The reaction was allowed to stir for 3 hours before solvent and ammonia were removed by evaporation. The crude product was dried under high vacuum for 30 minutes to afford 13 as an oily, translucent solid (75% yield). Expected MW: 802.50, Found M+H+: 803.63.

(1R,9S,12S,13R,14S,17R,18E,21S,23S,24R,25S,27R)-12-[(1E)-1-[(1R,3R,4R)-4-hydroxy-3-methoxycyclohexyl]prop-1-en-2-yl]-1-((3-chlorobenzyl)amino)-23,25-dimethoxy-14-hydroxy-13,19,21,27-tetramethyl-17-(prop-2-en-1-yl)-11,28-dioxa-4-azatricyclo[22.3.1.0(4,9)]octacos-18-ene-2,3,10,16-tetrone **(15)**

To a solution of **(13)** (12.5mg, 0.016mmol, 1eq) in 2mL DCM was added DMAP (0.6mg, 0.005mmol, 0.3eq) and allowed to stir under N_2. 3-chlorobenzyl bromide (9.9mg, 0.048mmol, 3eq) was added dropwise followed by the addition of DIEA (12.4mg, 0.096mmol, 6eq). After 24 hours, the solvent was removed by evaporation and the crude product dissolved in 1mL methanol and purified by HPLC (25% yield). Expected MW: 926.51, Found M+ACN$^+$: 968.93.

(1R,9S,12S,13R,14S,17R,18E,21S,23S,24R,25S,27R)-12-[(1E)-1-[(1R,3R,4R)-4-hydroxy-3-methoxycyclohexyl]prop-1-en-2-yl]-1-benzylamino-23,25-dimethoxy-14-hydroxy-13,19,21,27-tetramethyl-17-(prop-2-en-1-yl)-11,28-dioxa-4-azatricyclo[22.3.1.0(4,9)]octacos-18-ene-2,3,10,16-tetrone **(16)**

To a solution of **(13)** (20mg, 0.025mmol, 1eq) in 2mL DMF was added DMAP (1.0mg, 0.008mmol, 0.3eq) and allowed to stir under N_2. Benzyl bromide (42.8mg, 0.25mmol, 10eq) was added dropwise followed by the addition of DIEA (64.8mg, 0.5mmol, 20eq). The reaction temperature was raised to 50°C. After 24 hours, the crude product was purified by HPLC (10% yield). Expected MW: 892.54, Found M+H$^+$: 893.62.

(1R,9S,12S,13R,14S,17R,18E,21S,23S,24R,25S,27R)-12-[(1E)-1-[(1R,3R,4R)-4-hydroxy-3-methoxycyclohexyl]prop-1-en-2-yl]-1-((2-(tert-butoxy)-2-oxoethyl)amino)-23,25-dimethoxy-14-hydroxy-13,19,21,27-tetramethyl-17-(prop-2-en-1-yl)-11,28-dioxa-4-azatricyclo[22.3.1.0(4,9)]octacos-18-ene-2,3,10,16-tetrone **(18)**

To a solution of **(13)** (25mg, 0.031mmol, 1eq) in 2mL DCM was added DMAP (1.2mg, 0.010mmol, 0.3eq) and allowed to stir under N_2. Tert-Butyl bromoacetate (18.1mg, 0.093mmol, 3eq) was added dropwise followed by the addition of DIEA (24.1mg, 0.186mmol, 6eq). After 24 hours, the solvent was removed by evaporation and the crude product dissolved in 1mL methanol and purified by HPLC (25% yield). Expected MW: 916.57, Found M+ACN$^+$: 959.01.

(1R,9S,12S,13R,14S,17R,18E,21S,23S,24R,25S,27R)-12-[(1E)-1-[(1R,3R,4R)-4-hydroxy-3-methoxycyclohexyl]prop-1-en-2-yl]-1-((carboxymethyl)amino)-23,25-dimethoxy-14-hydroxy-13,19,21,27-tetramethyl-17-(prop-2-en-1-yl)-11,28-dioxa-4-azatricyclo[22.3.1.0(4,9)]octacos-18-ene-2,3,10,16-tetrone **(19)**

The protected derivative **(18)** (5mg, 0.005mmol, 1eq) was dissolved in a solution of DCM:TFA:TIPS:H_2O (45:45:5:5) and stirred for 30 minutes. TIPS was included as a cation scavenger. Solvent was evaporated and the crude product was purified by HPLC (5% yield). Expected MW: 860.50, Found M+H$^+$: 861.04.

(1R,9S,12S,13R,14S,17R,18E,21S,23S,24R,25S,27R)-12-[(1E)-1-[(1R,3R,4R)-4-hydroxy-3-methoxycyclohexyl]prop-1-en-2-yl]-23,25-dimethoxy-1-ethylamino-14-

hydroxy-13,19,21,27-tetramethyl-17-(prop-2-en-1-yl)-11,28-dioxa-4-

azatricyclo[22.3.1.0(4,9)]octacos-18-ene-2,3,10,16-tetrone (22)

To a solution of **(13)** (25mg, 0.031mmol, 1eq) in 2mL DMF was added DMAP (1.2mg, 0.010mmol, 0.3eq) and allowed to stir under N_2. Ethyl p-toluenesulfonate (124.2mg, 0.62mmol, 20eq) was added dropwise followed by the addition of DIEA (160.6mg, 1.24mmol, 40eq). The reaction temperature was raised to 50°C. After 24 hours, the crude product was purified by HPLC (5% yield). Expected MW: 830.53, Found M+Na$^+$: 853.58.

(1R,9S,12S,13R,14S,17R,18E,21S,23S,24R,25S,27R)-12-[(1E)-1-[(1R,3R,4R)-4-

hydroxy-3-methoxycyclohexyl]prop-1-en-2-yl]-1-(2-bromoacetamido)-23,25-

dimethoxy-14-hydroxy-13,19,21,27-tetramethyl-17-(prop-2-en-1-yl)-11,28-dioxa-

4-azatricyclo[22.3.1.0(4,9)]octacos-18-ene-2,3,10,16-tetrone (24)

To a solution of **(13)** (12.5mg, 0.016mmol, 1eq) in 2mL DMF was added DMAP (0.6mg, 0.005mmol, 0.3eq) and allowed to stir under N_2. 4-Nitrophenyl bromoacetate (4.2mg, 0.016mmol, 1eq) was added dropwise followed by the addition of DIEA (6.2mg, 0.048mmol, 3eq). The reaction temperature was raised to 50°C. After 24 hours, the crude product was purified by HPLC (5% yield). Expected MW: 924.42, Found M+ACN$^+$: 966.99.

(1R,9S,12S,13R,14S,17R,18E,21S,23S,24R,25S,27R)-12-[(1E)-1-[(1R,3R,4R)-4-

hydroxy-3-methoxycyclohexyl]prop-1-en-2-yl]-1-acetamido-23,25-dimethoxy-14-

hydroxy-13,19,21,27-tetramethyl-17-(prop-2-en-1-yl)-11,28-dioxa-4-

*azatricyclo[22.3.1.0(4,9)]octacos-18-ene-2,3,10,16-tetrone **(27)***

To **(13)** (12.5mg, 0.016mmol, 1eq) was added 1mL neat acetic anhydride and stirred under N_2. After 3 hours, the reaction was diluted with toluene and solvent was evaporated. This was repeated in total 3 times to remove as much unreacted acetic anhydride as possible. The crude product was dissolved in methanol and purified by HPLC (42% yield). Expected MW: 844.51, Found M+Na$^+$: 867.58.

(1R,9S,12S,13R,14S,17R,18E,21S,23S,24R,25S,27R)-12-[(1E)-1-[(1R,3R,4R)-4-

hydroxy-3-methoxycyclohexyl]prop-1-en-2-yl]-1-benzamido-23,25-dimethoxy-14-

hydroxy-13,19,21,27-tetramethyl-17-(prop-2-en-1-yl)-11,28-dioxa-4-

*azatricyclo[22.3.1.0(4,9)]octacos-18-ene-2,3,10,16-tetrone **(29)***

To a solution of **(13)** (12.5mg, 0.016mmol, 1eq) in 2mL DCM was added DMAP (0.6mg, 0.005mmol, 0.3eq) and allowed to stir under N_2. Benzoic anhydride (18.1mg, 0.08mmol, 5eq) was added dropwise followed by the addition of DIEA (20.7mg, 0.16mmol, 10eq). After 24 hours, the solvent was removed, crude product was dissolved in 1mL methanol and purified by HPLC (10% yield). Expected MW: 924.42, Found M+ACN$^+$: 966.99.

(1R,9S,12S,13R,14S,17R,18E,21S,23S,24R,25S,27R) -12-[(1E)-1-[(1R,3R,4R)-

4-hydroxy-3-methoxycyclohexyl]prop-1-en-2-yl]-23,25-dimethoxy-14-hydroxy-1-

sulfoamino-13,19,21,27-tetramethyl-17-(prop-2-en-1-yl)-11,28-dioxa-4-

azatricyclo[22.3.1.0(4,9)]octacos-18-ene-2,3,10,16-tetrone (34)

To a solution of **(13)** (12.5mg, 0.016mmol, 1eq) in 2mL DCM was added DMAP (0.6mg, 0.005mmol, 0.3eq) and allowed to stir under N_2. Chlorosulfonic acid (2.8mg, 0.024mmol, 1.5eq) was added dropwise followed by the addition of DIEA (20.7mg, 0.16mmol, 10eq). After 24 hours, the reaction had gone cloudy and solvent was removed. The crude product was dissolved in 1mL methanol and purified by HPLC (25% yield). Expected MW: 882.45, Found M-H$^+$: 881.87.

4.6   Notes

This chapter represents a portion of the work published in "Dunyak, B.M. & Gestwicki, J.E. Peptidyl-Proline Isomerases (PPIases): Targets for Natural Products and Natural Product-Inspired Compounds. *J. Med. Chem.* In press. (2016)." Bryan M. Dunyak and Jason E. Gestwicki designed the experiments and synthetic schemes. Bryan M. Dunyak performed the experiments and chemical syntheses with assistance from Daniel Schwarz.

4.7   Appendix

Characterization of compounds synthesized in Chapter 4.

Compound 15:

Expected MW: 926.51, Found M+ACN⁺: 968.93.
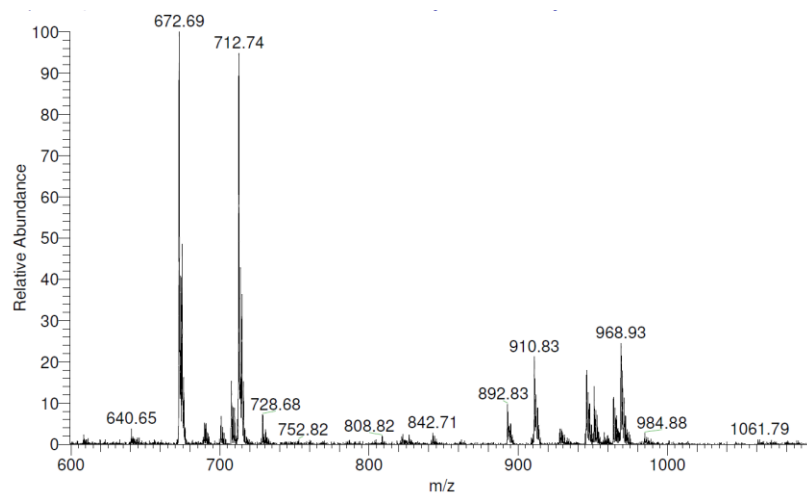
Compound 16:

Expected MW: 892.54, Found M+H⁺: 893.62.
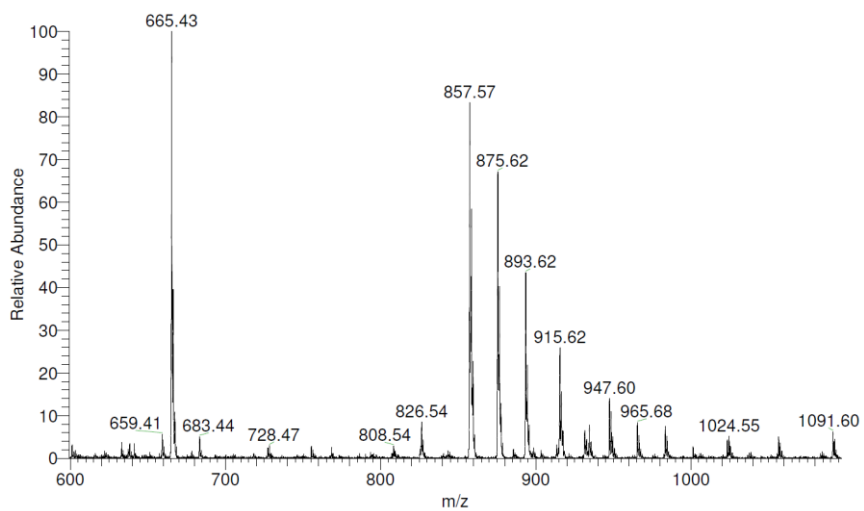
Compound 18:

Expected MW: 916.57, Found M+ACN$^+$: 959.01.
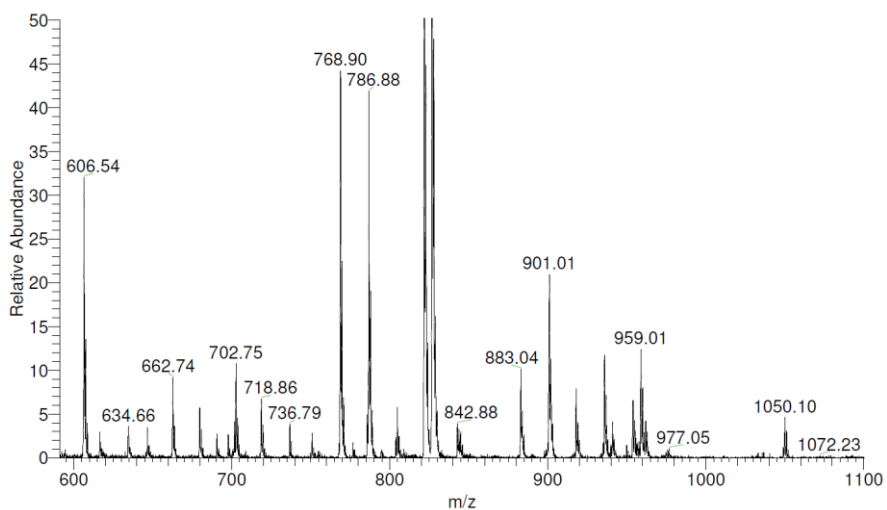
Compound 19:

Expected MW: 860.50, Found M+H$^+$: 861.04.

Compound 22:

Expected MW: 830.53, Found M+Na$^+$: 853.58.
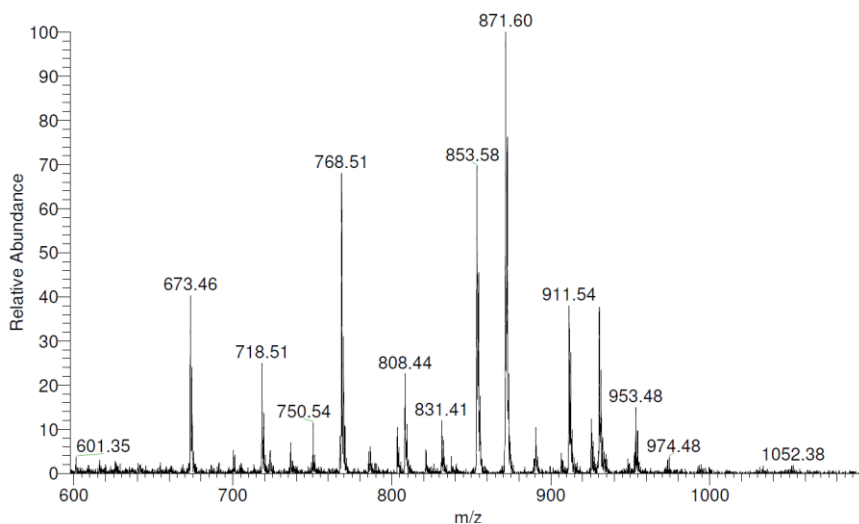
Compound 24:

Expected MW: 924.42, Found M+ACN$^+$: 966.99.
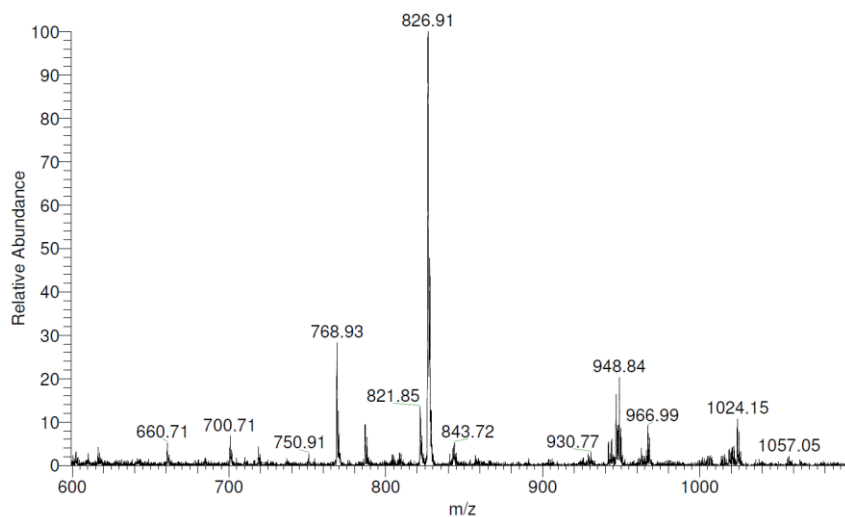
*Compound **27***:

Expected MW: 844.51, Found M+Na$^+$: 867.58.
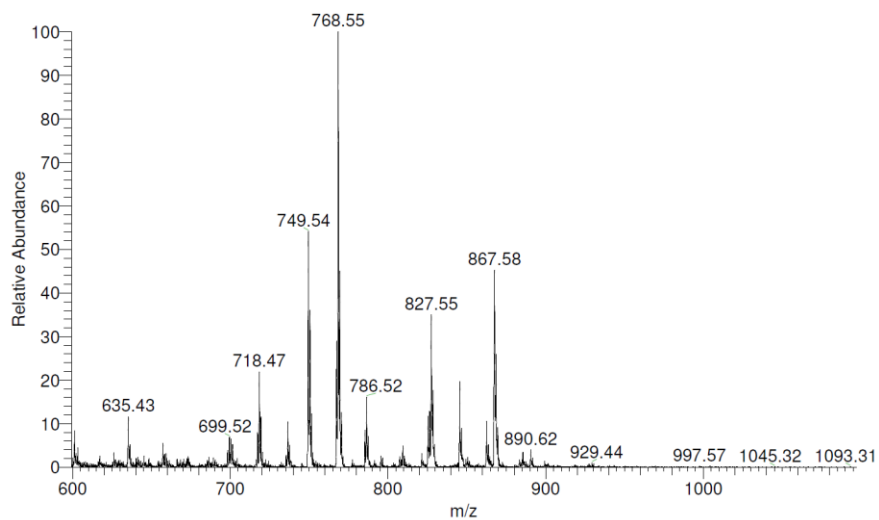
*Compound **29***:

Expected MW: 924.42, Found M+ACN$^+$: 966.99.
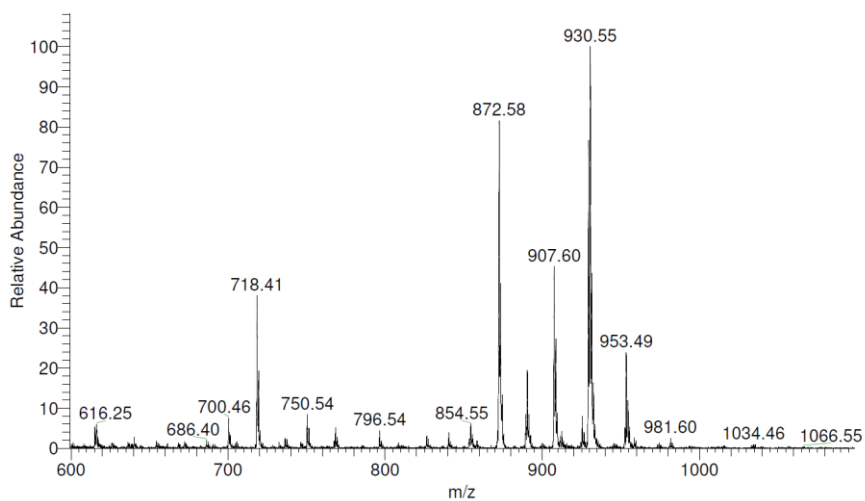
Compound 34:
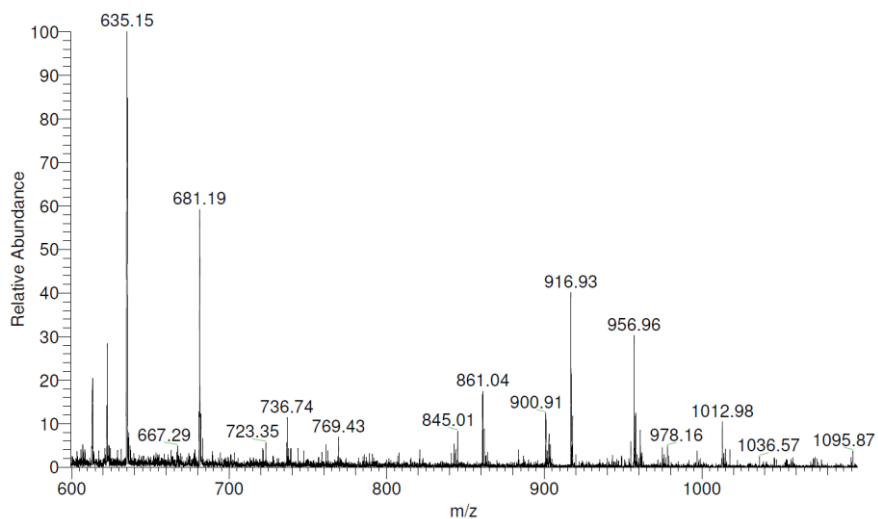
Expected MW: 882.45, Found M-H$^+$: 881.87.
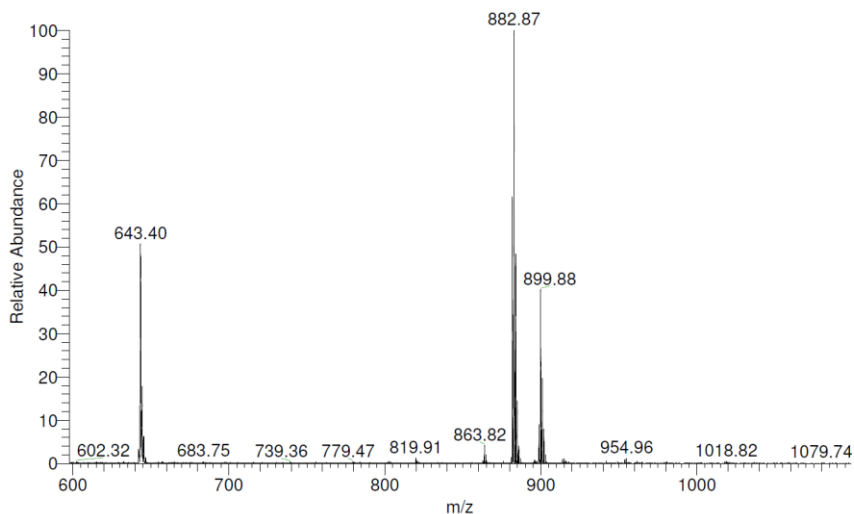
4.8   References

1.   Lu, K.P., Hanes, S.D. & Hunter, T. A human peptidyl-prolyl isomerase essential for regulation of mitosis. Nature 380, 544-7 (1996).
2.   Ranganathan, R., Lu, K.P., Hunter, T. & Noel, J.P. Structural and functional analysis of the mitotic rotamase Pin1 suggests substrate recognition is phosphorylation dependent. Cell 89, 875-86 (1997).
3.   Barman, A. & Hamelberg, D. Cysteine-mediated dynamic hydrogen-bonding network in the active site of Pin1. Biochemistry 53, 3839-50 (2014).
4.   Hanes, S.D., Shank, P.R. & Bostian, K.A. Sequence and mutational analysis of ESS1, a gene essential for growth in Saccharomyces cerevisiae. Yeast 5, 55-72 (1989).
5.   Schutkowski, M. et al. Role of phosphorylation in determining the backbone dynamics of the serine/threonine-proline motif and Pin1 substrate recognition. Biochemistry 37, 5566-75 (1998).
6.   Brister, M.A., Pandey, A.K., Bielska, A.A. & Zondlo, N.J. OGlcNAcylation and phosphorylation have opposing structural effects in tau: phosphothreonine induces particular conformational order. J Am Chem Soc 136, 3803-16 (2014).

7. Ryo, A., Liou, Y.C., Lu, K.P. & Wulf, G. Prolyl isomerase Pin1: a catalyst for oncogenesis and a potential therapeutic target in cancer. J Cell Sci 116, 773-83 (2003).

8. Bao, L. et al. Prevalent overexpression of prolyl isomerase Pin1 in human cancers. Am J Pathol 164, 1727-37 (2004).

9. Liou, Y.C. et al. Role of the prolyl isomerase Pin1 in protecting against age-dependent neurodegeneration. Nature 424, 556-61 (2003).

10. Lu, P.J., Wulf, G., Zhou, X.Z., Davies, P. & Lu, K.P. The prolyl isomerase Pin1 restores the function of Alzheimer-associated phosphorylated tau protein. Nature 399, 784-8 (1999).

11. Butterfield, D.A. et al. Redox proteomics identification of oxidatively modified hippocampal proteins in mild cognitive impairment: insights into the development of Alzheimer's disease. Neurobiol Dis 22, 223-32 (2006).

12. Ibanez, K., Boullosa, C., Tabares-Seisdedos, R., Baudot, A. & Valencia, A. Molecular evidence for the inverse comorbidity between central nervous system disorders and cancers detected by transcriptomic meta-analyses. PLoS Genet 10, e1004173 (2014).

13. Lim, J. et al. Pin1 has opposite effects on wild-type and P301L tau stability and tauopathy. J Clin Invest 118, 1877-89 (2008).

14. Moore, J.D. & Potter, A. Pin1 inhibitors: Pitfalls, progress and cellular pharmacology. Bioorg Med Chem Lett 23, 4283-91 (2013).

15. Hennig, L. et al. Selective inactivation of parvulin-like peptidyl-prolyl cis/trans isomerases by juglone. Biochemistry 37, 5953-60 (1998).

16. Uchida, T. et al. Pin1 and Par14 peptidyl prolyl isomerase inhibitors block cell proliferation. Chem Biol 10, 15-24 (2003).

17. Graber, M. et al. Selective targeting of disease-relevant protein binding domains by O-phosphorylated natural product derivatives. ACS Chem Biol 6, 1008-14 (2011).

18. Wei, S. et al. Active Pin1 is a key target of all-trans retinoic acid in acute promyelocytic leukemia and breast cancer. Nat Med 21, 457-66 (2015).

19. Wildemann, D. et al. Nanomolar inhibitors of the peptidyl prolyl cis/trans isomerase Pin1 from combinatorial peptide libraries. J Med Chem 49, 2147-50 (2006).

20. Zhang, Y. et al. Structural basis for high-affinity peptide inhibition of human Pin1. ACS Chem Biol 2, 320-8 (2007).

21. Guo, C. et al. Structure-based design of novel human Pin1 inhibitors (I). Bioorg Med Chem Lett 19, 5613-6 (2009).

22. Dong, L. et al. Structure-based design of novel human Pin1 inhibitors (II). Bioorg Med Chem Lett 20, 2210-4 (2010).

23. Potter, A. et al. Discovery of cell-active phenyl-imidazole Pin1 inhibitors by structure-guided fragment evolution. Bioorg Med Chem Lett 20, 6483-8 (2010).

24. Nussbaumer, P., Grassberger, M. & Schulz, G. C9-imino and C10-amino derivatives of ascomycin (21-ethyl-FK 506). Tetrahedron Letters 33, 3845-3846 (1992).

25.   Ham, Y.-B. & Koo, Y.-M. Identification of an 18-Methyl Derivative of Tacrolimus API in Streptomyces clavuligerus CKD-1119. *Bulletin of the Korean Chemical Society* **32**, 109-112 (2011).

Chapter 5

Conclusions and Future Directions

5.1   Conclusions

PPIases are challenging drug targets. Their active sites are shallow, hydrophobic, and often degenerate between family members. These complications are not unique to PPIases, however, as many viable protein targets exhibit "undruggable" features.[1] Despite these complications, the natural products FK506, rapamycin and cyclosporine bind PPIases with tight affinity and, in some cases, with some paralog specificity. Indeed, some of these PPIase natural products have even reached clinical approval for immune and oncology indications.[2] However, there have not been any approvals for small molecules that exert biological activity through inhibition of a PPIase. One of the major hurdles has been pharmacokinetics and membrane permeability. The natural products use the special properties of macrocycles, such as intramolecular hydrogen bonding, hydrophilic collapse, and cyto-specific targeting to achieve biological activity.[3-5] In this way, these macrocycles are able to access the important sites on the PPIase while maintaining intracellular partitioning. In this work, I have explored the characteristics underlying the mechanism of the natural product macrocycle

FK506 and its related derivatives to better understand how the mechanism of this molecule permits such a favorable pharmacological profile.

In Chapter 2, I synthesized a series of bifunctional molecules that have affinity for FKBP and HIV protease. Inspired by the mechanism of FK506, which is naturally bifunctional, we hypothesized that an "FK506-like" molecule capable of simultaneously binding FKBP12 and HIV protease might be selectively retained in cells that express both targets. I gained control over the FKBP12 binding by using either FK506 or the weaker ligand, SLF, while affinity for HIV protease was tuned by installing linkers at a region that was known to impact binding. Using biochemical assays, I characterized the library of bi-specific molecules and demonstrated that they possess variable affinity for each protein target.

In Chapter 3, I explored cyto-selective targeting of our bifunctional molecules. We hypothesized that coincident, high-level expression of both protein targets - such as in HIV-infected lymphocytes - would drive selective cellular targeting and sequestration of these compounds. In a cell-based GFP reporter assay, I confirmed that interactions with FKBP12 and HIV protease also control the cellular partitioning of these molecules. The cyto-selectivity effect was dominated by binding to FKBP12, likely because it represents a greater pool of available binding sites. Further exploring the impact of FKBP12 binding, pharmacological competitors and overexpression were used to systematically control the availability of FKBP12 for binding. Overexpression of an FKBP12 construct could enhance

partitioning (and anti-HIV protease activity), while binding competitors neutralized this effect. This concept is supported by the results of the live viral HIV-infectivity assays, in which FKBP12 binding determined the effectiveness of compounds. These results suggest that the key design principles in engineering cyto-selective bifunctional molecules are the abundance of the protein partners and the avidity of the interactions, reminiscent of what has been found for bi-specific antibodies.

In Chapter 4, I wanted to see if the features outlined in Chapters 1, 2 and 3, could be exploited to design novel Pin1 inhibitors. The pipecolate core found in FK506 and rapamycin provided the basis for early Pin1 inhibitors, and this scaffold exhibited a bound conformation highly reminiscent to that of FK506 bound to FKBP12. While FK506 has no measurable affinity for Pin1, we hypothesized that installation of an electronegative functional group could impart Pin1 binding. Thus, FK506 was systematically modified at the C10-hydroxyl to furnish an amine substituted derivative, FK-NH2. This position is in close proximity to the cationic groove in Pin1. Using a one-pot strategy for subsequent derivatization, we found that anhydrides allowed robust product formation in excellent yields (~100% in most cases). Direct alkylation with alkyl halides or amide formation with activated carboxylic acids and acyl chlorides was only moderately effective. These synthetic studies are expected to facilitate the creation of the next generation of potential Pin1 inhibitors bearing substituents designed for Pin1 binding like the sulfamic acid-containing compound **34**. In preliminary *in vitro* studies, this compound had modest affinity for Pin1 with FKBP12 activity significantly impacted.

Overall, this work has contributed to our understanding of the effectiveness of bifunctional molecules. We found that these compounds sequester into cells at levels unexpected by their physicochemical properties. This effect is "tunable", and mediated by the affinity and availability of the intracellular targets. In particular, we have demonstrated that bifunctional molecules are able to selectively partition into relevant cell populations, enhancing efficacy. Further, this mechanism has inspired the development of novel macrocyclic Pin1 inhibitors. These compounds are designed to address limitations in the cellular activity and usefulness of current Pin1 candidates. The design principles outlined here provide a framework for the continued development of new Pin1 inhibitors in this class.

5.2   Future Directions

5.2.1 Bifunctional molecules as a partitioning platform technology

In this work, we demonstrated the ability of bifunctional molecules to partition molecules with limited permeability into relevant cells and dramatically improve their cellular activity. Other strategies have been commonly used for internalizing impermeable payloads, such as TAT-fusion proteins or octa-arginine tags,[6] which undergo macropinocytosis to gain entry to the intracellular space. However, these techniques are often complicated by limited escape from endocytotic vesicles in the cell[7] and/or insufficient uptake and absorption in more complex animal models.[8] One potential way to address these problems is with FK506 variants. As outlined in Chapter 2, modification of the extracyclic alkene provides

an easily reactive handle for attachment of nearly any substrate. The favorable ADME properties of FKBP ligands could lead to rapid absorption and tissue distribution of desired cargo. Further, this attachment point on FK506 abrogates its immunosuppressive effects, which is a concern for FK506-based therapeutics. Beyond typical bioavailability of drugs, complex blood-brain barrier (BBB) permeability dynamics significantly limit feasible therapeutics for neurological conditions like neuropathic pain and neurodegenerative disease. Most BBB permeable molecules are very lipophilic, with both low molecular weight and polar surface area being a requirement, preventing the BBB penetration of many compounds. Surprisingly, both FK506 and rapamycin have significant BBB permeability despite their large size and a polar surface area two- to three-times the predicted cutoff.[9] Appending drugs to these macrocycles to shuttle them across the BBB could be a viable strategy to enhance their activity in the brain.

5.2.2   Engineering bifunctional macrocycles for clinical candidates

Co-opting the natural mechanism of the macrocyclic PPIase ligands, recent synthetic derivatives containing the PPIase region fused to a "variable" region have been heavily pursued as pre-clinical candidates (Figure 5.1).[10] This strategy takes advantage of two features; the FKBP partitioning effect reported in this work and the intracellular ternary complex formation central to the mechanism of FK506 and related macrocycles. FKBPs have been shown to have a highly dynamic surface that is capable of productively interacting with other proteins to dramatically stabilize a ternary complex. This feature contributes to complex
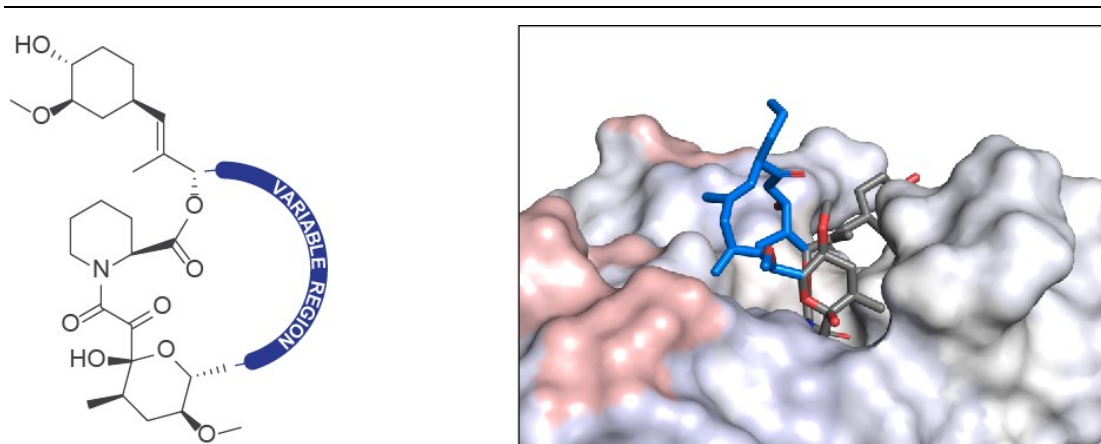
Figure 5.1) Artificial PPIase macrocycles that exploit the PPIase composite surface for inhibitory activity. FK506 is modified in the variable region through total synthesis or biosynthetic engineering. The highly plastic FKBP12 surface is able to cooperatively facilitate novel protein-protein interactions to inhibit desired targets. The variable region amenable for modification is shown in blue. (PDB: 1FKF, partial charges represented on the surface)

formation mediated by FK506 and rapamycin in the FKBP12-FK506-Calcineurin and FKBP12-rapamycin-mTOR interactions, respectively. Attaching the FKBP pipecolate core to peptides targeting mutated K-RAS G12V effectively inhibits the RAS-RAF interaction while simultaneously binding FKBP12.[11] A similar approach is being developed commercially for pre-clinical testing, instead using the core of the bifunctional molecule Cyclosporine to inhibit RAS signaling.[12] Generating synthetic macrocycles built off the PPIase binding core of these natural products is likely to be an effective strategy at inhibiting challenging targets through newly formed protein-protein interactions.

5.2.3 "Pinamycin" as an anti-cancer therapeutic

In Chapter 4, we systematically explored the reactivity of the semisynthetic derivative FK-NH2. As mentioned, similar conversion of the tertiary hydroxyl in
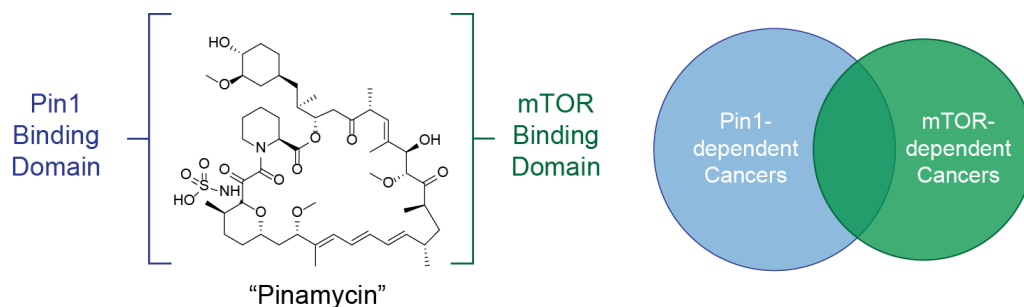
Figure 5.2) Pin1 and mTOR are validated targets in numerous human cancers. A modified "pinamycin" derivative is expected to potently inhibit proliferation of cancer cells with a large therapeutic window.

rapamycin is also effective (Figure 4.9). In part, we chose to first explore the reactivity of FK-NH2 because the chemical stability is greater than that of rapamycin. In particular, the triene region of rapamycin is highly reactive and prone to degradation. Thus, we characterized the FK-NH2 reactivity first so that we can now derivatize rapamycin under optimized conditions. Rapamycin, like Pin1, is a validated target in a variety of human cancers.[13, 14] Analogous to our strategy in Chapter 4, installation of electronegative groups at the position of the C10-hydroxyl is designed to afford both Pin1 and mTOR inhibitory activity. In this way, "Pinamycin", a novel rapamycin analog, would gain additional anti-cancer activity through its effects on Pin1 (Figure 5.2). In contrast, FKBP12 traditionally acts as a scaffold and is typically a bystander to the inhibitory effects of rapamycin on mTOR. Inhibiting both Pin1 and mTOR is reminiscent of cocktail therapies commonly used in oncology, where the effects of multiple drugs synergize to enhance efficacy. Additionally, mTOR and Pin1 and their respective clients are often over-expressed in cancer. So, as we have observed with other bifunctional

molecules, we expect Pinamycin to possess cyto-selectivity, increasing its accumulation and therapeutic index in desired cell populations.

5.2.4 Paralog specificity of FK-NH2 derivatives

Finding selective molecules for individual members of the FKBP family has been considered a major challenge, with FK506 and other ligands being nearly equipotent for the majority of FKBP paralogs. Recently, Hausch et al. investigated a "bump-hole"[15] mutagenesis approach to engineer specificity for FKBP51 and FKBP52. While testing expanded derivatives of SLF (**3**) against mutant FKBP51 and FKBP52, it was discovered that a subset of complementary ligands still had modest affinity for the wild-type FKBP51.[16] The expanded SLF derivative was found to induce a conformational rearrangement of the active site, with Phe-67 rotating away from the proline pocket (Figure 5.3). This induced fit conformation does not appreciably occur in FKBP12 or FKBP52. A brief SAR series produced a compound that bound FKBP51 with single digit nanomolar potency and greater

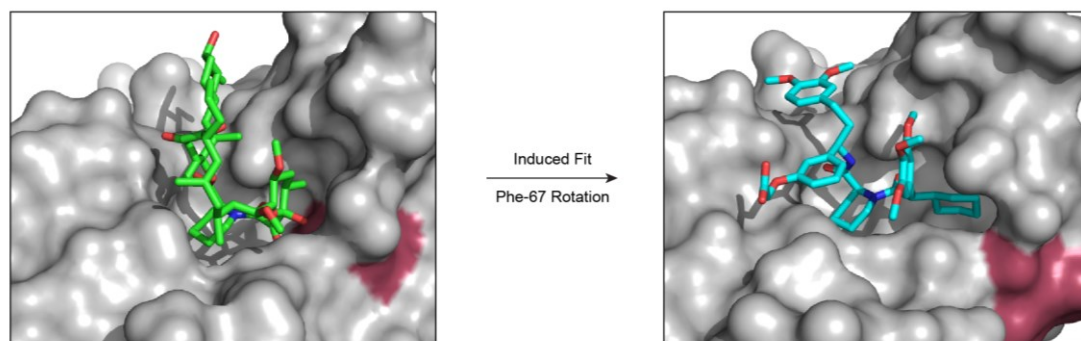
Figure 5.3) FKBP51 undergoes an expansion of the active site to tolerate high-affinity SLF derivatives substituted on the α-ketoamide. Phe-67 (red) rotates to allow the expansion and is in close proximity to the C10 modification point of FK506 and FK-NH2. (PDB: 3O5R and 5DIU)

than 10,000-fold selectivity over FKBP52 and only minimal FKBP12 binding. This work presents a promising therapeutic strategy for FKBP51-dependent pathologies.

The position of modification in FK-NH2 is in close proximity to Phe-67 of FKBP51. Small hydrophobics here are expected to be oriented in a similar pose as the highly selective SLF derivatives just mentioned. The semisynthetic approaches discussed in Chapter 4 provide an immediate path towards testable FKBP51-specific ligands. In parallel to our work engineering FK-NH2 derivatives to enable Pin1 binding, we are also exploring the ability of these molecules to gain FKBP51 selectivity. Highly specific, cell permeable FKBP51 molecules would address a long-standing complication in the field of FKBP ligands with immediate translational potential.

5.3   References

1.   Makley, L.N. & Gestwicki, J.E. Expanding the number of 'druggable' targets: non-enzymes and protein-protein interactions. Chem Biol Drug Des 81, 22-32 (2013).
2.   Giordanetto, F. & Kihlberg, J. Macrocyclic drugs and clinical candidates: what can medicinal chemists learn from their properties? J Med Chem 57, 278-95 (2014).
3.   Rezai, T., Yu, B., Millhauser, G.L., Jacobson, M.P. & Lokey, R.S. Testing the conformational hypothesis of passive membrane permeability using synthetic cyclic peptide diastereomers. J Am Chem Soc 128, 2510-1 (2006).
4.   Rezai, T. et al. Conformational flexibility, internal hydrogen bonding, and passive membrane permeability: successful in silico prediction of the relative permeabilities of cyclic peptides. J Am Chem Soc 128, 14073-80 (2006).

5. Dunyak, B.M., Nakamura, R.L., Frankel, A.D. & Gestwicki, J.E. Selective Targeting of Cells via Bispecific Molecules That Exploit Coexpression of Two Intracellular Proteins. ACS Chem Biol 10, 2441-7 (2015).

6. Bechara, C. & Sagan, S. Cell-penetrating peptides: 20 years later, where do we stand? FEBS Lett 587, 1693-702 (2013).

7. Khalil, I.A., Kogure, K., Akita, H. & Harashima, H. Uptake pathways and subsequent intracellular trafficking in nonviral gene delivery. Pharmacol Rev 58, 32-45 (2006).

8. Weiss, H.M. et al. ADME investigations of unnatural peptides: distribution of a 14C-labeled beta 3-octaarginine in rats. Chem Biodivers 4, 1413-37 (2007).

9. Meikle, L. et al. Response of a neuronal model of tuberous sclerosis to mammalian target of rapamycin (mTOR) inhibitors: effects on mTORC1 and Akt signaling lead to improved survival and function. J Neurosci 28, 5422-32 (2008).

10. Sheridan, C. Recasting natural product research. Nat Biotechnol 30, 385-7 (2012).

11. Wu, X., Upadhyaya, P., Villalona-Calero, M.A., Briesewitz, R. & Pei, D. Inhibition of Ras-Effector Interaction by Cyclic Peptides. Medchemcomm 4, 378-382 (2013).

12. Sheridan, C. Drug developers refocus efforts on RAS. Nat Biotechnol 34, 217-8 (2016).

13. Easton, J. & Houghton, P. mTOR and cancer therapy. Oncogene 25, 6436-6446 (2006).

14. Yeh, E.S. & Means, A.R. PIN1, the cell cycle and cancer. Nat Rev Cancer 7, 381-8 (2007).

15. Shah, K., Liu, Y., Deirmengian, C. & Shokat, K.M. Engineering unnatural nucleotide specificity for Rous sarcoma virus tyrosine kinase to uniquely label its direct substrates. Proc Natl Acad Sci U S A 94, 3565-70 (1997).

16. Gaali, S. et al. Selective inhibitors of the FK506-binding protein 51 by induced fit. Nat Chem Biol 11, 33-7 (2015).